Development and Optimisation of New Methodology for use in Solid-Phase Organic Synthesis.

a thesis presented by

Duane Stones

to the

UNIVERSITY OF ST ANDREWS

in application for

THE DEGREE OF DOCTOR OF PHILOSOPHY

St Andrews December 2000

Copyright.

In submitting this thesis to the University of St. Andrews I understand that I am giving permission for it to be made available for use in accordance with the regulations of the University library for the time being in force, subject to any copyright vested in the work not being affected thereby. I also understand that the title and abstract will be published and that a copy of the work may be made and supplied to any bona fide research worker.

Date 19 Dec 2000 Signature of Candidate.. .....

Declarations.

I, Duane Stones, hereby certify that this thesis, which is approximately 36000 words in length, has been written by me, that it is the record of work carried out by me and that it has not been submitted in any previous application for a higher degree.

date 19 Dec 2000 signature of candidate.. .....

I was admitted as a research student in October, 1996 and as a candidate for the degree of Ph.D. in October, 1997; the higher study for which this is a record was carried out in the University of St Andrews between 1996 and 1998, and the University of Birmingham between 1998 and 2000.

date 19 Dec 2000 signature of candidate. .....

I hereby certify that the candidate has fulfilled the conditions of the Resolution and Regulations appropriate for the degree of Ph.D. in the University of St Andrews and that the candidate is qualified to submit this thesis in application for that degree.

date 19 Dec 2000 signature of supervis

Acknowledgements.

Work:

Firstly, I should acknowledge my supervisor Professor Gani for letting me have a free rein on a very interesting project. Good luck for the future.

Thanks to Stacey, for helpful hints (has he gone yet??), Luci and Lynn.

For their excellent technical support and advice, I thank Melanja, Jim and Bobby (can you guys do everything?), and Colin in St. Andrews, along with Neil, Malcolm, Pete, Nick, Leanne and Roy in Birmingham, along with the Glasses, Phil and Steve.

Thanks to the Universities of St. Andrews and Birmingham for funding.

Other Stuff:

After 4 years, there are many people to thank, and I do not apologise if I miss you!

To members of the group for various 'episodes' along the way: Graham "Bomber" Allan and Roger Pybus for military golf games, and a cracking Raisin Sunday (never again!!), Donald McNab for introducing me to fantasy liqueurs, Mark "Scroat" Hillier and Arwel "Prof. Pop" for dragging me to the fantastic Cellar Bar Quiz, and John "Sportsbra" Pollard and Trevor "Lenin" Rutherford for poker nights, impromptu visits to Tenerife, Cupartastic drinking sessions, the Royal Family, and the School Run!!!! Thanks also to Cambridge for giving me a place to live, Dave and Jon S, Thierry, Ozzie Mick, Bashir and Amit.

To housemates everywhere, thanks for being a great crowd, but no more nasty Bulgarian wine please Birdmate!!!

To G and Fi, (and Fi's parents) for giving me a place to escape to in Aberdeen, and pushing me down the Lecht, I would have gone mad without you! Lets drink to KBC.

To the guys in Birmingham, Coops, Monkey, Cookie, Skip, Mikeeeeeee, Aario a.k.a Speedwagon and Gerby, things will never be the same again!

The many football teams in which I have played (**!!??**), including Bomber (again), Cabbage, Roger, Jules, Dave, Brian, Pete and Martin (Ski & Freybentus), Damage, Doug, Daz, Max, Raf, DC, Andy (Halfway!!!), Luca, Simon (Chemistry PGFC), cheers guys, try and keep up the winning run!!!

Thanks to Nicola for all the smiles, hugs, tears and support, and for introducing me to some of the delights of Peterhead (Nicola H). I hope to see you soon in the Toon!

To Malcolm and Ellis, The Cellar Bar and the regulars for fine beer, food, music and chat, and also the free shirts and testers, and lock-ins---so that's where my money went???

To the Chemistry Birds FC, Banjo, PC Pigby, Boot, Big Bird, Paddy, Amanda, I always knew you could do it!

To the Philp Group in St. Andrews, keep smiling and I'll see you all soon, especially Doug....I know a great place for dinner if you're paying!

To Sam for being a star and making me laugh again, come and see me, I meant everything!

I hope you can all make it to Edmonton to see me sometime.

Finally, to Mum and Dad, Donna and Neil, and Grandma for always being there when I needed anything, and quite often everything, without you it would not mean anything. Also to the people who are not here to see this happen, I think about you always.

God Bless you all.

Abstract.

This thesis describes developments in three areas associated with combinatorial solid-phase chemistry.

Firstly, the initial development of a method for the parallel synthesis of libraries of discrete, individual compounds, POSAM™, is described. This includes the design of microreactors that contain the polymer support, and the design, improvements and testing of the apparatus used in library synthesis.

Secondly, a method of accurately quantifying the loading of any fluorinated species onto a solid support is described. This method can be used at any point in of a synthetic procedure to monitor the extent of a reaction on a solid support.

Finally, the design and development of a resin-immobilised, heterogeneous catalyst is described. The supported species serves as a stable and re-usable alkene hydroformylation and hydrogenation catalyst.

Contents.

List of Figures.

List of Schemes.

List of Tables.

List of Graphs.

Abbreviations.

Å	angstroms (10^{-10}m)
Bn	benzyl
Boc	*tert*-butoxycarbonyl
Bpoc	2-(4-biphenylyl)*iso*propyl phenyl carbonate
CAN	ceric ammonium nitrate
DCA	dichloroacetic acid
DCE	1,2-dichloroethane
DCM	dichloromethane
DIPEA	*N,N*-di*iso*propylethylamine
DMAP	4-dimethylaminopyridine
DMF	*N,N*-Dimethylformamide
DMSO	Dimethyl sulfoxide
DMT	4,4´-dimethoxytrityl
DVB	divinylbenzene
e.e.	enantiomeric excess
Et	ethyl
Fmoc	9-fluorenylmethoxycarbonyl
GC	gas chromatography
HPLC	high pressure liquid chromatography
IMPase	Inositol monophosphatase
IR	Infrared
LC	liquid chromatography
MAS	magic angle spinning
*m*CPBA	*meta*-chloroperbenzoic acid

Me	methyl
Mpoc	2-(4-methylphenyl)*iso*propyl phenyl carbonate
MS	mass spectrometry
NMM	*N*-methylmorpholine
NMO	*N*-methylmorpholine *N*-oxide
NMP	*N*-methylpyrrolidinone
NMR	Nuclear Magnetic Resonance
PEG	polyethyleneglycol
POSAM™	Permutational Organic Synthesis in Addressable Microreactors
ppm	parts per million
PS	polystyrene
PSP	polymer-supported perruthenate
PTFE	polytetrafluoroethylene
PyBOP	Benzotriazol-1-yloxytris(pyrrolidinyl)phosphonium hexafluorophosphate
RF	radiofrequency
S_NAr	nucleophilic aromatic substitution
SASRIN	superacid sensitive resin
SPOC	solid-phase organic chemistry
SPOS	solid-phase organic synthesis
SPPS	solid-phase peptide synthesis
T_1	Spin lattice relaxation time
TES	triethylsilane
TFA	trifluoroacetic acid
THF	tetrahydrofuran

TLC	thin layer chromatography
TMS-CN	trimethylsilyl cyanide
TPAP	tetra-*n*-propylammonium perruthenate
Triflate	trifluoromethanesulfonate
Triflic	trifluoromethanesulfonic
Ts	4-toluenesulfonyl

Amino Acid Abbreviations.

Three Letter Code	Amino Acid	One Letter Code
Ala	Alanine	A
Arg	Arginine	R
Asn	Asparagine	N
Asp	Aspartic acid	D
Cys	Cysteine	C
Gln	Glutamine	Q
Glu	Glutamic acid	E
Gly	Glycine	G
His	Histidine	H
Ile	Isoleucine	I
Leu	Leucine	L
Lys	Lysine	K
Met	Methionine	M
Phe	Phenylalanine	F
Pro	Proline	P
Ser	Serine	S
Thr	Threonine	T
Trp	Tryptophan	W
Tyr	Tyrosine	Y
Val	Valine	V

CHAPTER ONE

INTRODUCTION

1.1 Background.

The discovery of new and biologically active compounds for use in all sectors of the chemical industry has historically relied upon the identification and optimisation of lead structures from many different sources, including plant, animal and microbiological fermentations. However, this process of identification is very time consuming and expensive in terms of synthesis and screening. Finding new biologically active molecules is becoming increasingly difficult, due to the increasing number of receptors and enzymes that are being identified as possible therapeutic targets.[1, 2]

The way the pharmaceutical companies have traditionally tackled this expansion in the number of targets is by screening the vast numbers of compounds present in their existing libraries. This, coupled with automated high throughput screening methods (HTS) has allowed testing of thousands of compounds per week.[3-6] However, one drawback in this approach is that the structural diversity of the compounds in the company portfolios has been significantly influenced by the requirements of previous drug discovery programs.

With the identification of new lead compounds from synthesised libraries, initially there is no attempt to design an active moiety. The advantage of this method is the library offers a large number of compounds with a vast degree of structural variety present. Often, any preconceptions of which core structures should, or might, display affinity for the target are ignored in favour of the chance that there will be a serendipitous discovery of a lead. However, such a strategy does not exclude the 'rational design' of potential drugs in a combinatorial approach in which knowledge of the structure of the receptor or enzyme being targeted is used to design the library. At the other extreme, the identification of a lead compound can be used in the design of a library of closely related structural analogues. These can be used in structure activity relationship (SAR) studies. In such cases, the use of combinatorial chemistry impacts

on the drug discovery process at the lead compound optimisation stage, rather than the lead discovery stage, Figure 1.1.

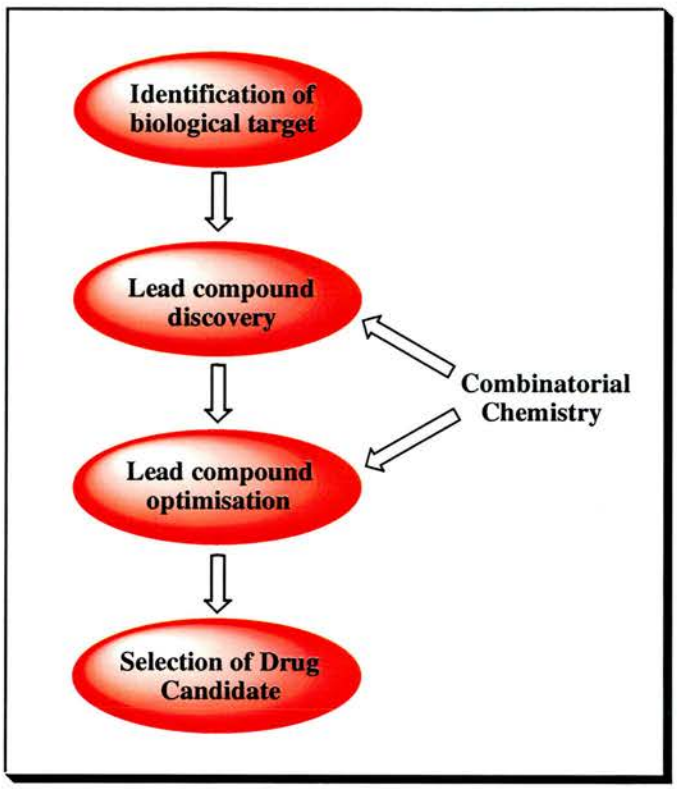

Figure 1.1: *The drug discovery process and the impact of combinatorial libraries.*

1.1.1 The Principles of Combinatorial Chemistry.

In lead discovery, combinatorial synthesis should facilitate the rapid production of as many different structural variants as possible. This method takes its lead from nature, which succeeds in obtaining a large number of products with diverse functionalities, for example peptides and proteins, from only a small number of starting materials, amino acids, by combinatorial principles. Other examples include polysaccharides from sugars and lipids from fatty acids. In nature, only useful, functionally active molecules persist. All of the permutations that do not confer advantage are lost. Thus, synthesis and selection are intimately linked.

The principles behind combinatorial synthesis are very straightforward. In classical organic synthesis, reactions are carried out with one reagent, from different chemical classes, **A** and **B** to obtain a single, if not major, product **A-B**. In the case of combinatorial synthesis, instead of a single compound from the class **A** or **B**, a series of structurally similar compounds of each class, $\mathbf{A^1....A^n}$ and $\mathbf{B^1....B^n}$, are reacted together according to the principle that each of the compounds reacts with all the others, as shown in Scheme 1.1. These reactions can take place simultaneously in a mixture, or in individual reaction chambers or wells.

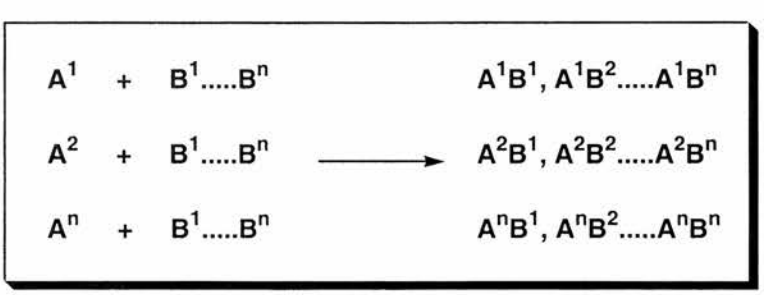

Scheme 1.1: *Principles of Combinatorial Synthesis.*

Starting this synthesis with a group of *n* building blocks **A**, and reacting these with a group of *n'* building blocks **B,** would give us all the possible combinations of products $\mathbf{A^1B^1}$ to $\mathbf{A^nB^{n'}}$. Starting with ten of each building block would give us a total of 100 (*n* x *n'*) products. If this principle is then extended to a multi-step reaction, then

from only a very small number of building blocks, a large number of products can be rapidly synthesised. This principle is shown in Figure 1.2.

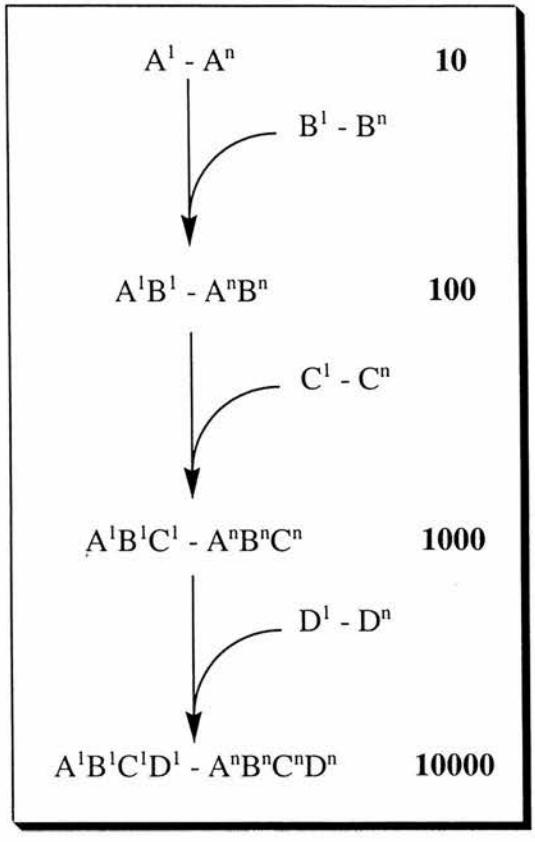

Figure 1.2: *Multi-step Combinatorial Synthesis*

In Figure 1.2, ten structurally similar compounds from four classes **A**, **B**, **C** and **D,** are reacted together to form ten thousand compounds as a mixture. These compounds are collectively known as a library, and in the case of a multi-step synthesis, the magnitude of the library produced is dependent upon two factors. These factors are;

(i). The number of reactants used in each step.

(linear relationship)

(ii). The number of reaction steps.

(exponential relationship)

This process of combinatorial synthesis may be carried out using either traditional solution-phase methodologies, or solid-phase chemistry. Of these methods, the main focus has been on solid-phase chemistry. The reason for this is the ability to

increase the yield of the reactions by using excess reagents, improve the purity of the final compound by eliminating side product formation and also make product isolation as easy as possible. Both approaches to combinatorial library synthesis will now be discussed.

1.1.2 Solution-Phase Combinatorial Chemistry.

The main focus of combinatorial chemistry has been towards the synthesis of compounds on solid supports. However, the synthesis of combinatorial libraries using solution-phase techniques has also been carried out. In solution-phase synthesis, the components can be attached to a rigid central molecular scaffold,[7, 8] and then reactions are carried out on the attached compound. Examples of the scaffolds used are shown in Figure 1.3.

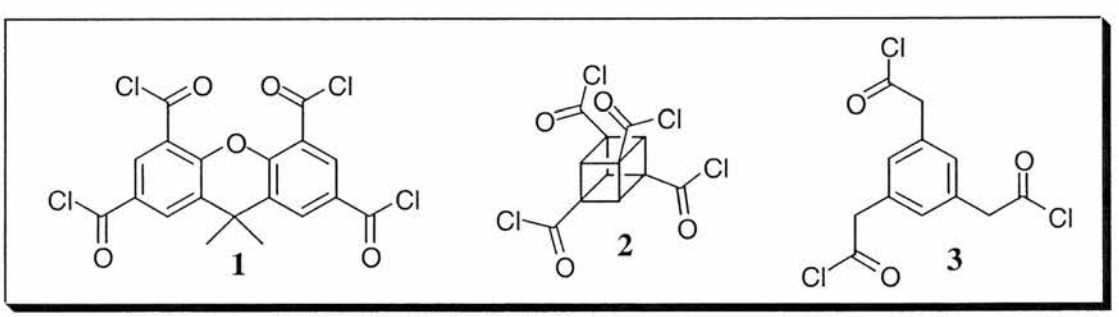

Figure 1.3: *Scaffolds used in solution-phase library synthesis.*

The reactions performed on these scaffolds were amide formation and reactions of isocyanates with amines. These three molecular scaffolds were chosen, as the reactivities of the functional groups are very similar. Also, the distance between the functional groups ensures that the compounds being synthesised on the scaffold have very little steric influence on each other. One interesting point to note with the scaffolds is that as the symmetry of the core decreases, the number of compounds that it is possible to synthesise increases. To show this, if **1,2** and **3** were each reacted with 19 amines, the number of compounds produced would be 65341, 11191 and 1130

respectively. Work with these core molecules has led to the discovery of a trypsin inhibitor, **4**, with a $K_i = 9\mu M$, Figure 1.4.[8]

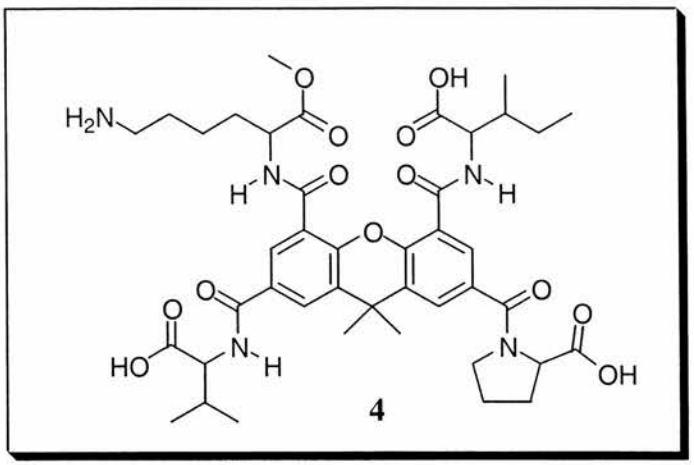

Figure 1.4: *Trypsin inhibitor identified using molecular scaffolds.*

Examples of solution-phase combinatorial syntheses where a core scaffold is not used include the production of a 72 member tetrahydroacridine library by Pirrung,[9] Scheme 1.2 and also the synthesis of a library of 54 carbamates by Smith,[10] Scheme 1.3.

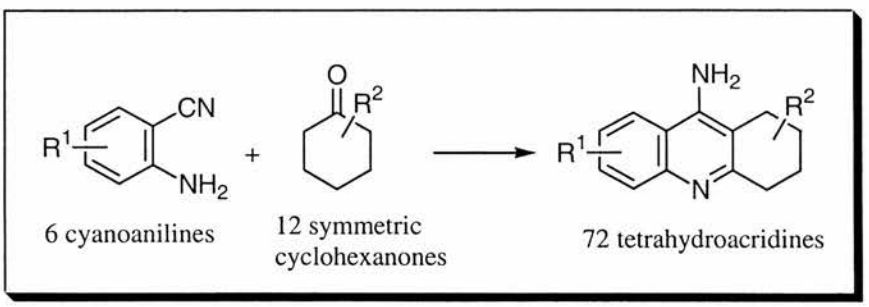

Scheme 1.2: *Solution-phase synthesis of a tetrahydroacridine library*

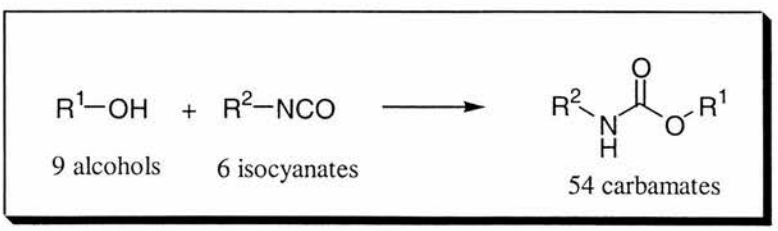

Scheme 1.3: *Solution-phase synthesis of a carbamate library*

The synthesis of libraries using solution-phase methods does hold some advantages over synthesis on solid supports. The major advantage is that existing methodology and established reaction conditions can be used, and also no method of

attaching or cleaving the compounds from the solid supports has to be used or developed.

1.1.3 Solid-Phase Combinatorial Chemistry.

The first reported synthesis on a solid support was carried out by R.B. Merrifield, in 1963.[11] Merrifield described the preparation of the solid-support, now know as Merrifield Resin, by cross-linking styrene, **5**, with 1% divinylbenzene (DVB). The cross-linking gives the solid support a degree of mechanical stability, but still allows the flexibility required when swelling the support prior to, or during a reaction. Polymerisation of the cross-linked styrene gives the solid support, which is then functionalised, Scheme 1.4. Functionalisation of the support may be carried out prior to polymerisation through the use of suitably functionalised starting materials.

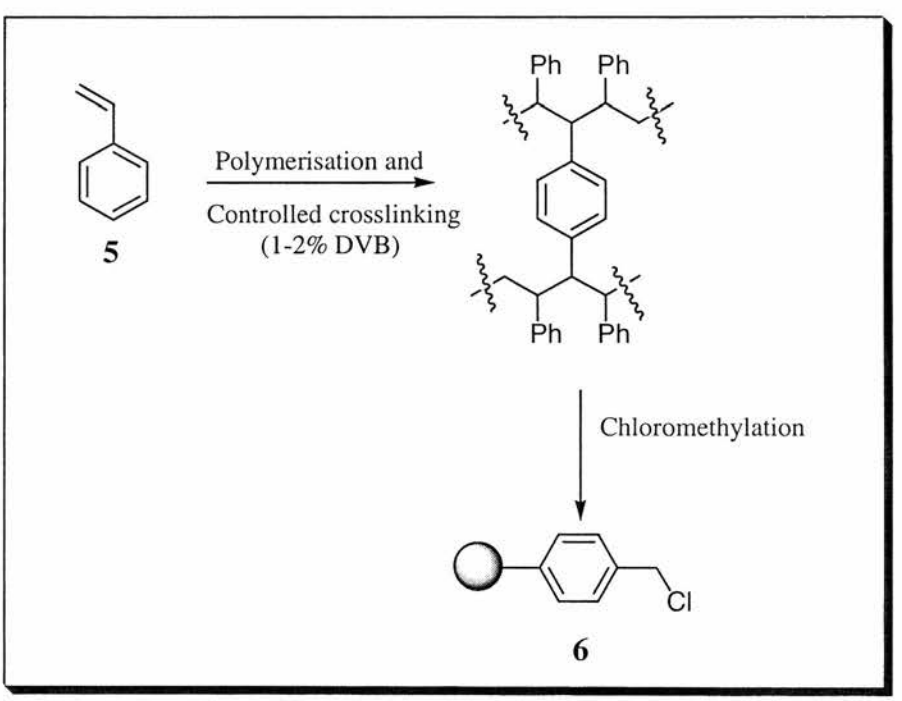

Scheme 1.4: *Preparation of Merrifield Resin.*

In his original work,[11] Merrifield coupled the C-terminus of an N-protected amino acid to the solid support. This was followed by synthesis of a solid-supported tetrapeptide using standard peptide chemistry, Scheme 1.5.

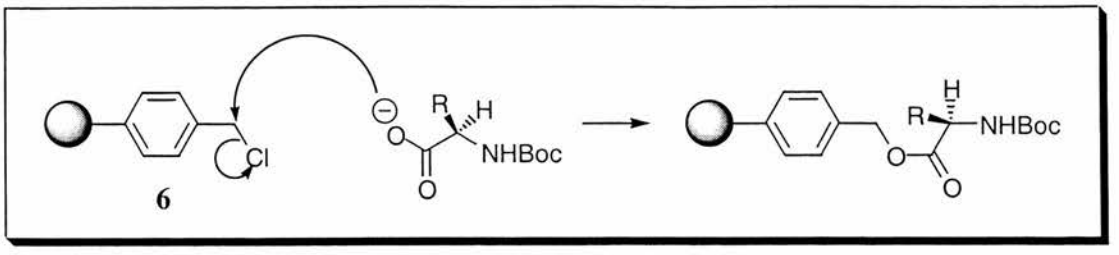

Scheme 1.5: *Coupling to Merrifield Resin.*

The ester bond formed on attachment to the solid support is stable to conditions used in peptide synthesis. The product is cleaved from the solid support under vigorous acid conditions.

The first methods for the combinatorial synthesis of peptides on solid supports were developed in the mid-1980's, by Geysen and Houghten.[12, 13] Geysen described how peptides could be synthesised on polymer supports in numbers that were three orders of magnitude greater than by conventional synthesis. This was achieved by synthesising the peptides on polyethylene rods, onto which had been grafted acrylic acid. The synthesised peptides could then be assayed free in solution, or, still attached to the solid support. This technique is commonly known as the 'Multipin method'.

The method of Houghten is commonly referred to as the 'Tea-Bag method'. Here, small amounts of the solid support are enclosed in labelled, porous polypropylene containers. These are immersed into solutions of amino acids, to couple the amino acids to the solid support. Any deprotection and washing steps all take place in one vessel. The 'Tea-Bags' are then separated for the next synthetic step. The process is repeated until the desired length of peptide chain has been synthesised. Cleavage of the peptide is again achieved using vigorous acid conditions.

With the development of these methods, peptide chemistry was revolutionalised. However, it was not until the work of Furka[14] that the true combinatorial synthesis of peptides became possible. He described a principle known as 'Split and Mix',

Figure 1.5. The appearance of 'Split and Mix' synthesis is considered to be the actual birth of combinatorial chemistry.

In a 'Split and Mix' synthesis, the solid support is divided into x equal portions. Figure 1.5 shows three portions. Each of the portions are treated with a synthetic building block **A** ($\mathbf{A^1}$, $\mathbf{A^2}$, $\mathbf{A^3}$). This approach gives uniform coupling, as any competitive coupling between building blocks has been eliminated. The portions of supports are then mixed together for any deprotection or washing steps, then re-divided into equal portions. The portions now show a statistical distribution of sequences attached to the support. Treatment of these mixtures with a different synthetic building block **B** ($\mathbf{B^1}$, $\mathbf{B^2}$, $\mathbf{B^3}$) gives nine solid-supported permutations. With repetition of the mix, spilt and reaction steps, it can be seen that large numbers of compounds can be rapidly synthesised, with all products in approximately equimolar quantities.

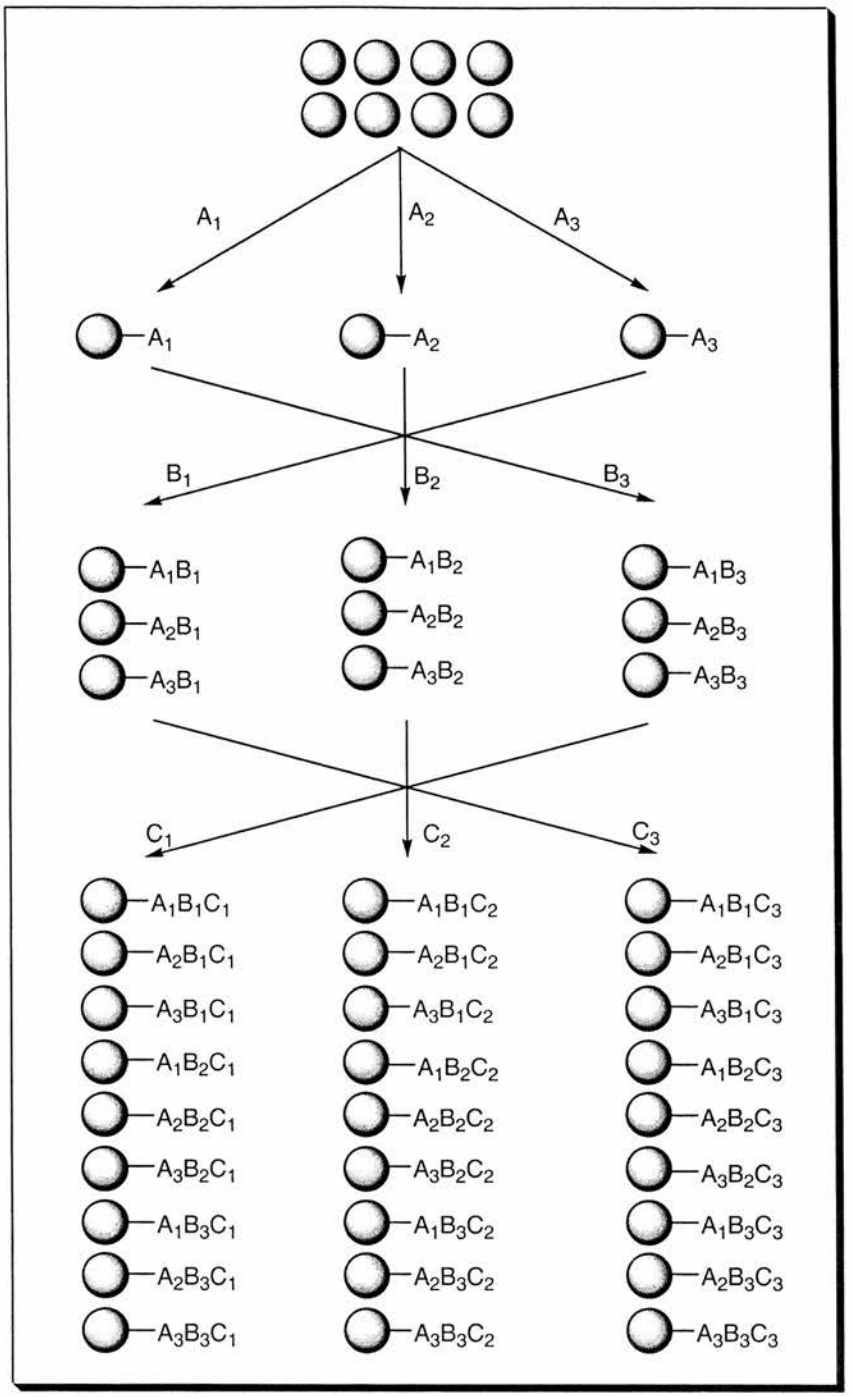

Figure 1.5: *'Spilt and Mix' synthesis of peptides.*

In Figure 1.5, twenty-seven products are formed, in three mixtures of nine compounds. These products have been formed in nine reaction steps from nine building blocks. For the individual synthesis of these compounds, eighty one reaction steps would be required. Using the 'Split and Mix' method with the twenty naturally occurring amino acids, sixty coupling reactions would be required to produce all possible eight thousand tripeptide permutations.

1.1.4. Solution-Phase Synthesis versus Solid-Supported Synthesis.

Synthesis on solid supports holds a number of advantages over conventional solution-phase synthesis.

The rate of reaction can be accelerated through using an excess of the soluble reactant, leading to complete conversion of the solid-supported compound. Complex isolation and purification steps are replaced by simple washing of the solid support, so that excess reagents and any impurities are removed. This subsequently enables the process to be fully automated at each step, even for multi-step syntheses.

However, solution-phase combinatorial chemistry also has advantages that should not be overlooked. Combinatorial synthesis in solution does not require any additional reaction steps to establish linkage to a solid support, or for cleavage from that support. The reactivity and stability of the linker groups do not have to be considered when planning a synthetic route. The biggest advantage is that the reaction conditions do not have to be adapted to solid-supported synthesis. A large number of reactions have now been reported on solid supports.[15-17]

These advantages and disadvantages are outlined in Table 1.1.

Table 1.1: *Advantages and disadvantages of Solution-Phase and Solid-Supported chemistry.*

	Solid-Supported chemistry	**Solution-Phase chemistry**
Advantages	Use excess reagents to drive reaction to completion	Any organic reactions can be carried out.
	Product purification by washing	No adaptation of existing reaction conditions required
	Full automation of all steps possible	No additional reaction steps required (cleavage, linking)
	'Split and Mix' synthesis possible	Unlimited quantity of product can be produced
Disadvantages	Require time to develop synthesis	Cannot use excess reagents without additional purification
	Additional reaction steps required (linkage, cleavage)	Automation of isolation and purification steps is difficult
	Restrictions from support and linker	
	Difficult reaction monitoring	

The nature of the solid supports used, common linkers currently available, methods of analysis and also encoding are discussed in the following sections.

1.2 Solid Supports.

As discussed in Section 1.1.3, the first synthesis on a solid support was carried out by R. B. Merrifield in 1963.[11] In this work, the production of a functionalised solid support, Merrifield Resin, is described, Figure 1.6. This worked earned Merrifield the Nobel Prize for Chemistry in 1981.

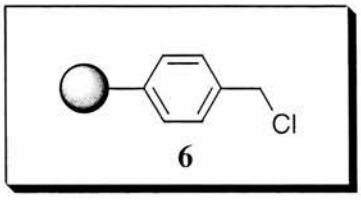

6

Figure 1.6: *Merrifield Resin.*

On this solid support, Merrifield synthesised peptides through the attachment of amino acids to the support, then using standard peptide synthesis to produce a peptide attached to the support.

After Merrifields work, much of the early work in this area was concerned with solid-phase peptide synthesis (SPPS). Recently, work has moved towards the generation of small organic molecules on the supports, termed solid-phase organic synthesis (SPOS) or solid-phase organic chemistry (SPOC).

When performing SPOS or SPOC, there are three considerations to be made in choosing the solid support for the synthesis.

(i). The solid support should be insoluble, and inert to the reaction conditions.

(ii). The molecule is linked to the solid support by a linker that facilitates easy cleavage from the support.

(iii). The synthetic procedure should be compatible with the support and linker at all times.

There are many different types of available solid supports, with the majority based on the PS/DVB co-polymer, as described by Merrifield, Table 1.2.

Table 1.2: *Commonly used solid supports and their properties.*

Solid Support	Properties
PS/DVB co-polymer	Good swelling, limited thermal stability
Polyamide Resin	Good swelling in polar solvents
TentaGel™	Polar resin, pressure stable, swells in H_2O, MeCN, MeOH, DMF, DCM
MultiPins (polyethylene rods)	Grafted acrylic acid pins
Controlled Pore Glass	Pressure & heat stable, low loading

Some of the types of solid supports are discussed below.

1.2.1. Polystyrene-Divinylbenzene (PS/DVB) co-polymers.

Merrifield Resin is a PS/DVB co-polymer. DVB is added during the polymerisation step to link the floppy polystyrene chains together. This gives a greater degree of mechanical stability. The cross-linking also makes the solid support insoluble, an important feature in solid-supported synthesis. This essentially makes the polymer bead one single macromolecule. There are two main classes of solid-supports. These are known as macroporous supports and gel-type supports. Of these, it is the gel-type supports that show significant degrees of swelling when suspended in a suitable medium. The macroporous supports possess little or no swelling abaility.

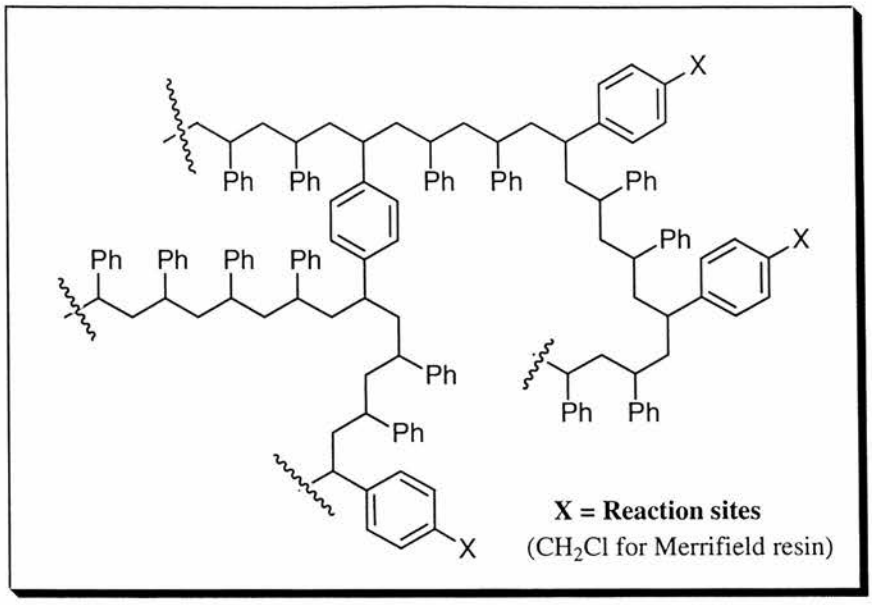

Figure 1.7: *Structure of polystyrene.*

However, this cross-linking is not sufficient to prevent swelling of the solid support in the reaction medium. The swelling of the solid support is an essential feature in these resins, as it demonstrates flexibility of the polymer backbone. This flexibility is required to allow movement of solid-supported compounds in order to maximise the availability of the functionality present on the compound. The swelling property also allows free diffusion of any solvents and reagents into the solid support, aiding accessibility to the reaction sites. The swelling properties of PS resins with common organic solvents has been investigated.[18] Some work carried out using PS solid supports has indicated that the resin is not completely inert during the course of a reaction.[19] After synthesis, analysis of the compound shows the presence of impurities from the solid support. Investigations into removing these impurities found that pre-washing the support before a reaction reduced the level of impurities. The solid support was also exposed to the strong acidic cleavage conditions before synthesis, again to remove excess impurities. However, the impurities returned, due to the general degradation of the polystyrene backbone of the solid support.

One drawback in synthesis on solid supports is the possibility of site-site interactions within the polymer framework. This can cause problems when synthesising peptides on supports at high loading levels. At high levels of loading, interactions between the peptide chains on the support can occur, due to the hydrophobicity of the polymer backbone, and the hydrophilicity of the peptide chain. These interactions can have significant effects on the synthetic efficiency of the reaction. The hydrophobicity of the support causes the peptide chain to fold, reducing the availability of the free end of the peptide chain.

This problem has led to the design and development of a new class of solid supports. It was hoped that this new class of supports would mimic the properties of the peptide.

1.2.2. Polyamide Supports.

The polyamide supports were expected to mimic the properties of peptide chains,[20] and also have improved characteristics in polar solvents such as DMF and NMP, which solvate peptide chains. The constituents of a polyamide support are shown in Figure 1.8.

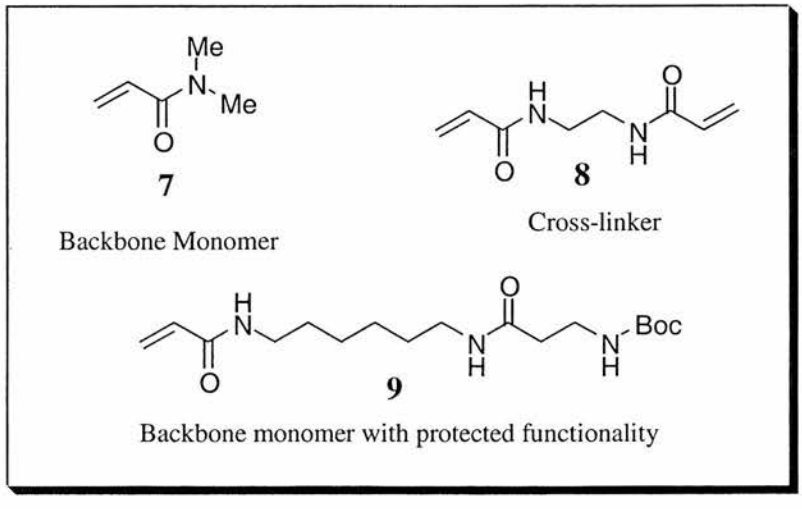

Figure 1.8: *Monomer units of a polyamide support.*

Polyamide supports with different polymer backbones have also been investigated. Replacing *N,N*-dimethylacrylamide with *N*-acryloylpyrrolidine as the backbone monomer gives a solid support that swells in water, ethanol and methanol, Figure 1.9.[21]

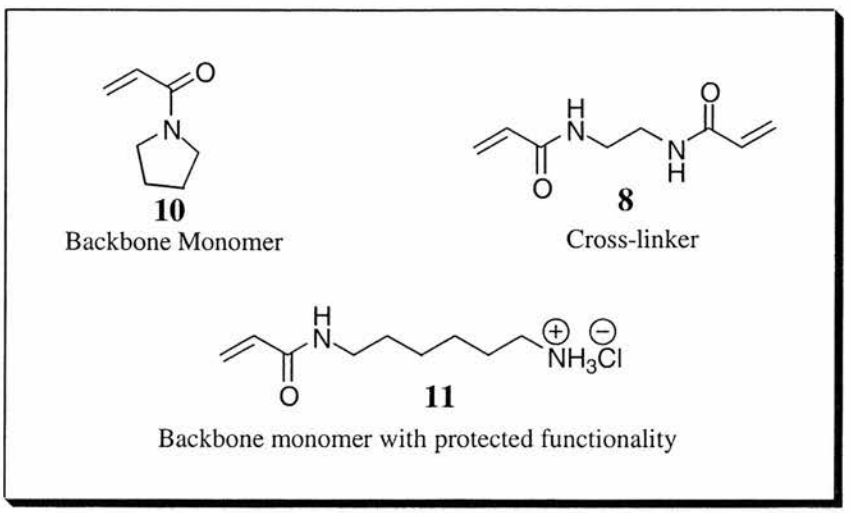

Figure 1.9: *Alternate backbone monomers for polyamide support.*

1.2.3. TentaGel Supports.

Another solid support to have a dramatic effect on solid-phase synthesis is the TentaGel resin. The resin is constructed from polyethylene glycol (PEG) attached to a cross-linked polystyrene support, through an ether link, Figure 1.10.

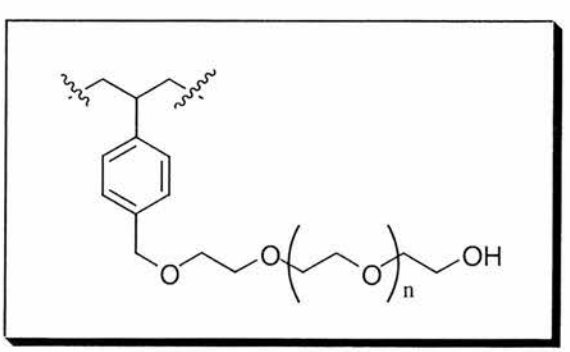

Figure 1.10: *TentaGel Resin.*

The resin has the benefits of a soluble PEG support,[22] combined with the characteristics of the polystyrene support. The resin was prepared from the

polymerisation of ethylene oxide on cross-linked polystyrene, previously derivatised with tetraethylene glycol, giving the PEG chains shown in Figure 1.10. The resins generally carry PEG chains with a molecular weight of around 3000 Da, however, the loading level of the resin, 0.2-0.4 mmol g^{-1} is lower than that commonly seen with cross-linked PS supports, 0.5-1.2 mmol g^{-1}. The environment within the support closely represents that of diethyl ether and THF, commonly used solvents in solution-phase synthesis, and so has the potential to be used for a large range of reactions when synthesising a compound library, where the use of polystyrene supports is not practical. One example of this is the synthesis of a library of β-turn mimetics by Ellman.[23] This work could not be carried out on PS/DVB supports, as the support did not swell in the aqueous reaction conditions.

1.2.4. Controlled Pore Glass (CPG) Supports.

One drawback in using the polymer supports described in this section is that they all behave differently dependent on the solvent being used for the reaction. Different solvents swell the polymers to different degrees, having effects on the reaction rates, coupling efficiency and general accessibility to reaction sites. Many of these disadvantages can be overcome by the use of an inorganic support, such as controlled pore glass. With CPG, the accessibility to reaction sites is not dependent on the reaction medium. The support is rigid, incompressible and allows for high flow rates, hence applicability to continuous flow synthesis. The support is very stable, and can be reused. The preparation of such a support, **12**, was reported by Eby and Schuerch,[24] Scheme 1.6.

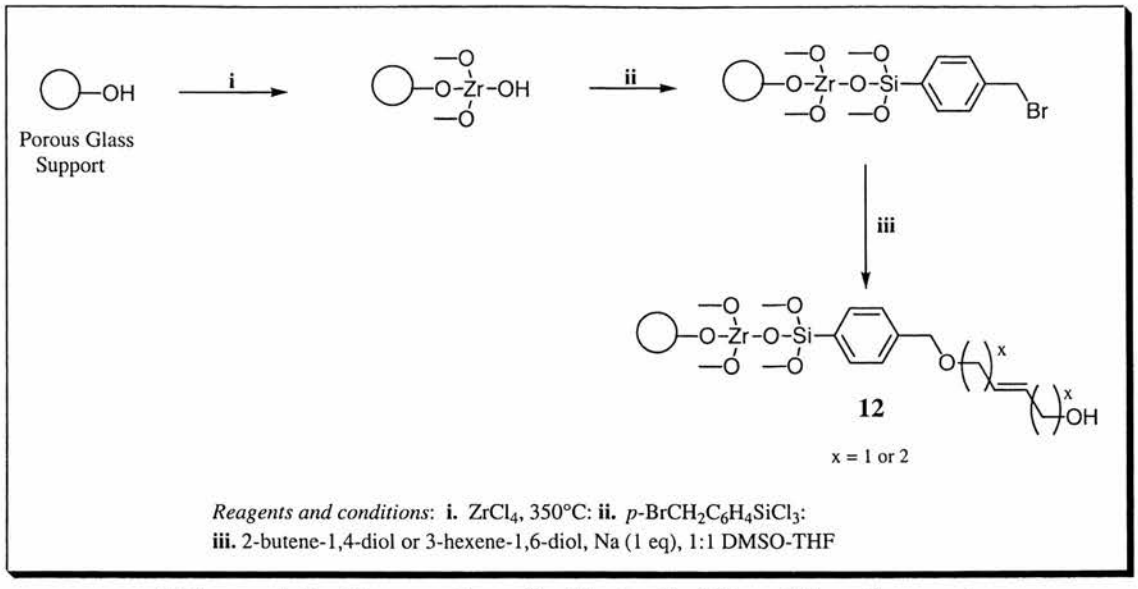

Scheme 1.6: *Preparation of a Controlled Pore Glass Support.*

Initially, this support contained silicon-oxygen-silicon bonds. However, it was found that these bonds were not stable under basic conditions, and so were replaced with silicon-oxygen-zirconium bonds. Coupling of a saccharide to the support was then attempted, with the yield determined by the weight gain of the support. The best coupling yield observed was 20%. As the reason for the low conversion was not known, it was thought that CPG could not be used in solid-phase synthesis of oligosaccharides. Another attempt at using CPG in oligosaccharide synthesis was attempted by Heckel *et al.*.[25] They looked at using a different linker system between the support and the first sugar residue, and developed mercaptopropyl functionalised controlled pore glass (MP-CPG), **13**, Scheme 1.7.

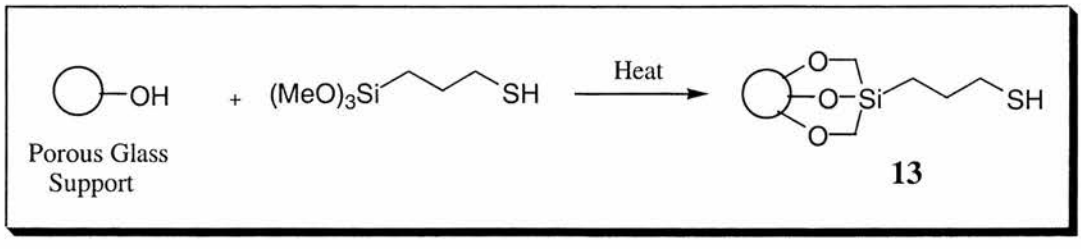

Scheme 1.7: *Mercaptopropyl-Controlled Pore Glass Support.*

This support gives a thioglycosidic link to the first sugar residue which is resistant to the conditions used in extending the oligsaccharide chain length. The linker

can also be selectively cleaved with no affect on the synthesised compounds. The support was found to have a loading of the free thiol groups of 0.3 mmol g^{-1}, and was successfully used in the solid-supported synthesis of oligosaccharides.

1.2.5. Fluoropolymer Supports

Due to limitations with polystyrene based solid supports, Gani and co-workers evaluated the potential of more stable polymers, including ones containing perfluorocarbon backbones.[26, 27] The thermal, mechanical and chemical stabilities of polytetrafluoroethylene (PTFE) are well established, and appear to be ideally suited for SPOS applications. However, the preparation of suitably functionalised perfluorinated supports is extremely difficult, due to the high toxicity and explosive nature of the monomer, tetrafluoroethylene (TFE). Initial work used Nafion®50NR, **14**, a co-polymer of TFE and trifluorovinyl ethers, in the synthesis of sulfonamides. This form of Nafion® has a sulfonic acid functionality present on the polymer side-chains, so that reactions may be carried out on the support. Reaction of the activated support with the dye Disperse Orange 11 gave a highly coloured sulfonamide, **15**, Scheme 1.8.

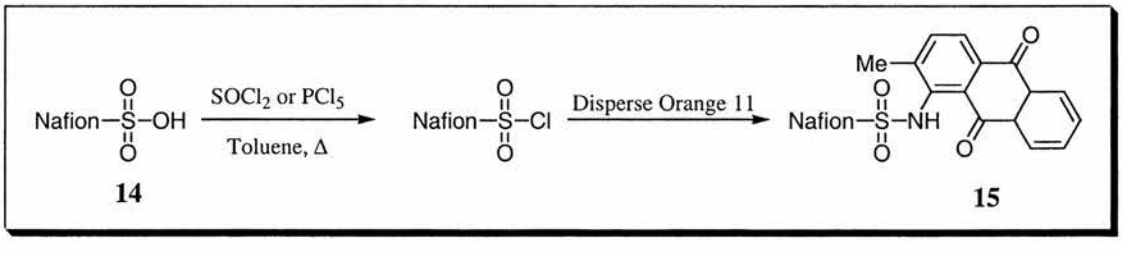

Scheme 1.8: *Synthesis of sulfonamides on Nafion®.*

From this work it was evident that fluoropolymers offered considerable potential as SPOS supports. However, the combination of non-lipophilic side chains and polar functional groups, which do not allow the support to swell in organic solvents and the low loading levels of Nafion® make this solid support unattractive. Alternative polymers possessing a perfluorinated backbone and lipophilic side chains were

investigated. The first example was based on poly(α,β,β-trifluorostyrene), (PTFS),[26] an analogue of polystyrene, Figure 1.11.

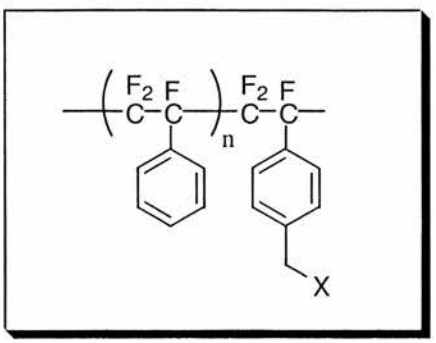

Figure 1.11: *Perfluoropolymer based on poly(trifluorostyrene).*

The PTFS polymers are thermally stable and DSC analysis showed no observable T_g or T_m. At about 350°C, the polymer began to show signs of decomposition, so the support can be used over a large temperature range. The support either swelled, or was soluble in a range of solvents, making its use in liquid-phase organic synthesis a possibility. The accessibility of the functional sites to reaction was tested by reaction with 4-fluorophenol, using real-time *in-situ* NMR spectroscopy. The rate of the reaction was found to be comparable to the same reaction on Merrifield Resin.

Another reported fluoropolymer support is polystyrene grafted fluoropolymer MicroTubes, by IRORI and Illumina, Inc..[28] These were developed for use in conjunction with their encoding strategy, section 1.5. The MicroTubes were immersed in a solution of styrene, methanol and mineral acid, and then γ-irradiated with a ^{60}Co source to radiolytically graft the polystyrene to the fluoropolymer.[29-31] Following aminomethylation of the grafted polymer,[32] a large variety of linkers may be attached to the support. The support was used in reactions at elevated temperatures, notably a [4+2] cycloaddition between a supported alkene and 1-phenylbutadiene at 145°C.[28] Under these reaction conditions, polystyrene and polyethylene glycol based supports would rapidly disintegrate.

1.3 Linkers used in Solid-Phase Synthesis.

As has already been discussed, the molecule to be synthesised is attached to the solid support through a cleavable linker group. A linker is described as a bifunctional protecting group, as it is attached to the molecule being synthesised through a cleavable bond, and also to the solid support through a bond that is more stable to reaction conditions. Linkers perform many similar functions to protecting groups, and the majority of new linkers developed have been based on solution-phase protecting groups. Other linkers fall into a broader definition, as a connection between the solid support and the molecule being synthesised. An ideal linker would have to satisfy certain criteria:

- Readily available and inexpensive
- Attachment to linker is easy and high yielding
- Stable to reaction chemistry
- Efficient cleavage that does not affect product
- Cleavage method should not introduce impurities

Many of the current available linkers do not pass all of the criteria. In some cases, the method of attachment is difficult, and the cleavage conditions are usually too strong. This is a situation that has to be rigorously addressed before any attempt is made at synthesising a library. As the number of reactions carried out on solid-phase has increased over the last few years, so has the number of linkers.[33-39] The next section outlines some of the more common linkers in current use.

1.3.1 Acid Labile Linkers.

Peptides attached to Merrifield resin form a very stable ester bond to the solid support.[11] This ester bond is cleaved by treatment with hydrogen fluoride (HF). This gives high purity products, in good yield. Due to the volatility of HF, excess reagent is easily removed. However, low temperatures and short reaction times are advised to avoid side reactions.[40] Trifluoromethanesulfonic acid (TFMSA) has also been used to cleave peptides from Merrifield resin.[41] The need for special glassware as with HF is eliminated, but TFMSA is non-volatile, so removal is difficult. However, the ester linkage is not 100% stable to treatment by TFA.[42] In the synthesis of ribonuclease A, 1.4% of the peptide chain was lost after each deprotection step.[40] Sparrow[43] believed this loss was due to incomplete coupling, arising from hindrance of the peptide from the polystyrene backbone of the support. He inserted a spacer between the first residue and the point of attachment to the support, Figure 1.12. Using this spacer and linker, a 3-fold increase in the yield of a 19-residue peptide was observed.

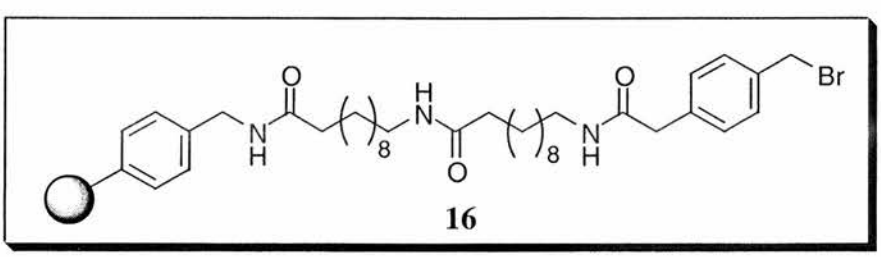

16

Figure 1.12: *Sparrows linker and spacer group.*

Merrifield suggested that the loss of material after each deprotection step was due to partial cleavage, rather than incomplete coupling. He prepared a phenylacetamidomethyl (PAM) linker,[44] **17**, Figure 1.13. This linker made the ester bond 100 times more stable to the cleavage conditions relative to the ester formed on Merrifield resin.[45]

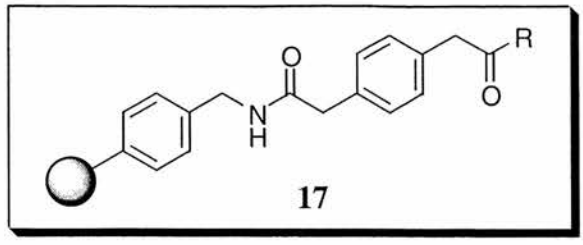

17

Figure 1.13: *PAM linker.*

The hazardous nature of HF cleavage has led to the production of new linkers that require mild conditions for cleavage. The sensitivity of a linker to acidic cleavage conditions relates to the stability of the carbocation formed on cleavage. Therefore, the inclusion of electron donating groups in the linker should decrease the strength of acid required for cleavage. This has led to the inclusion of alkoxy groups and phenyl groups in the linker. Wang[46] described a *p*-benzyloxybenzyl alcohol linker, **18**, Figure 1.14, which allows cleavage of peptides from the support using TFA. Used in conjunction with Fmoc protection, the Wang linker is widely used in SPPS and SPOC.

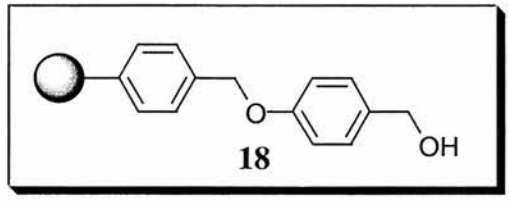

18

Figure 1.14: *Wang Linker*

This linker can be converted into the chloro,[47, 48] bromo,[48, 49] or iodo[49] derivatives, providing variations of the standard Merrifield resin. The SASRIN linker is linked to the support through an ether bond, **19**, Figure 1.15, and is formed by the addition of a methoxy group to the Wang linker. Compounds attached via this linker can be cleaved using 1% TFA.

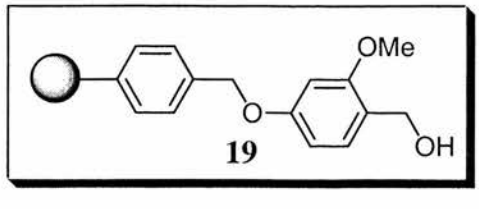

19

Figure 1.15: *SASRIN Linker.*

The introduction of alkoxy groups onto a benzhydryl system led to linker, **20**, a *p*-methoxybenzhydrylamine linker.[50] A similar linker was reported by Brown,[51] **21**, who named it MAMP (Merrifield α-methoxyphenyl), and used it in the synthesis of secondary amines.

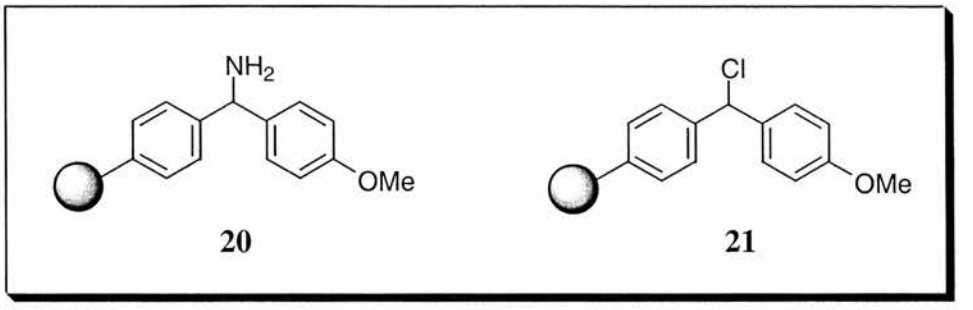

Figure 1.16: *Benzhydryl linkers.*

The inclusion of additional alkoxy groups gives the Rink linker, Figure 1.17.[52] This system allows the cleavage of peptides under extremely mild conditions, 0.2% TFA. The Rink linker is so sensitive to acid that coupling with HOBt required buffering with DIPEA.

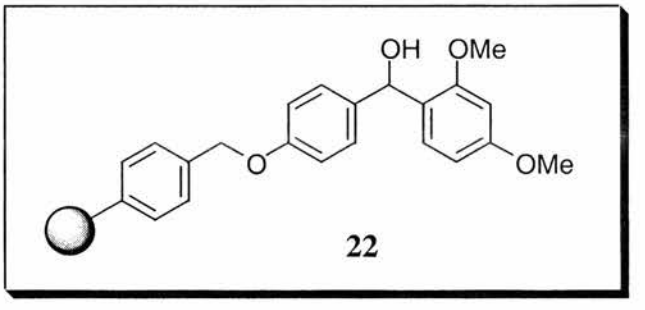

Figure 1.17: *RINK Linker.*

Trityl linkers were initially developed as insoluble protecting groups for the monoprotection of symmetrical molecules.[53-55] Later, the trityl chloride linker, **23**, was used to immobilise amino acids.[56] Cleavage was carried out using *p*-TsOH in THF, 1M HCl in THF, or 2% TFA. A range of trityl linkers are currently commercially available, **23-27**, Figure 1.18.

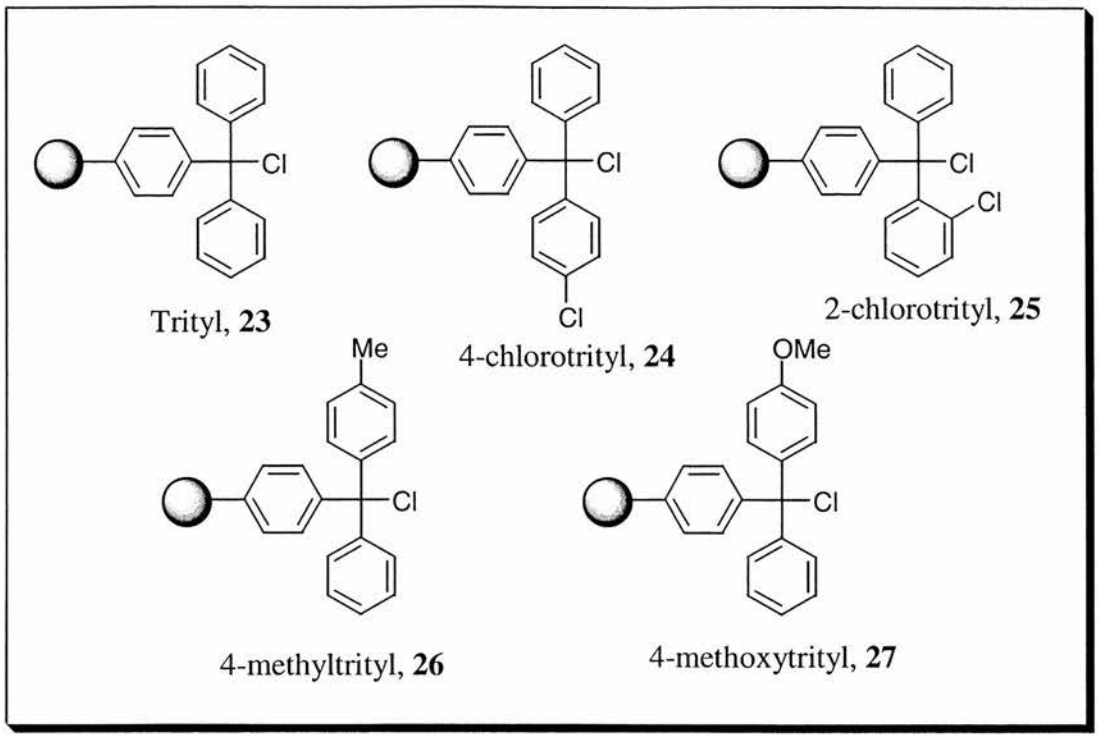

Figure 1.18: *Trityl Linkers.*

1.3.2. Base Labile Linkers.

The REM (REgenerated resin and Michael addition) linker, **28**, was developed for the synthesis of tertiary amines.[57] This was achieved through Michael addition of a secondary amine to an acrylate resin. The amine is then quaternarized by alkylation with a variety of alkyl halides, and treated with base to give the tertiary amine product *via* a Hoffman elimination, Scheme 1.9.

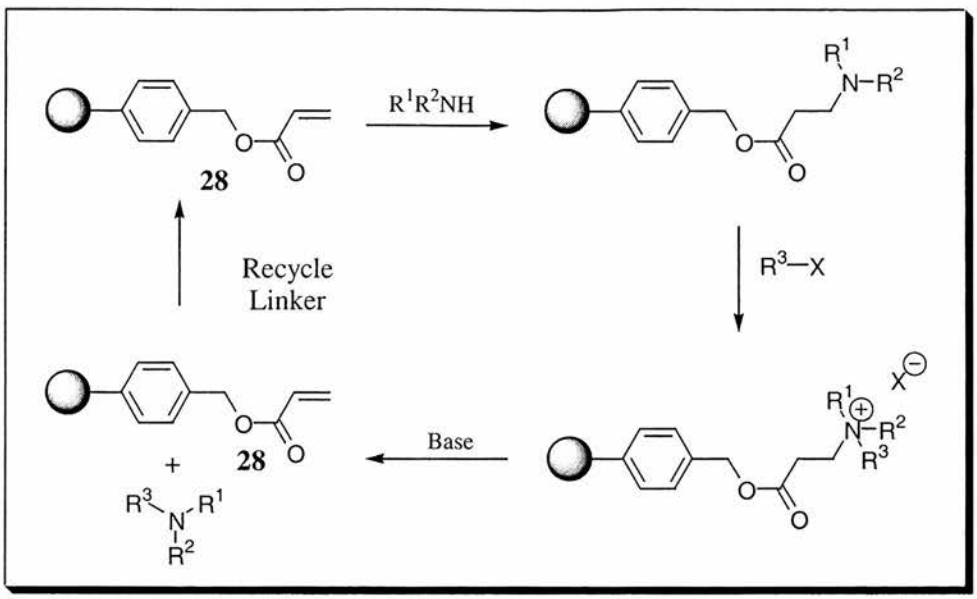

Scheme 1.9: *Synthesis of tertiary amines using REM resin.*

Vinyl sulfone linkers, **29-31**, have been developed as alternatives to the REM linker, Figure 1.19.[36, 58]

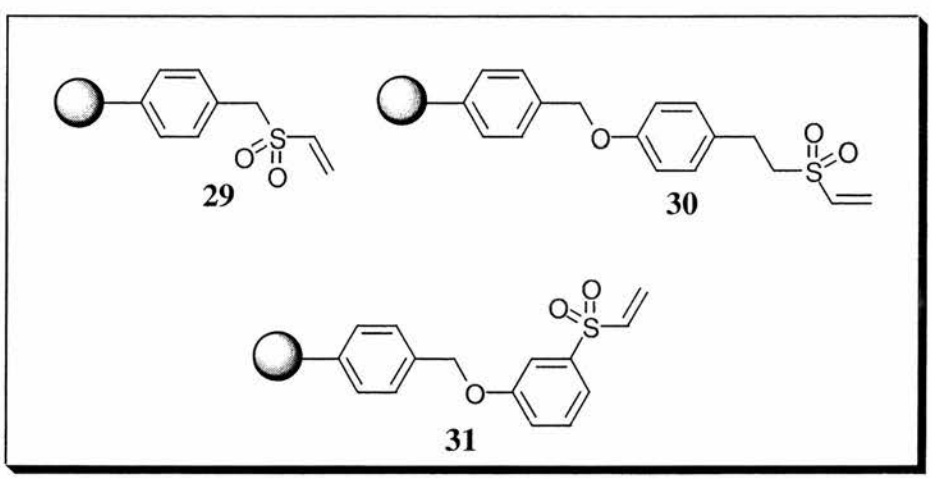

Figure 1.19: *Vinyl sulfone linkers in solid-phase synthesis.*

As with the REM linker, the vinyl sulfones are recyclable and can be used repeatedly with high purity. Sulfone linkers have also been used in heterocyclic chemistry, Scheme 1.10.[59]

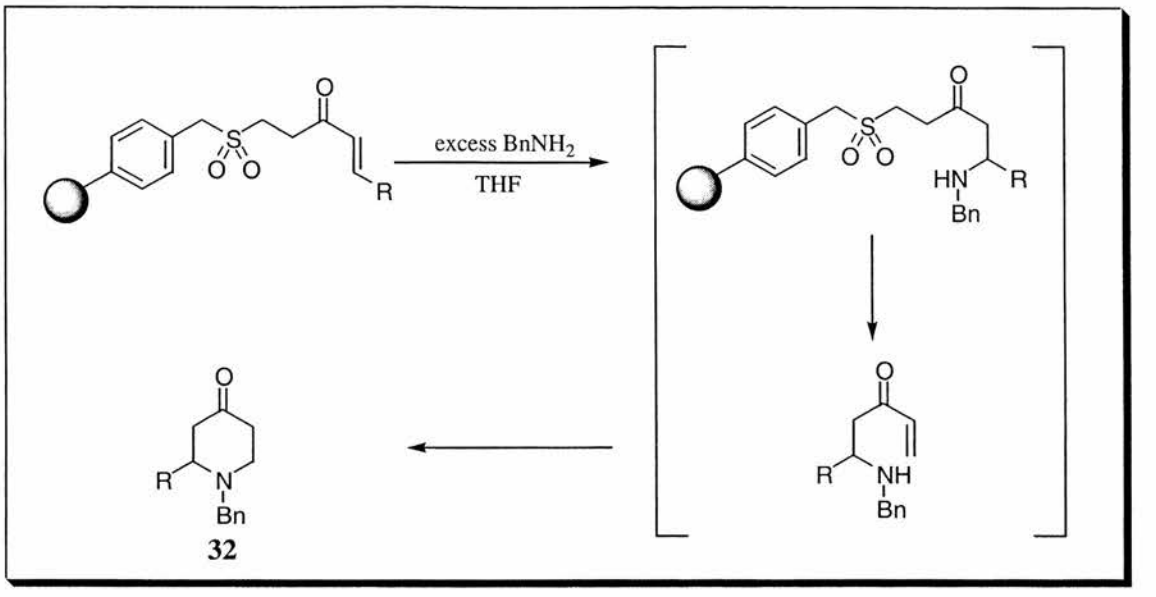

Scheme 1.10: *Sulfone linkers in synthesis of heterocycles.*

In Scheme 1.10, benzylamine behaves as a nucleophile in a Michael addition to the linker, then as a base, inducing elimination of the compound from the support. A second Michael addition then gives the 2-substituted-*N*-benzylpiperidin-4-ones, **32**, in moderate yields.

1.3.3. Traceless Linkers.

After cleavage of a synthesised molecule from a solid support, functionality is usually left on the molecule, at the point of attachment, which is not always desirable. This has led to investigations of linkers that leave no functionality behind, so called 'traceless linkers'.*

The most common of this type of linker is the aryl silyl linker. Silicon attached to a phenyl group undergoes a protodesilylation reaction under acid conditions, cleaving the silicon-carbon bond. The first linkers of this type were produced by Ellman, **33**,[37] and Veber, **34**,[60] Figure 1.20.

* A traceless linker is defined as one where a new carbon-hydrogen or carbon-carbon bond is formed at the linkage site of the cleaved material.

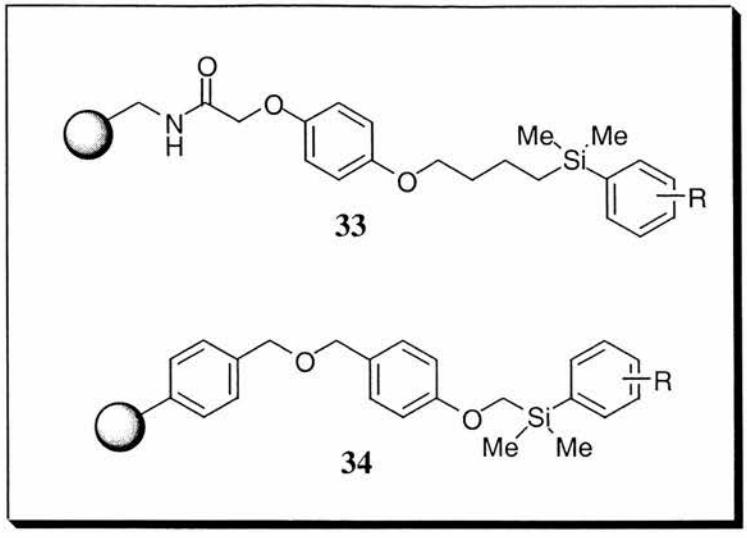

Figure 1.20: *Aryl silyl linkers of Ellmad and Veber.*

Linker **33** has been used in the synthesis of a benzodiazepinone library,[37] while linker, **34**, has been used to demonstrate palladium catalysed couplings to aromatic rings.[60]

1.3.4. Photocleavable Linkers.

Photolysis is a mild method of cleavage, carried out under neutral conditions. The use of photocleavable protecting groups in synthesis has been limited by the sensitivity of molecules to irradiation. The linker should absorb the radiation, so the molecule is not altered in any way. The first use of a photocleavable linker was carried out by Rich.[61] The linker, **35**, Figure 1.21, was prepared by nitration of 1% cross-linked PS support. However, over nitration gave only moderate yields. Another linker, **36**, Figure 1.21, was prepared by coupling 3-nitro-4-bromomethylbenzoic acid onto 1% cross-linked PS support. Boc-protected peptides were released from this linker by irradiation at 350 nm.

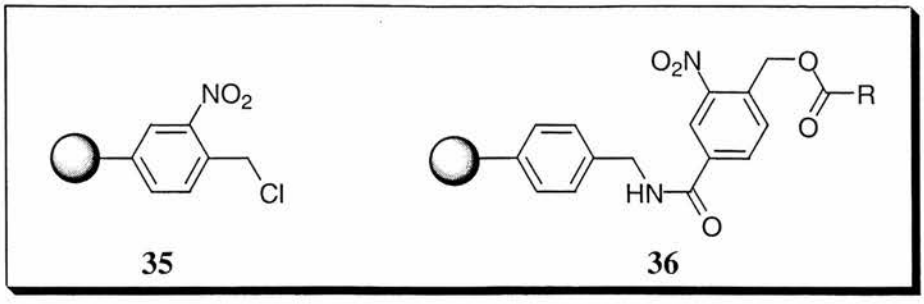

Figure 1.21: *Examples of photocleavable linkers.*

The low yield of the cleavage reaction can be addressed by using α-substituted *o*-nitrobenzyl linkers,[62] Figure 1.22. Two of these linkers, **37** and **38**, have been used in peptide synthesis,[63, 64] and give higher yields, due to better photocleavage efficiency compared to *o*-nitrobenzyl linkers.

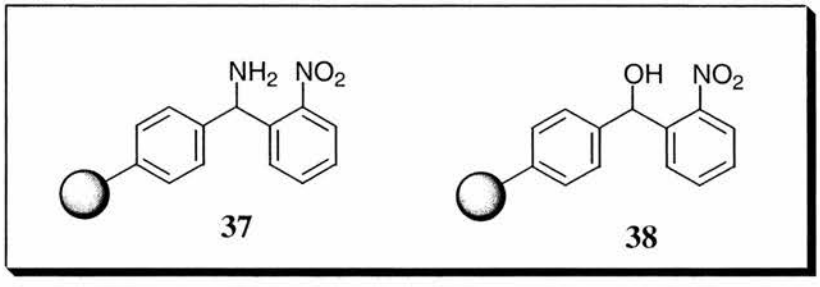

Figure 1.22: *α-substitued* o-*nitrobenzyl linkers.*

An increase in the photolysis yield has also been observed for the phenacyl linker,[65] **39**, Figure 1.23.

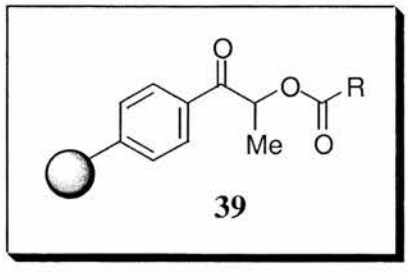

Figure 1.23: *Phenacyl linker showing improved photolysis yield.*

Other photocleavable linkers include the NpSSMpact linker, **40**, developed by Sucholeiki.[66, 67] The linker is attached to TentaGel resin, deprotected then alkylated. Upon irradiation at 350nm, tolyl formation takes place. However, the use of this linker

appears to be restricted to the formation of *p*-phenyltolyl products. With other groups in the *para* position, irradiation leads to formation of the disulfide product, Scheme 1.11.

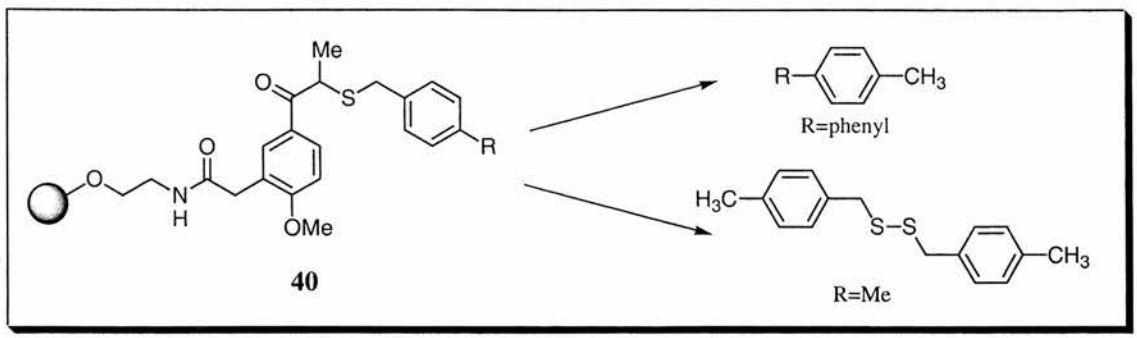

Scheme 1.11: *Cleavage products from NpSSMpact linker.*

1.4 Analysis of resin-bound species

As combinatorial chemistry and solid-phase synthesis have made rapid advancements, the analytical techniques required to support developments in the area have improved. Every reaction carried out on solid-phase has to be monitored in some manner, to assess the progress of the reaction. Knowing how fast a reaction occurs, and when an end-point has been reached allows the optimisation of reaction yields and aids scale-up work. In a classical solution-phase organic reaction, **A** reacts with **B** to form a product **C** and possible side product **D**, Scheme 1.12. Here, x ranges from 0-1 equivalent of the reacting species.

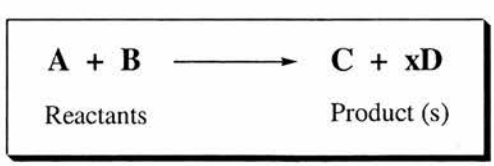

Scheme 1.12: *A Classical Solution-Phase Reaction.*

This reaction may be followed by observing changes in colour, pH, or by following the appearance or disappearance of any of the individual components. The most useful methods for following reactions in solution are thin layer chromatography (TLC), gas chromatography (GC), liquid chromatography (LC), infrared spectroscopy (IR), ultraviolet/visible spectroscopy (UV/vis), nuclear magnetic resonance

spectroscopy (NMR) and mass spectrometry (MS). Samples can be removed from the reaction mixture, or, can be monitored directly, as in the case for NMR spectrometry. However, monitoring any reaction carried out on a solid support is much more challenging. In a typical reaction on solid-phase, the reacting species **A** is covalently attached to the solid support through a linker, and reacted with **B**, which is in the solution-phase, Scheme 1.13.

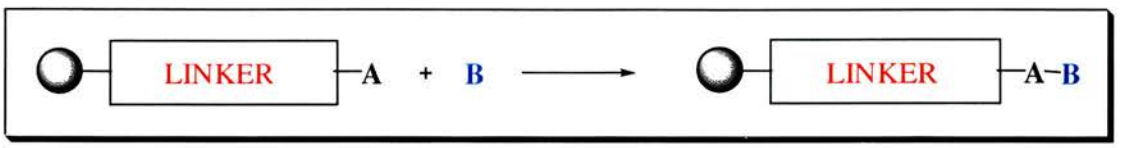

Scheme 1.13: *A Solid-Phase Supported Reaction.*

As **A** is attached to the solid-support, it is difficult to follow its conversion by conventional methods, for example, by TLC. Moreover, how much of species **A** is available to take part in the reaction depends acutely on the efficiency of previous chemical steps and the loading capacity of the solid-support. The reactant **B** and any other reagents are usually present in large excesses, such that its change in concentration does not reflect the full extent of the conversion to **A**.

Probably the most common method for monitoring reactions is the small scale cleavage of resin bound intermediates and subsequent analysis of the released material by conventional solution-phase methods. This process is very time consuming, so to save time, the process has been automated.[68]

Another useful method is the semi-quantitative analysis of functional groups on the solid-support. The appearance or disappearance of certain functional groups is monitored by colorimetric tests. Of these tests, the Kaiser test[69] is probably the most widely used, to detect primary amines on a solid support. This allows the determination of the extent of reaction for an amino acid coupling step, thus avoiding the formation of incomplete peptide chains. The method is both rapid and sensitive, indicating whether ≥99% of the terminal primary amino groups have reacted. In another method, described

by Reddy and Voelker,[70] the initial loading level of an amine functionalised resin is determined by reaction with 4,4′-dimethoxytrityl chloride (DMT-Cl). Subsequent treatment with mild acid results in the liberation of the DMT cation, **41**, which can be measured spectrophotometrically. The resin is then coupled with a Boc-protected amino acid, and the amine groups which failed to couple are quantified by repeating the tritylation/detritylation reactions.

The authors claim this method to be more sensitive than the Kaiser test. Both methods of analysis detect the presence of primary amines. Another method uses nitrophenylisothiocyanate-*O*-trityl (NPIT)*, **42**, for monitoring less reactive amines on solid supports during combinatorial synthesis.[71] The reagent consists of an activated isothiocyanate functionality which reacts with the solid-supported amine, Scheme 1.14.

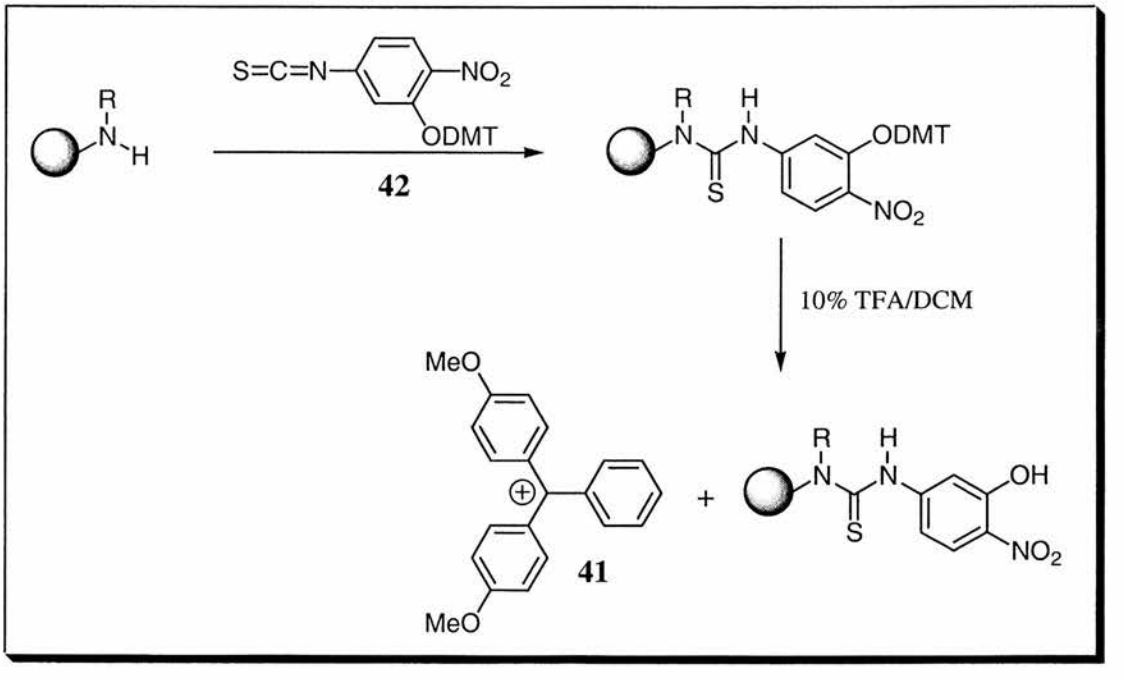

Scheme 1.14: *Reaction monitoring with NPIT*

The trityl ether is then released through treatment with mild acid and measured spectrophotometrically as in the method of Reddy and Voelker.[70] With the exclusion of amines, very few functional groups have been quantified on the solid-phase. However,

* IUPAC nomenclature 3-(4,4′-dimethoxytrityl)-4-nitrophenyl isothiocyanate.

the extent of thiol production during the synthesis of β-turn mimetics has been quantified using Ellman's reagent.[23, 72]

Significant efforts have been made more recently to adapt common spectroscopic analytical techniques, such as IR, MS and NMR, for the analysis of resin-bound organic compounds. Success would provide convenient methods for monitoring and optimising reactions rapidly. Some important advances are discussed below.

1.4.1 NMR. Spectroscopy for resin-bound species.

Two methodologies exist for monitoring reactions on solid supports using NMR techniques. These are gel-phase NMR spectroscopy and magic angle spinning (MAS) NMR spectroscopy.

1.4.1.1 Gel-Phase NMR Spectroscopy.

Gel-phase NMR spectroscopy is normally performed on the resin-bound compound as a slurry, with conventional NMR solvents, in a standard NMR tube. This method has the advantage that it is non-destructive, such that the sample can easily be recovered after analysis. Since the resin-bound compound is in the form of a slurry, there are three important practical considerations concerning the physical stability of the sample during the NMR experiment that have to be addressed. Firstly, the density of the solvent used to swell the solid support must closely match the density of the support. If this is not the case, then the solid support will tend to float or sink. The second consideration is the solvation of the resin in the NMR solvent, leading to problems occurring from the heterogeneity of the gel-phase sample. If the resin beads are not uniformly solvated, differences in the magnetic susceptibility throughout the sample result in line broadening of signals. This limits the technique to nuclei, such as ^{13}C, ^{19}F

and ^{31}P, which all have large chemical shift dispersions. The final consideration is the position of the solid support, within the NMR tube, in relation to the NMR receiver coils. If the resin beads tend to float or sink, the number of beads within the instrument's coils will be very small, giving very little or no information. One solution to this is to overload the gel-phase sample with resin beads. However, the amount of material required for this is significantly greater than is actually required.

1.4.1.1.1 ^{13}C-Gel-Phase NMR Spectroscopy.

One of the earliest applications of ^{13}C gel-phase NMR to combinatorial synthesis was in its use to monitor the growth of a peptide chain on a solid support.[73] The signals for most of the peptide side chains were observed, together with those for the *tert*-butyl protecting group. As the presence of the *tert*-butyl signal was easy to detect, the protection/deprotection reaction was easy to follow, allowing rapid reaction optimisation. The application of ^{13}C gel-phase NMR spectroscopy to solid-phase organic synthesis was first reported in 1980, when it was used in the quantification of CH_2Cl and CH_2OH groups present on the solid support.[74] This work was then extended to show that ^{13}C NMR data could be obtained from polymer-supported diols and insect pheromones, and reaction yields could be optimised from the spectra obtained.[75] Another use of ^{13}C gel-phase NMR spectroscopy was in the functional group interconversion of supported cholic acids[76] where information about the reaction was obtained, without cleavage of material from the solid support. The quality of the spectra obtained was improved by including a *p*-alkoxybenzyl spacer group between the support and the compound. The difference between the chemical shifts of the solid-supported and the solution-phase cholic acids was negligible, significantly aiding the spectral assignment of the compounds. The method continues to be used to evaluate reaction progress on solid supports. However it is generally impractical as a method for

the real-time monitoring of reaction courses, as often many thousands of scans are required to obtain an acceptable signal-to-noise ratio, especially for quaternary carbon atoms. To use ^{13}C gel-phase NMR as a rapid method of monitoring reactions, the use of ^{13}C-labelled building blocks has been reported[77, 78] with some success. In one experiment, the gel sample was locked in place by using an insert, and the spectrum obtained in 64 transients, using 20 mg of resin containing approximately 1 mg of compound.[77]

1.4.1.1.2 ^{19}F Gel-Phase NMR Spectroscopy.

No commercially available solid supports contain fluorine. As the natural abundance of ^{19}F is 100%, ^{19}F is potentially a very sensitive probe for monitoring reactions on solid-supports. Moreover, ^{19}F-signals have a wide chemical shift distribution (around 200 ppm), reducing the chances of obtaining overlapping signals. Structural modifications, such as functional group interconversions and reactions, carried out quite remote from the fluorine atom can result in sufficiently large chemical shift changes in the spectrum to be able to monitor the reaction directly.[79] The first use of ^{19}F gel-phase NMR spectroscopy was to observe the assembly of a peptide chain.[80] This was achieved by incorporating fluorine into the side chain protecting groups, fluorobenzyloxycarbonyl, F-Boc. Recently, ^{19}F gel-phase NMR has been used to study the S_NAr reaction[81] shown in Scheme 1.15.

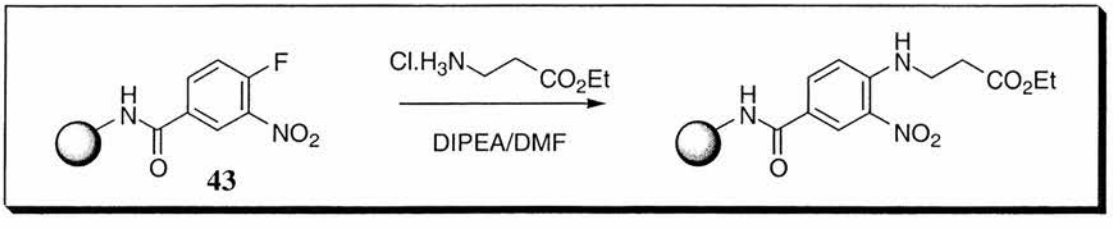

Scheme 1.15: *S_NAr Reaction followed by ^{19}F Gel-Phase NMR spectroscopy.*

During the reaction, fluoride is displaced from the aromatic ring of **43**, such that the disappearance of the resin-bound aromatic fluorine signal and appearance of a new

^{19}F-fluoride signal in solution could be used to monitor the progress of the reaction. The spectrum also contained a large broad peak, not associated with the solid-supported compound. The authors declared that this was due to components of the quadranuclear probe that contained fluorine. However, the presence of this broad peak gave a very reliable external standard for monitoring the reaction progress. ^{19}F gel-phase NMR spectroscopy has also been used to monitor the synthesis of a peptoid.[82] The fluorine-atom was incorporated into the linker, rather than the compound being synthesised, thus the reaction conditions for any step of the synthesis could be rapidly optimised, Scheme 1.16.

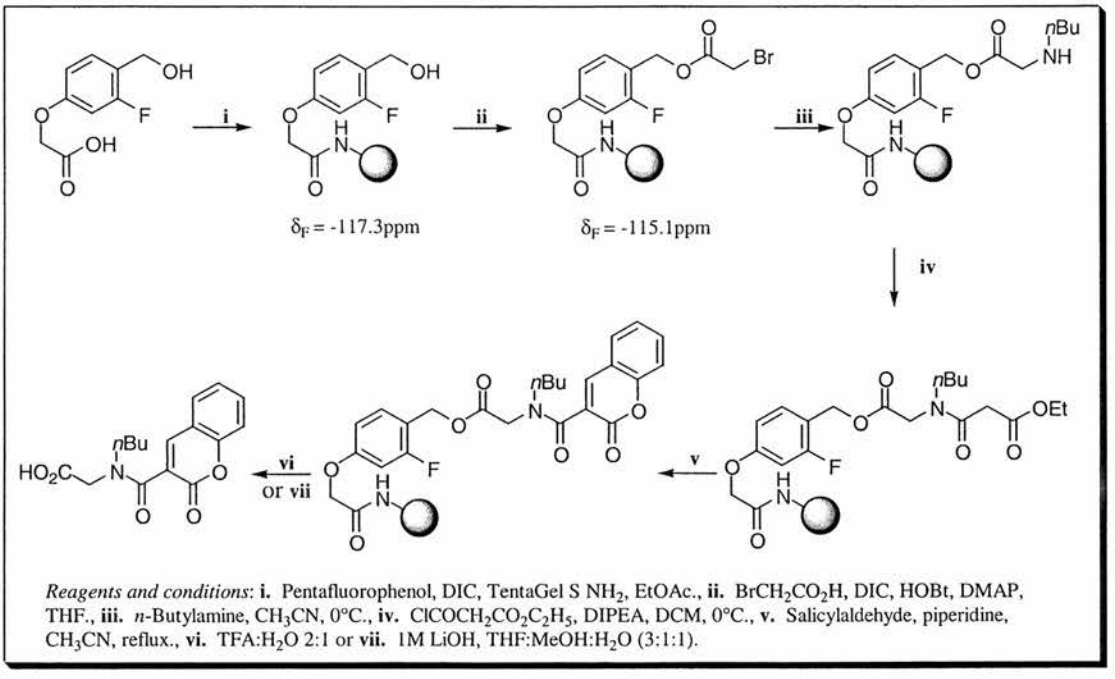

Scheme 1.16: *Monitoring changes in δ_F during solid-phase synthesis of a peptoid.*

Recently, fluorine containing polymers have been developed[83] by the co-polymerisation of styrene, **5**, 4-fluorostyrene, **44**, 1,4-divinylbenzene, **45**, and 4-vinylbenzylchloride, **46**, Scheme 1.17.

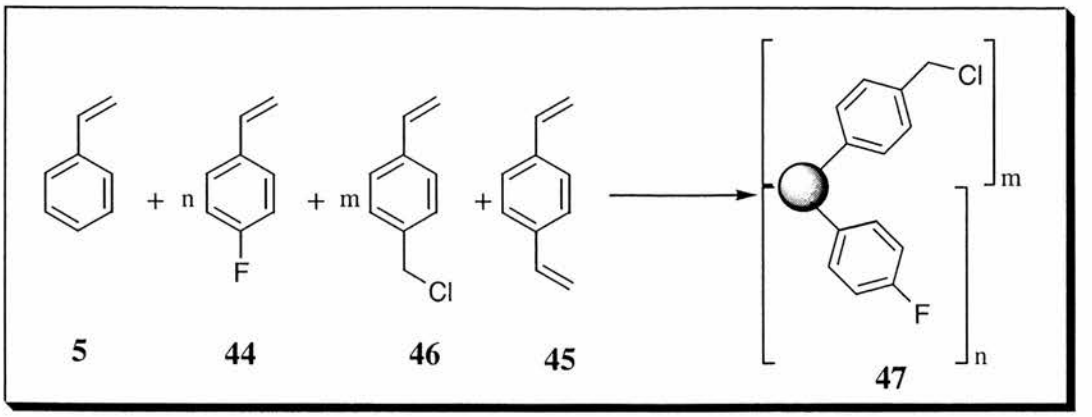

Scheme 1.17: *Synthesis of fluorine containing polymer support.*

This gave a functionalised fluorinated support, **47**, with a loading of approximately 0.3 mmol F g^{-1} of the internal standard, determined by fluoride ion chromatography[84] and which also gave a single signal in the NMR spectrum at -121 ppm. With this level of internal fluorine loading, spectra could be acquired with approximately 50 mgs of resin in 6 minutes on a 200 MHz instrument, and 1 minute on a 500 MHz NMR machine.

1.4.1.1.3 ^{31}P Gel-Phase NMR Spectroscopy.

As was the case with ^{19}F gel-phase NMR spectroscopy, ^{31}P NMR spectra can be rapidly acquired. This method has been successfully applied to monitoring reactions, and was first described for the oxidation of phosphite to phosphate in solid-phase oligonucleotide synthesis.[85] A second coupling reaction was then carried out, so the reappearance of the phosphite peak was used to monitor the progress of the coupling reaction, Scheme 1.18.

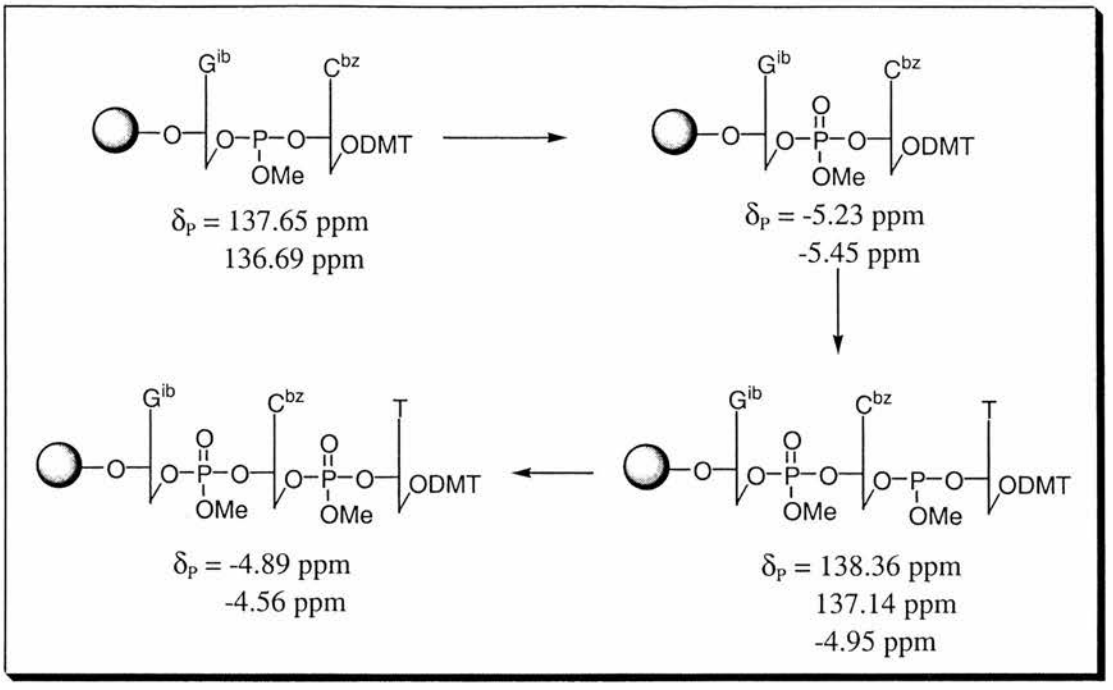

Scheme 1.18: *Oligonucleotide synthesis monitored by ^{31}P gel-phase NMR spectroscopy.*

Another application of ^{31}P gel-phase NMR spectroscopy was the analysis of a Horner-Wadsworth-Emmons olefination reaction, Scheme 1.19.[86] The reaction was followed by monitoring the disappearance of the phosphonate signal in the starting material, and the appearance of a new signal corresponding to the diethyl phosphate formed. In addition to this, the method also picked up a competing side reaction, which would have been very difficult to detect using any other analytical technique.

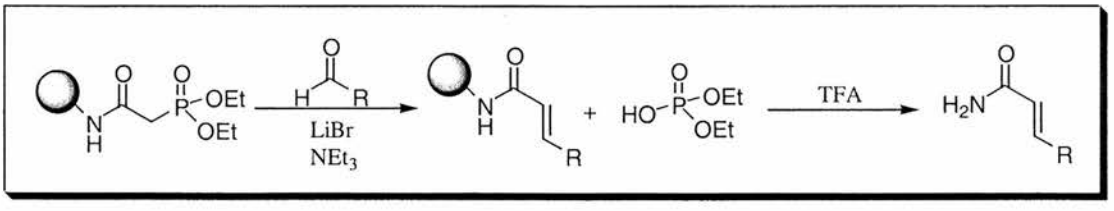

Scheme 1.19: *^{31}P monitoring of solid-supported Horner-Wadsworth-Emmons reaction.*

1.4.1.1.4 ^{15}N Gel-Phase NMR Spectroscopy.

Due to ^{15}N having a low natural abundance (0.37%), the method requires the use of isotopically labelled ^{15}N compounds. Swayze[87] demonstrated the use of this technique by monitoring the functionalisation of a supported amine.

1.4.1.2 Magic Angle Spinning (MAS) NMR Spectroscopy.

In analysis by gel-phase NMR spectroscopy, line broadening can be a problem, due to residual dipolar interactions and also variations in the magnetic susceptibility. To obtain spectra of solid-supported compounds with comparable resolution to compounds in solution-phase, these problems need to be addressed. Both dipole-dipole coupling, which is dependent on the angle between the dipole pair, the static field in the form of $(3\cos^2\theta\text{-}1)$, and any line broadening due to magnetic susceptibility can be removed by MAS.[88] By spinning the sample at an angle of 54.7° relative to the static magnetic field, the dipolar couplings are averaged out to zero, so $3\cos^2\theta\text{-}1=0$. Sample spinning also averages the magnetic susceptibility, helping to reduce line broadening. The best solvent with which to carry out MAS NMR has been investigated, and it has been found that the choice of solid support and solvent can considerably influence the quality of the specta obtained. Keifer[89] looked at nine commercially available resins in conjunction with seven different NMR solvents, to determine the best combinations. He found that the best solvents were CD_2Cl_2, $CDCl_3$, C_6D_6, d_6-DMSO and d_7-DMF. When analysed under MAS conditions, the polymeric backbone of the resin sometimes gave intense spectral signals that could make interpretation of the resin-bound compound difficult. It has been found that presaturation can improve the spectral quality for TentaGel resins.[90] However, while decreasing the magnitude of some background signals, other residual signals from the backbone can still make spectral

assignment very difficult. The nature of the compound attached to the resin linker also exerts an important influence on the quality of the recorded spectrum.

1.4.1.2.1 ^{13}C MAS NMR Spectroscopy.

In the late 1980's, it was shown that ^{13}C NMR data could be obtained from a compound on resin using MAS NMR spectroscopy.[91] However, the approach was not widely applied for many years. The first example of the application of ^{13}C MAS NMR analysis in combinatorial chemistry demonstrated that spectra of sufficient quality to monitor the course of reactions could be obtained.[92] A distinct advantage of the MAS method is the short data acquisition time required, 20 minutes, compared to 120 minutes for ^{13}C gel-phase NMR. MAS NMR spectroscopy has been used to measure the enantiomeric excess (e.e.) of a product formed during a reaction on solid-phase.[93] When compared to the measurements after cleavage from the resin and analysis by HPLC, the e.e. measured using MAS NMR agreed to closer than 1%. ^{13}C MAS NMR has also used to follow the progress of the S_NAr reaction previously discussed in Section 1.4.1.1.2 (Scheme 1.15),[81] where the appearance of a methyl signal was indicative of product formation. At this time, ^{31}P and ^{15}N MAS NMR analyses for resin-bound compounds have not been reported.

1.4.2. Infrared Spectroscopic Techniques.

Infrared spectroscopy has been routinely used for many years. It is a convenient and sensitive technique for the characterisation of solid-supported compounds. IR spectroscopy allows direct measurement of the appearance or disappearance of building blocks or protecting groups that possess an IR active species. Thus the kinetics of a reaction on a solid support can be monitored directly, and the influence of variations in the reaction conditions can be probed. Moreover, the utility of different resin types can be compared and the extent of a reaction can be determined semi-quantitatively. There are many different variants of infrared spectroscopy, as discussed below.

1.4.2.1. Infrared Transmission Spectroscopy

Transmission spectroscopy is the simplest of the infrared techniques used for analysing solid-supported compounds. It is used for routine spectral measurements on many diverse samples, and is usually applied to polystyrene or PS-PEG resins. To carry out the analysis, 1-5 mg of resin-supported compound are required, prepared as a KBr disc or pellet. Relative quantitation of the yield of a reaction on solid support is generally possible with infrared spectroscopy, by means of internal reference bands.

The extent of appearance or disappearance of a specific absorption band enables the calculation of the percentage of product formed at that point in the reaction. For absolute quantitation, cleavage of the product from the solid support and analysis by other methods is required.

Although infrared transmission spectroscopy has the advantage of not requiring cleavage of material prior to analysis, there are also disadvantages. Large amounts of material (1-5 mg) are required for the analysis, and the sample is also being distorted, through crushing and grinding when forming the KBr pellet, when using this technique.

1.4.2.2. Internal Reflectance Spectroscopy.

Internal reflectance spectroscopy, also known as attenuated total reflectance (ATR) is a highly versatile, non-destructive technique for obtaining the infrared spectrum of the surface of a material. ATR dates back to original work by Newton, who when studying the total reflectance of light at an interface between two media of different refractive indices, discovered that an evanescent wave found in the less dense material extended beyond the reflecting interface. Infrared spectra can be obtained by measuring the interaction of this wave with the less dense material. The sample, usually a single resin bead, is placed in contact with the internal reflection element. This element is made from a material with a high refractive index, such as silicon or diamond. The light is then totally reflected, and the sample interacts with the evanescent wave, resulting in the absorption of radiation by the sample in contact with the element. The method is highly sensitive as an analytical technique, with data being collected from only a small percentage of the solid-supports surface area. It has been estimated that the detection limit is in the femtomole (10^{-15}) region, corresponding to approximately 0.025% of the total resin bead loading. ATR has been used to monitor the rate of the esterification of hydroxyl groups on TentaGel® and Wang resins.[94] This work showed that there is little difference in the rate of the solid-supported reaction compared to solution-phase. ATR has also been used to show that absorbances from protecting groups that contain deuterium can provide a quantitative measurement of resin loading. This is achieved by measuring the deuterium content of an immobilised compound.[95]

1.4.2.3. Diffuse Reflection Spectroscopy.

Diffuse-reflectance infrared fourier transform spectroscopy (DRIFTS),[96] allows analysis of samples where other spectroscopic methods fail. When large particle faces

are present in the sample, analysis by this method can cause specular reflection, which produces *reststrahlen* bands (inverted bands) in the diffuse-reflectance spectrum. However, due to the relatively small particle size of the resin beads, information can often be taken from the spectra of untreated, *i.e.* diluted as a KBr disc, or crushed beads directly. An automated method of carrying out DRIFTS is now commercially available and provides a very good method for high throughput on-bead analysis of solid-phase reactions.[96]

1.4.2.4. Photoacoustic Spectroscopy.

This is a fast non-destructive method of analysis that requires no sample preparation, complementing the other available IR techniques. The photoacoustic effect occurs due to infrared radiation absorbed by the sample being converted into heat energy. This heat diffuses to the surface of the sample, then into an adjacent gas atmosphere. The thermal expansion of the gas produces a photoacoustic signal that is detectable by microphone. The use of this method to monitor a reaction on solid-phase has been reported.[97] As no sample preparation is required, analysis of a series of reactions on the same resin can be performed. This method of analysis appears to offer a convenient alternative, although less sensitive, to ATR spectroscopy.

1.4.3. Mass Spectrometry.

Mass spectrometric (MS) techniques generally provide the most useful methods for analysing combinatorial mixtures, as well as individual products from solid-phase synthesis. MS is highly sensitive, yet destructive, and to a certain degree, lacks the ability to quantify reactions on solid-phase like other analytical techniques discussed in this section. Initial studies began with the analysis of peptide mixtures produced in a combinatorial manner.[98] Since then, many examples of the application of MS

techniques to the analysis of the components of small organic molecule libraries have appeared. MS methods useful in the analysis of products from solid-phase syntheses are discussed below.

1.4.3.1. Electrospray Mass Spectrometry (ES-MS).

ES-MS has been successfully applied to the analysis of the products formed in a solid-phase Bischler-Napieralski reaction. Analysis of the mixture of dihydroisoquinoline and tetrahydroisoquinoline products, Scheme 1.20, showed the presence of all the expected molecular ions in the ES mass spectrum.[99]

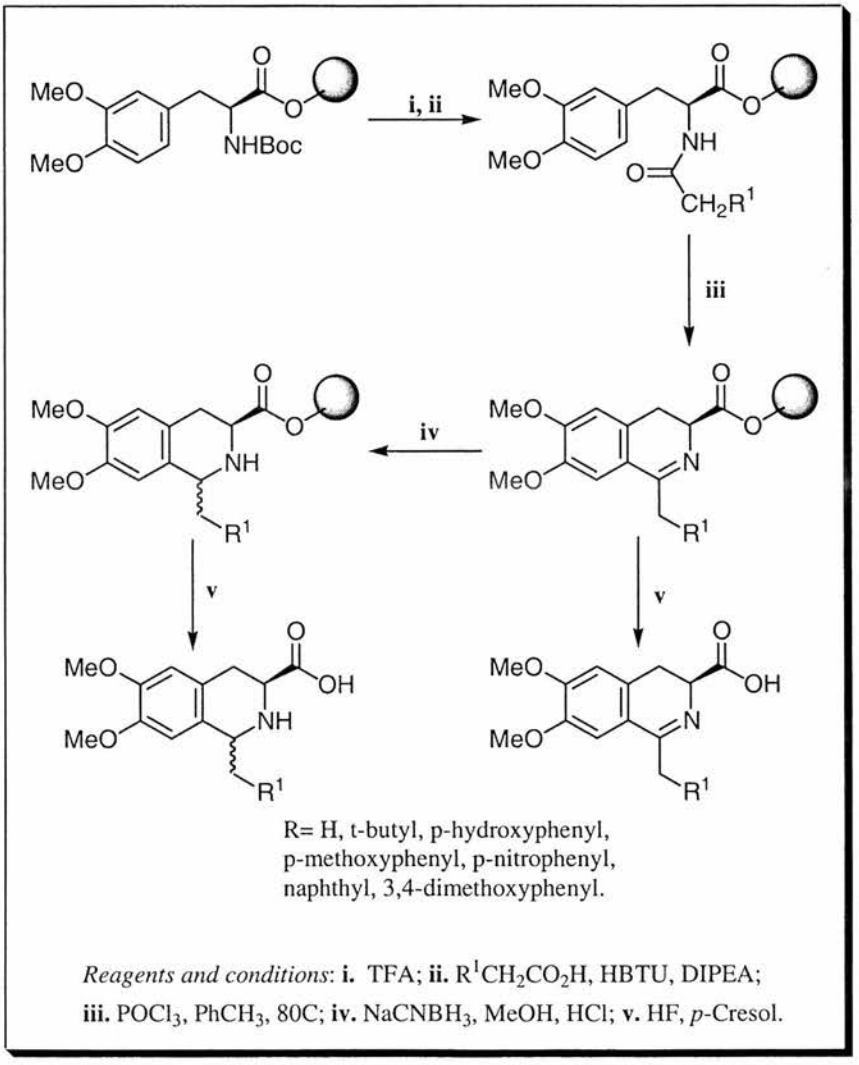

Scheme 1.20: *Solid-supported Bischler-Napieralski reaction.*

1.4.3.2. Matrix Assisted Laser Desorption Ionisation-Time-of-Flight-Mass Spectrometry (MALDI-TOF-MS).

Bradley *et. al.*[100, 101] have utilised this method to analyse compounds attached to solid supports. In MALDI-TOF-MS, resin beads, or a single bead, are placed in a reaction well, and the compound is cleaved from the solid support. The nature of the linker group attaching the compound to the solid support, see Section 1.3., determines how this cleavage is performed. To the mixture of solid support and free compound is added the matrix, usually glycerol or 2,5-dihydroxybenzoic acid, and the mixture is left to crystallise. The mixture is then irradiated with multiple pulses of a 337nm N_2 laser. As used by Bradley *et. al.*, the technique was given the acronym SPIMS, (solid-phase *in situ* mass spectrometry), as the cleavage of the compound from the solid support is carried out only when required, and the support is not removed from the reaction mixture. The work was carried out on solid-supported compounds linked through an acid labile linker. In-situ cleavage was then carried out by treatment of the solid-supported compound with TFA vapour. Other work using this method, by Fitzgerald *et. al.*[102] attached a peptide to the solid support through a photolabile α-methyl-phenacyl ester linkage, from brominated-Wang resin. A single pulse from the laser directed at the resin bead crystallised in α–cyano-4-hydroxycinnamic acid, gave a clear molecular ion signal, Figure 1.24.

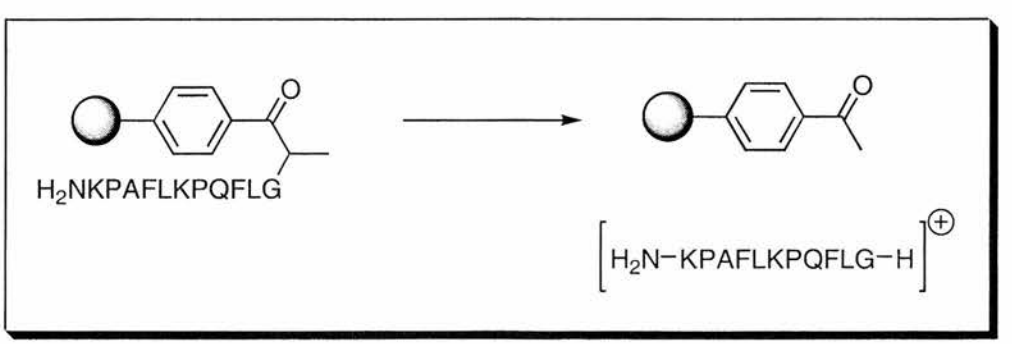

Figure 1.24: *Photolytic cleavage using MALDI-TOF MS.*

1.5. Encoding In Combinatorial Synthesis.

After a compound library has been synthesised, one of the major problems concerning testing of the library is the identification of compound(s) that show affinity for the target. In large library syntheses, the small amounts of compound produced make routine chemical or spectroscopic methods of identification difficult. The identity of the compound may be known from its position in a 96-well plate, however the compound may have to be identified using some form of deconvolution protocol. The most common of these is the resynthesis of the compound library, but resynthesised as mixtures that decrease in size, Figure 1.25.

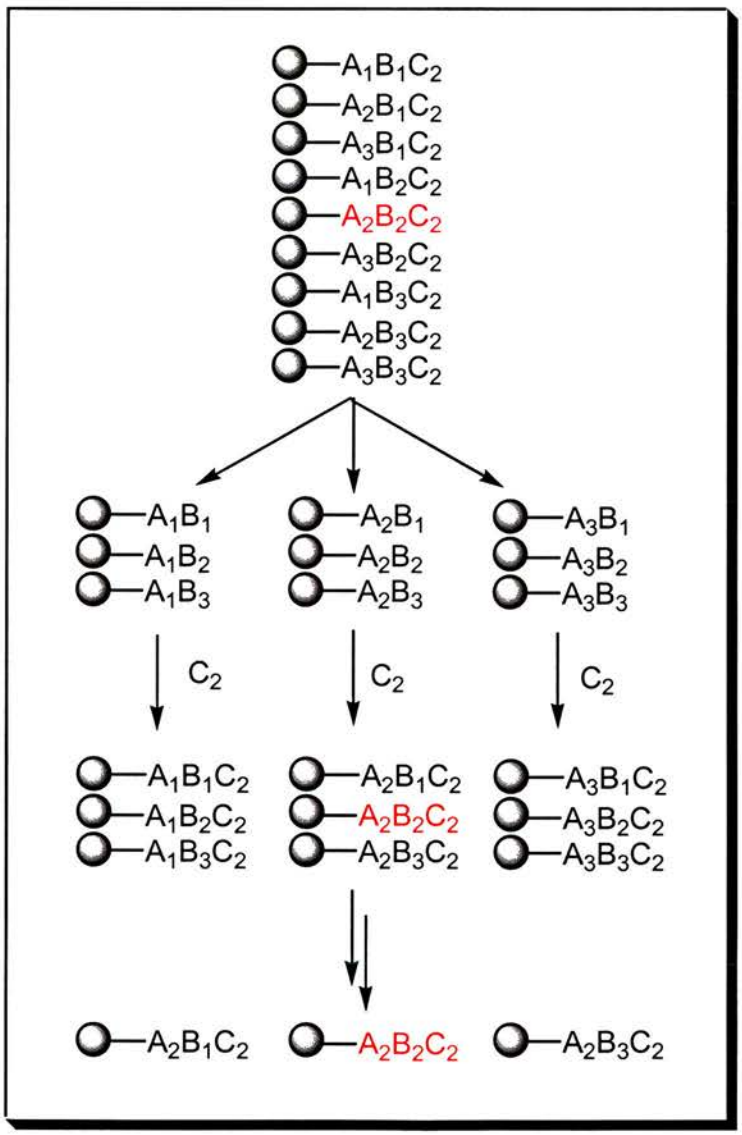

Figure 1.25: *Deconvolution through resynthesis.*

In Figure 1.25, an active compound has been identified in the mixture of nine resin-bound permutations, all of which were reacted with C_2 in the last step of the synthesis. This set of compounds is then taken back one step in the synthesis, and split into three further subsets, each containing three compounds. The subsets are reacted with C_2, and the active compound identified through rescreening. The subset containing the active compound is then subjected to this process again, until the active entity in the library is isolated and identified. In this example, starting from a mixture of nine compounds, the procedure is relatively quick and straightforward. However, when libraries containing 10000 compounds need to be deconvoluted, the process is both time consuming, costly and inefficient. Moreover, there may be several moderately active members of the library, all of which need to be identified.

To overcome these problems, moves towards encoding combinatorial libraries has occurred. Encoding combinatorial libraries offers two distinct advantages. These are relational nomenclature, and also the ability to utilise automated handling techniques. Czarnik[103] describes relational nomenclature using the idea of a library of books. These books are encoded with an alphanumerical 'call number', dictated by the Dewey decimal system.* This call number allows the books to be shelved in an organised way, permitting ease of retrieval. As stated previously, one of the other advantages of encoding is the possibility of using automated techniques for sample handling and also in the storage and retrieval of data.

The encoding of chemical libraries is not a new idea. The major pharmaceutical companies maintain libraries of hundreds of thousands of compounds, encoded with a bar code system. These libraries are encoded after synthesis, but it is far more efficient to encode during the synthesis. Encoding during synthesis requires that the tag, or other

* Books in a library are arranged on shelves according to the Dewey Decimal Classification System of 1876, developed by Melville Dewey (1851-1931). The system divides knowledge into ten different broad subject bands, called classes, numbered 000-999.

method of encoding, is directly attached to the solid support, or is attached to the compound being synthesised, as shown in Figure 1.26.

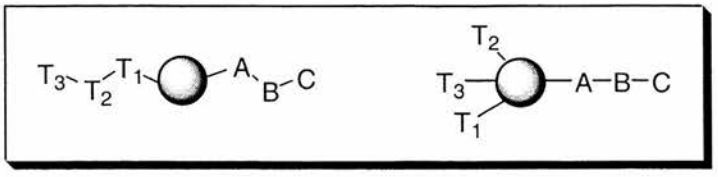

Figure 1.26: *Encoding of resin beads during solid-phase synthesis.*

Therefore, a prerequisite for this process is that the method used in attaching the tag does not alter the compound or the support in any way. It is also necessary that the chemistry used in the synthesis does not transform the tagging system in any way. The most common methods of encoding are discussed below.

1.5.1. Chemical Encoding.

Libraries can be tagged in many ways, including using isotopes, peptides, oligonucleotides and other organic compounds. In oligonucleotide tagging, the library is synthesised onto the solid support, and at each step, an oligonucleotide that specifically relates to that synthetic step is added to the support. As the components of the library are built up, the oligonucleotide chain grows. When the library has been assayed and tested, the identity of the active compound(s) in the library can be determined by using the polymerase chain reaction, (PCR), to sequence the oligonucleotide chain.[104] Using peptides to encode reactions on solid-phase is advantageous due to the quick processes available for the identification of sequences, such as Edman degradation.[105] There are advantages in using oligonucleotides over peptides to encode a combinatorial synthetic sequence, namely that the amount of material required for identification is much smaller than would be needed using a peptide tagging strategy. Encoding using organic compounds has moved the area away from peptides and oligonucleotides, as the use of such tags requires mild conditions of

synthesis. The utility of haloaromatic tags **48** and **49**, which are inert to the reaction chemistry, have been assessed.[106, 107] The tags are attached to the solid support during the synthesis of the library. Upon analysis of the library by MS methods, the presence or absence of the tags details the synthetic history of the solid-supported compound, leading to identification. The haloaromatic tags are shown in Figure 1.27.

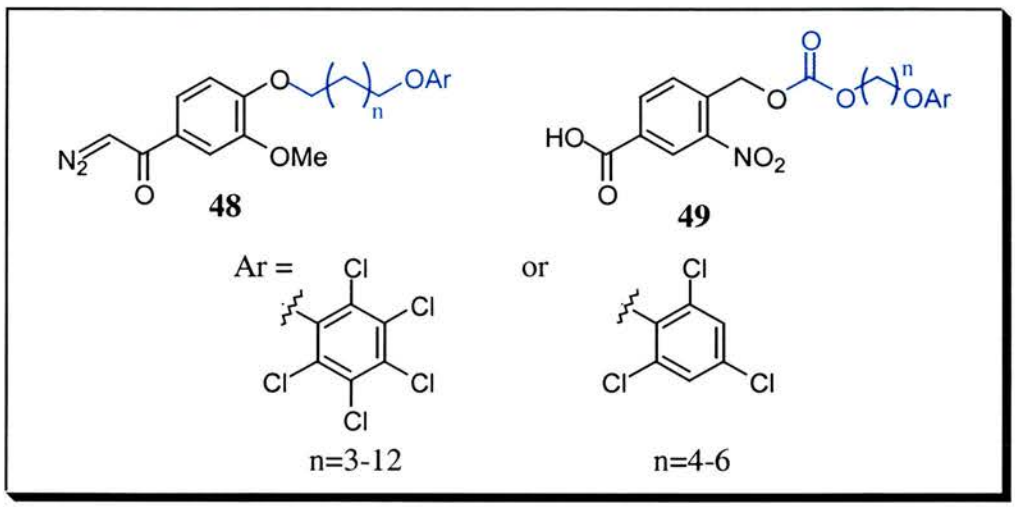

Figure 1.27: *Stills Haloaromatic tags.*

The tag portion of **49**, shown in blue, is attached to a photolabile linker through a carbonate functionality. The linker is then attached to an amine group on the solid-supported compound, through an amide bond. The release of the tag is carried out by photolysis of the solid support. The free tag is then silylated, and analysed by electron capture gas chromatography (ECGC). The tag portion of **48**, again shown in blue, is attached to an oxidative linker through an ether bond. This tag is directly attached to the solid support, not the compound of interest. The advantage of this attachment is that it is facile and versatile, and does not require any special functionality or complex protection/deprotection strategy, as is often required for other encoding systems. After synthesis, treatment of the support with ceric ammonium nitrate (CAN) liberates the tag, which is again silylated, and analysed by ECGC. The tags can be selectively detected in sub-picomole (10^{-12}) quantities, and the binary code, therefore the inferred compound structure, can be determined from the resulting chromatogram. The

stability of these tags allows the use of a wide range of reaction chemistries required to synthesise a library of diverse non-oligomeric compounds. The simplicity of introduction, removal and analysis makes the tags both a reliable and rapid way for the structural analysis of solid-supported compounds. The method has been successfully used in the synthesis of heterocyclic,[108] peptide[106, 109-112] and linear[108, 113] libraries, Figure 1.28.

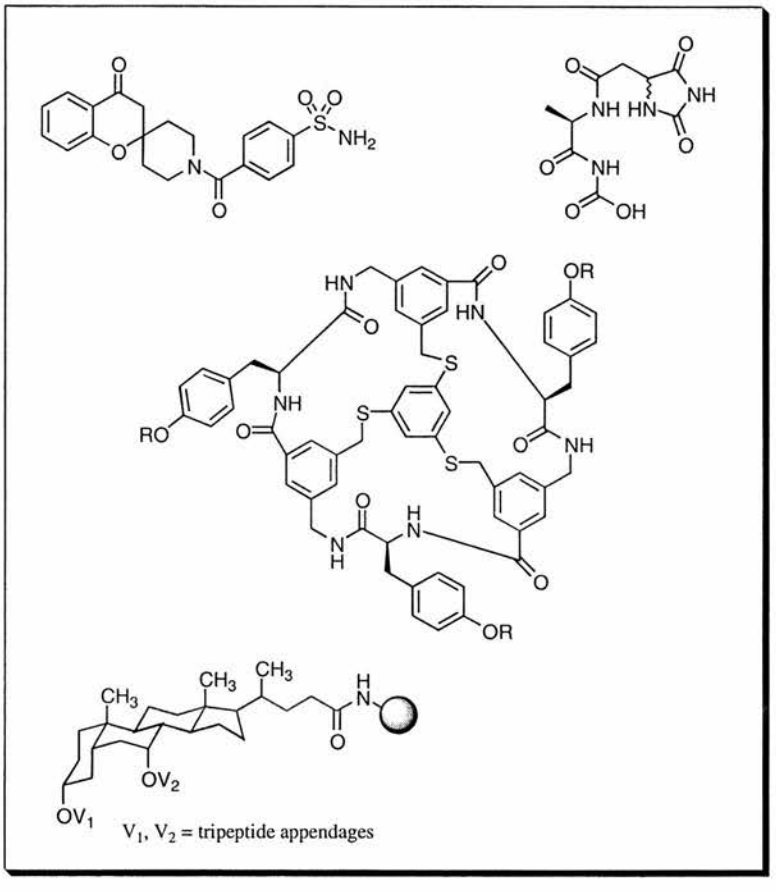

Figure 1.28: *Compounds produced using haloaromatic tagging.*

1.5.2. Electronic Encoding.

Chemical encoding can often cause problems through incompatibility of reaction conditions with the tagging system. Methods of non-chemical tagging have been investigated. Of these, radiofrequency (RF) tagging has been used for encoding libraries.[114] RF encoded microchips are commonly used to identify laboratory animals through subcutaneous insertion.[115] The tags are then encoded by downloading binary information onto the chip. Reading of the chip is achieved by reading the emitted RF signals at the end of the synthesis. The application of the technology to combinatorial synthesis used the RF chips in a reaction vessel that also contained the solid support. The RF chip is shown in Figure 1.29.

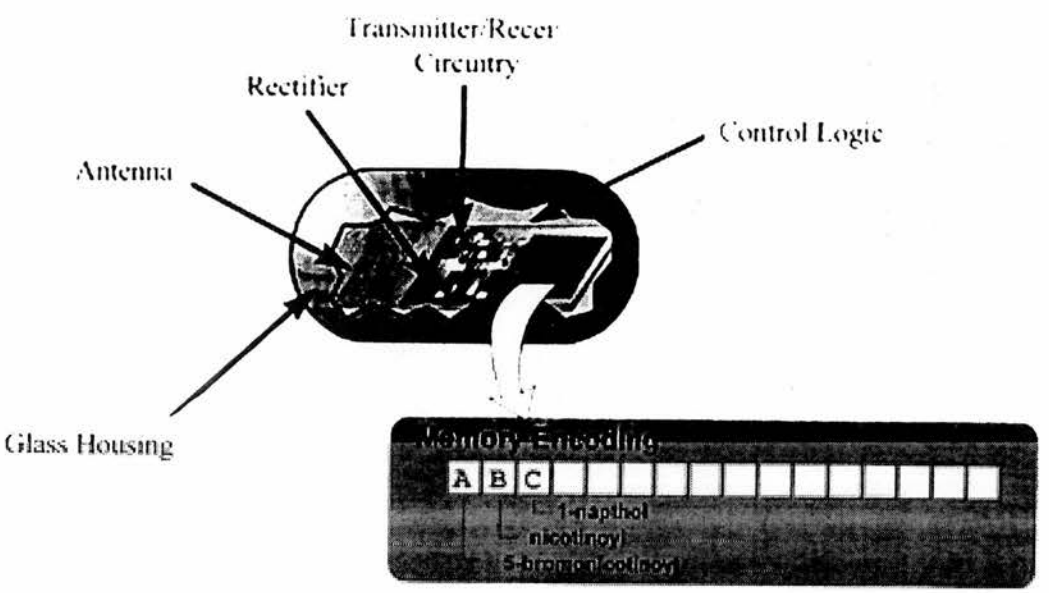

Figure 1.29: *RF encoding chip*

The chip is encased in glass, and consists of three components. The first of these is memory. Each chip is produced with a unique alphanumerical code, with no two chips every having the same code. The second component is a rectifying circuit that converts the absorbed RF energy into electrical energy, so no external power supply is required. The third component is an antenna, which receives and transmits the RF signals. The RF tags can then be placed into flasks, T-bags, tubes etc, enabling

identification of the container, and so its synthetic history, at any time. This tagging method has been used in the synthesis of a taxoid library.[116]

1.6. Solid-Supported Reagents.

The development of solid-phase organic synthesis methodology to meet the demand for high-throughput screening studies has basically removed the necessity for the time consuming process of compound isolation and purification as is required in solution-phase synthesis. Excesses of reagents, along with any by-products formed in solution are easily removed by filtration of the solid support from the reaction mixture. Cleavage from the solid support then gives the target molecule with a suitably high enough purity to begin biological testing directly. This method has been successfully applied, however, there are still limitations and difficulties present with this method.

One of these problems is when a known solution-phase synthetic protocol is transferred to the solid-phase, the molecule being synthesised requires a covalent link to the solid support. When cleaved from the support after the synthesis has been carried out, artefacts of this linker group may remain on the synthesised molecule, adding an element of similarity into a library of compounds. Methods have been developed that incorporate the linker group into the molecule upon cleavage. In the same area, work has been carried out on the design and use of some form of traceless linker strategy, as outlined in Section 1.3.3.

Another problem is that many well known synthetic procedures, routinely carried out in solution-phase synthesis, do not immediately transfer very well to the heterogeneous conditions that are distinctive of solid-phase organic synthesis.[117] This problem is in addition to the problems associated with compound analysis, as shown in Section 1.4., and can result in long periods of synthetic development and reaction

optimisation before the production of any libraries can begin, making solid-phase organic synthesis methodology impractical in any lead compound optimisation process.

A solution to these problems would be the development of a method where the parallel synthesis of target molecules can be carried out using traditional solution-phase techniques and methods, but with the requirement for purification removed from the process. This also removes any need for a covalent linker group, giving another available site for synthetic modification. Several strategies have been described which detail such an approach. Current work in this field has moved into two distinct areas, the production of solid-supported reagents and the development of polymer-supported scavengers which remove excess reagents and materials from the reaction mixture.

1.6.1. Polymer-Supported Reagents.

Work in the area of polymer-supported reagents began in the early 1970's with the development of solid-supported Wittig reagents. Diphenylphosphine derivatised polystyrene was developed in order to perform olefinations of solution-phase compounds.[118-121]

The rebirth of the area occurred when Ley began adapting existing solution-phase methodologies for use on solid-phase. Previously, the use of tetra-*n*-propyl-ammonium perruthenate (TPAP) as a mild, room temperature, catalytic oxidant for converting primary and secondary alcohols to aldehydes and ketones had been described.[122] The immobilisation of this reagent onto a solid support was achieved by ultrasound treatment of an Amberlyst anion exchange resin, containing quaternary ammonium groups, with an aqueous solution of potassium perruthenate.[123] When the polymer-supported perruthenate (PSP) was used in a series of alcohol oxidation reactions, the yields of the desired carbonyl compounds was found to be good to excellent, and upon comparison to other supported reagents, the PSP-reagent was

generally found to be superior, with the only by-product in the synthesis being the unreacted starting material. An added advantage of the PSP-reagent is that after use, it can easily be regenerated by treatment with *N*-methylmorpholine-*N*-oxide (NMO). The PSP-reagent has been used extensively in work by the Ley group, including its use in conjunction with polymer-supported cyanoborohydride (PSCBH) and polymer-supported aminosulfonylpyridinium chlorides, to form a library of sulfonamides.[124] The use of PSP with polymer-supported Wittig reagents has also been described. Ley used this idea to synthesise a series of six Wittig reagents, according to the literature procedure of Bernard *et. al.*,[125] and used them in the synthesis of β-hydroxylamines from alcohols.[126]

The same group then began to investigate the use of other polymer-supported reagents which would be capable of performing a wide variety of oxidative functional group transformations, therefore increasing their desirability for use in generating compound libraries. It was decided that hypervalent iodine reagents would offer good properties, due to their diverse chemistry in solution. This work was begun by looking at the use of polymer-supported (diacetoxyiodo)benzene, (PSDIB), the preparation of which was already known,[127] in oxidative reactions, and also looking at its potential as a catalyst through recycling of the reagent. Other hypervalent iodine reagents have been prepared, and are shown in Figure 1.30. All reagents are prepared from poly(iodostyrene).

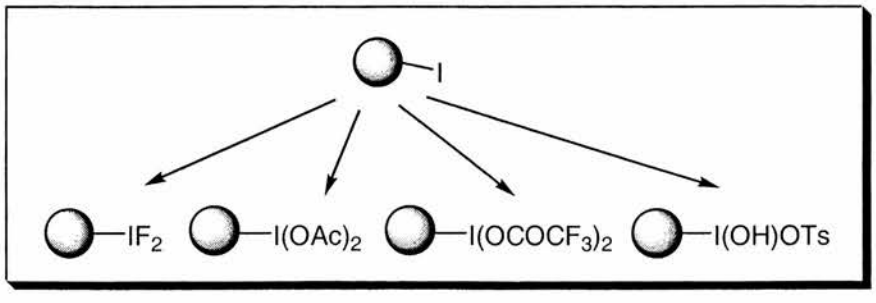

Figure 1.30: *Hypervalent iodine reagents used as solid-supported reagents.*

PSDIB has been used in the oxidation of quinols to quinines, oxidation of primary alcohols and α-hydroxylation of ketones. After use, the polymer-supported reagent is regenerated by reoxidation with peracetic acid, for PSDIB. Repeating the oxidation reactions after regeneration shows no loss of activity for the reagent. This work with polymer-supported reagents has recently been published in the syntheses of (±)-oxomaritidine,[128] **50**, (±)-epimaritidine,[128] **51**, and (±)-epibatidine,[129] **52**, Figure 1.31.

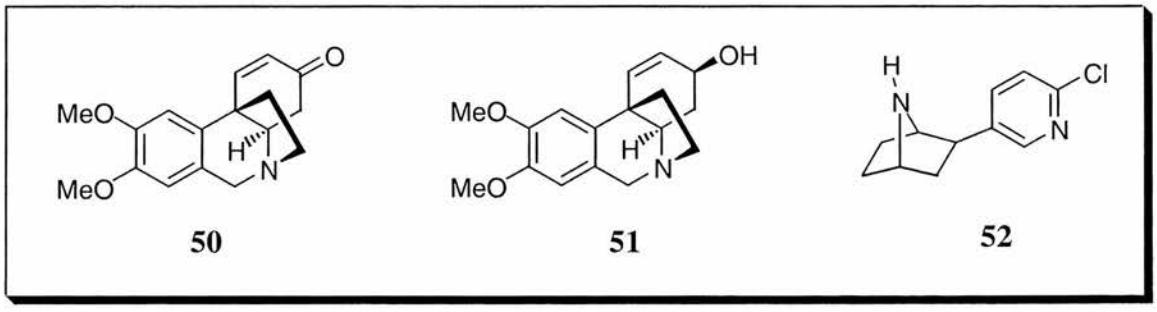

Figure 1.31: *Natural products using polymer-supported reagents.*

Other examples of polymer-supported reagents include the preparation of polyallylscandium trifylamide ditriflate, **53**, by Kobayashi.[130] This water tolerant catalyst has been used to catalyse a number of organic reactions and can be used many times without any loss in catalytic activity. The use of it to catalyse three component reactions between amines, aldehydes and silylated nucleophiles has been described,[131] and is shown in Scheme 1.21.

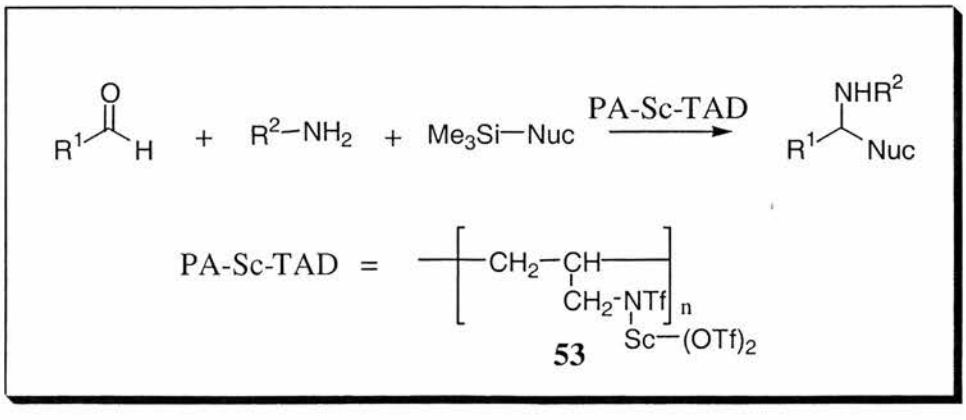

Scheme 1.21: *Three-component reaction catalysed by polymer-supported catalyst.*

1.6.2. Polymer-Supported Scavengers.

Polymer-supported scavengers, or quench reagents, are used to remove impurities from reaction mixtures upon completion of a solution-phase reaction. This can be done either in a covalent manner, or ionically. Kaldor *et. al.*[132] have developed polymer-supported nucleophiles and electrophiles that can be used for the selective removal of reaction impurities. The use of these reagents means that the solution-phase synthesis of small molecule libraries can be carried out in a much cleaner fashion, and removes the need for purification. The choice of scavenger used depends upon the impurities that are present in the reaction mixture. The scavengers developed are shown in Figure 1.32.

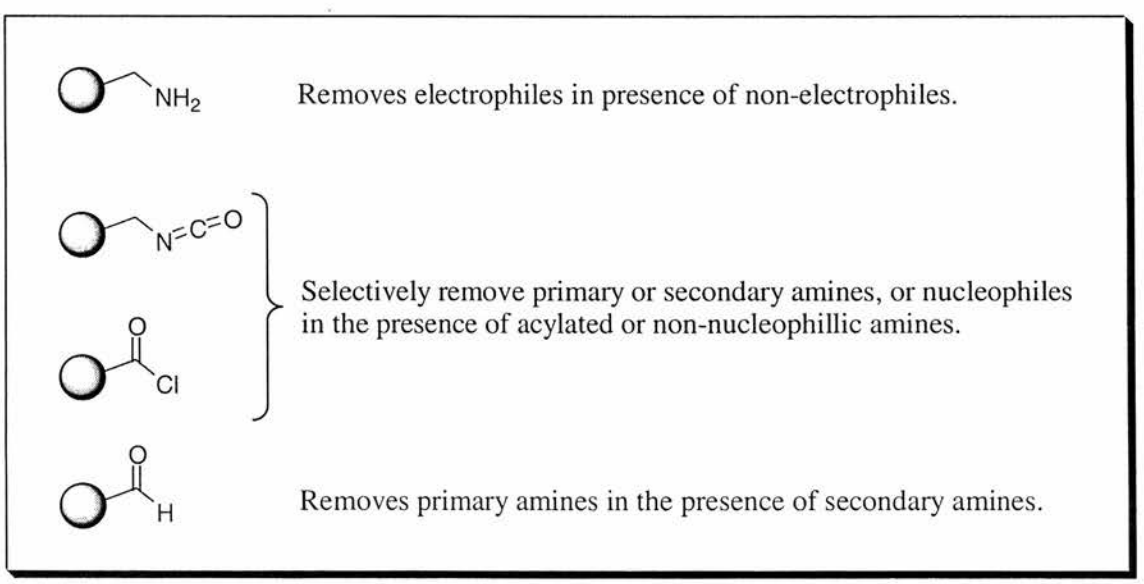

Figure 1.32: *Polymer-supported scavengers.*

The use of these scavengers in a solution phase reaction is outlined in Scheme 1.22.

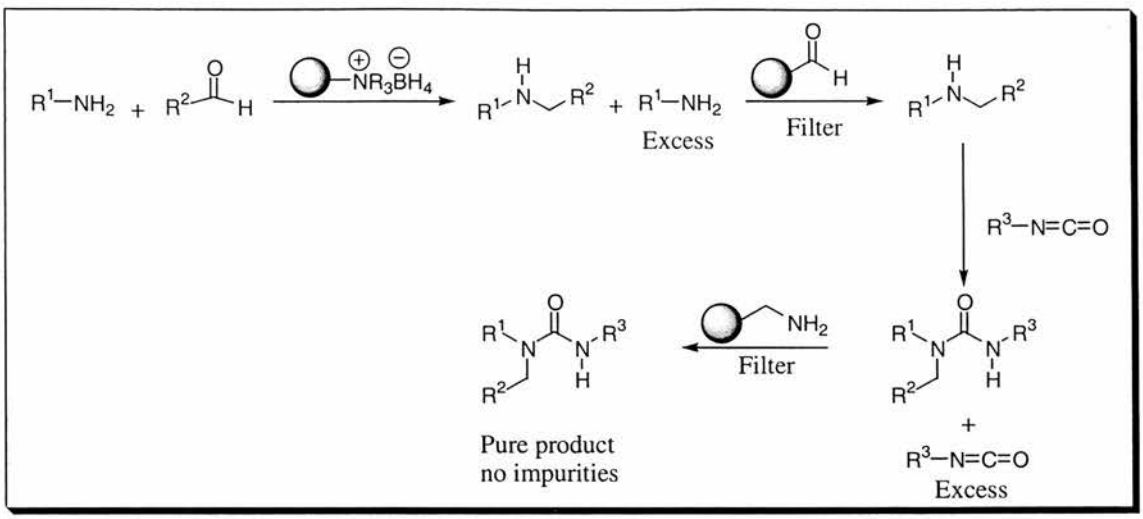

Scheme 1.22: *Use of polymer-supported scavengers in the synthesis of ureas.*

Workers at Parke-Davis recently described the use of two polymer-supported quench reagents (PSQ),[133] **54** and **55**, shown in Figure 1.33. The PSQ's are used in the generation of a library of 4-thiazolidinones, **56**, Scheme 1.23.

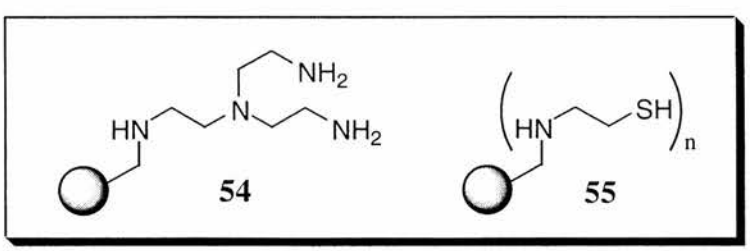

Figure 1.33: *Parke-Davis polymer-supported quench reagents.*

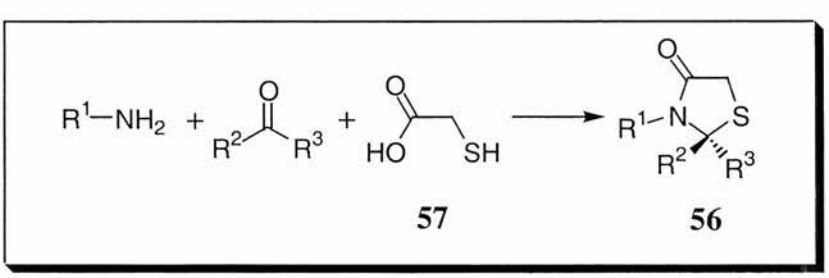

Scheme 1.23: *Synthesis of 4-Thiazolidinones.*

It was envisaged that the polymer-supported quench reagent **54** could remove both excess mercaptoacetic acid, **57**, and the aldehyde present in the reaction mixture through formation of a polymer-bound thiazolidinone, and could also remove mercaptoacetic acid, **57**, from solution by acting as a simple anion exchange resin. With PSQ reagent **55**, the removal of mercaptoacetic acid, **57**, should be achievable by

disulfide formation, while the removal of the aldehyde will be achieved by hemi-thioaminal formation.

A supported scavenger resin for the removal of amines from solution has been described by Coppola.[134] In this case, isatoic anhydride, **58**, is taken and reacted with Merrifield resin as shown in Scheme 1.25.

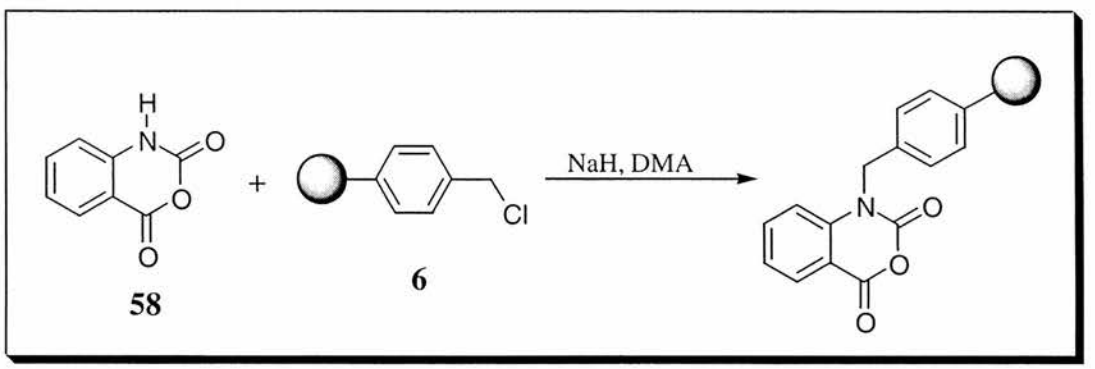

Scheme 1.24: *Scavenger resin for amines.*

The anhydride is an internally protected and activated form of 2-aminobenzoic acid. This makes the C4 carbonyl of the heterocyclic ring very susceptible to attack by nucleophiles, leading to ring opening and the production of CO_2 as the only by-product in the reaction. When tested in the synthesis of thioureas and anthranilamides, total removal of the excess amine present in the reaction mixture was observed in 30-90 minutes.

1.7. Inositol Monophosphatase.

1.7.1. Manic Depression and Lithium Therapy.

Inositol Monophosphatase (IMPase) plays a very important role in the dephosphorylation of secondary messengers, which are involved in the cell signalling process.[135-139] Problems that occur in the recycling process of these secondary messengers results in an overactivity of the signalling pathway, which subsequently leads to problems in the subject. The resulting chemical imbalance in the brain is responsible for causing manic depression and other related bipolar disorders in

approximately 1% of the world's population.[140] Currently the treatments for manic depression include Carbazepine™ and Depakote™, epilepsy drugs that contain valproic acid as their active ingredient, and also lithium therapy.[141-144] Lithium carbonate is used as the source of lithium, and it is this that is believed to inhibit IMPase. However, at the same time, lithium only has a very narrow therapeutic window with many side effects, including its high toxicity.[141, 145] Another way to try and treat the disease is to use structural analogues of the natural substrate, inositol-1-phosphate, in order to try and inhibit the function of the enzyme.[146-148] Some of the compounds produced using this technique have been shown to be potent inhibitors of the enzyme. However, due to their poor bioavailability *in vivo*, the compounds do not act as drugs. A variety of new modified compounds have been designed, and it is hoped that these will have improved bioavailabilities, allowing them to pass through the blood brain barrier.

1.7.2. Inositol Monophosphatase.

The hydrolysis of the phosphate ester of inositol-1-phosphate, inositol-3-phosphate and inositol-4-phosphate to *myo*-inositol, as shown in Scheme 1.26, is catalysed by the enzyme IMPase.

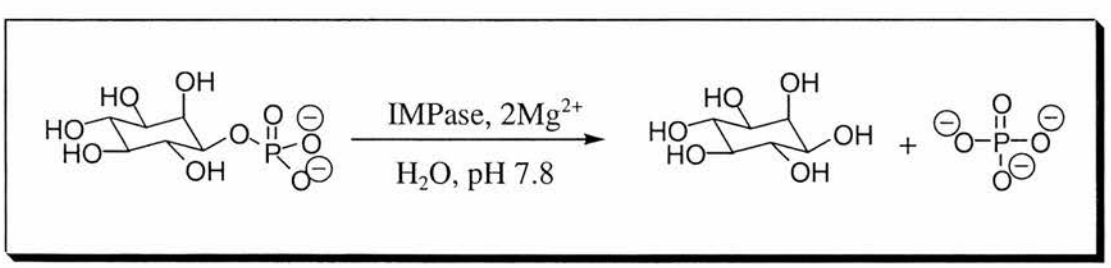

Scheme 1.25: *Hydrolysis by IMPase.*

IMPase is a homodimeric enzyme, with a molecular weight of 58kDa. Each of the monomers has an active site, and requires two Mg^{2+} metal centres as cofactors. Mg^{2+} is the natural cofactor, however, the enzyme has also been shown to work with Mn^{2+} Co^{2+} and Zn^{2+} as cofactor.[140] The structure of the active site of IMPase, bound with the

natural substrate, *myo*-inositol-1-phosphate, has been determined by X-Ray crystallographic techniques.[146-148] This work on the enzyme structure also included important results obtained from deletion studies carried out on the substrate. This has led to the identification of the C1, C2 and C4-hydroxyl groups of inositol as being essential for binding, and the hydroxyl group at C6 being involved in some form of catalytic role. X-Ray studies have also shown the presence of a water molecule in the enzyme active site, which appears to be bound to Mg^{2+}. It was postulated that this water molecule acts as an attacking nucleophile in the phosphoryl transfer reaction, yielding inorganic phosphate, P_i. This has recently been confirmed by Cullis *et. al.*[149] who showed that hydrolysis of a chiral [^{17}O,^{16}O]-phosphorothioate derivative of inositol-1-phosphate in $H_2{}^{18}O$ occurred with an inversion of stereochemistry at the phosphorus atom. This implies that an in-line displacement mechanism occurs, and this is more likely to occur when the nucleophilic water molecule is bound to Mg^{2+}.

1.7.3 Inhibitors of IMPase.

In order to be able to probe the active site geometry of IMPase, a variety of mechanistic probes and potential inhibitors have already been designed and tested,[150] and some examples are shown in Figure 1.34.

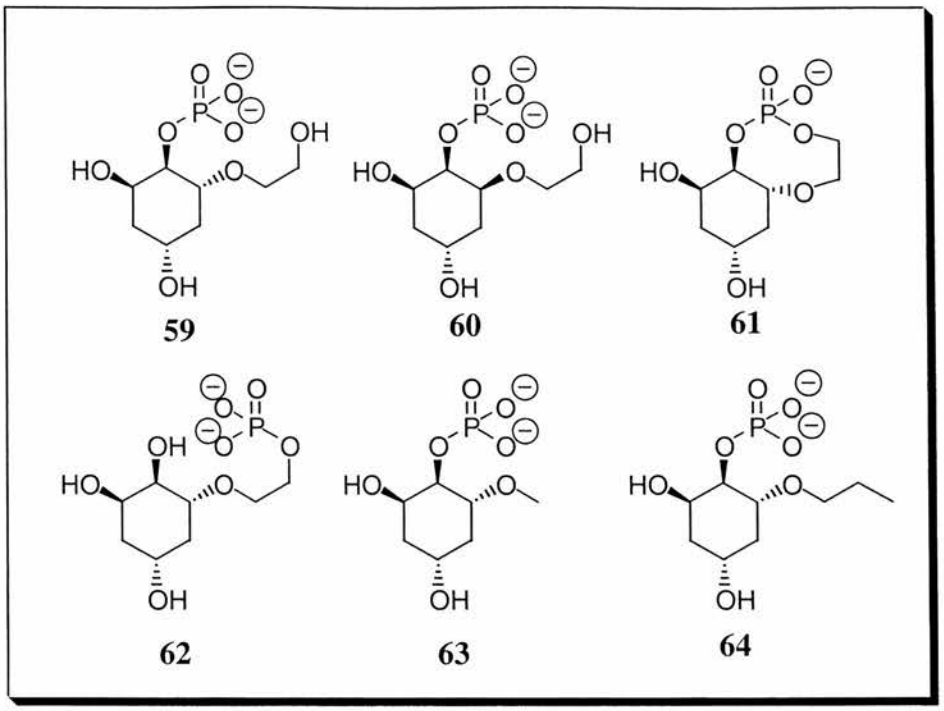

Figure 1.34: *Examples of inhibitors of IMPase.*

These so called pendant arm structures, **59-64**, have been designed with the intention that the alcohol of the arm would extend into the enzyme active site and exclude the nucleophilic water molecule, therefore preventing attack at the phosphorus centre. Addition of alkyl groups at the C6 position, such as methyl and propyl, alters the binding properties, so these compounds act as inhibitors, not substrates. This supports the role of the C6 hydroxyl as a catalytic one. A number of other molecules have also been tested for activity against the enzyme, including α-hydroxytropolones,[151, 152] **65**, a tricyclic spirane structure, L-671,776,[112] **66**, and also simple thiol derivatives of inositol,[153] **67** and **68**. These compounds are shown in Figure 1.35.

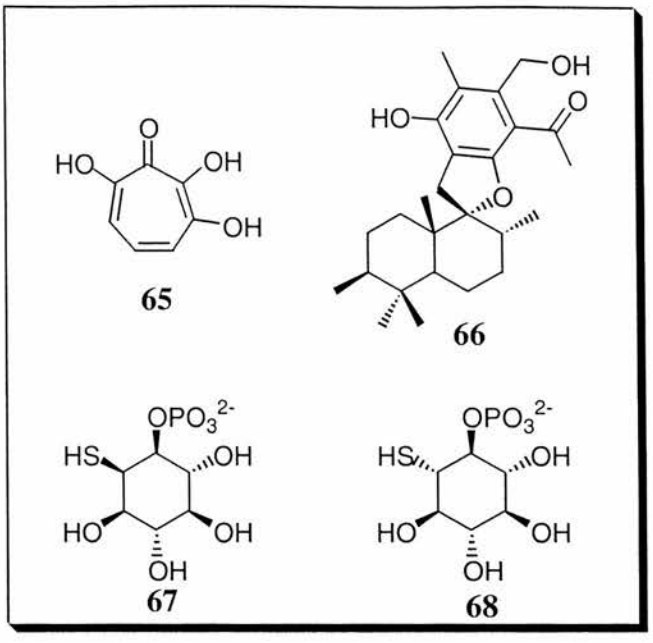

Figure 1.35: *Other examples of IMPase inhibitors.*

As mentioned earlier, the C3 and C5 hydroxyl groups in *myo*-inositol-1-phosphate have been shown not to contribute significantly to the binding or catalytic activity of the enzyme through deletion studies. As a consequence, the two stereocentres are omitted from the target molecules, giving the generic target molecule **69**, Figure 1.36, as possible targets for the enzyme.

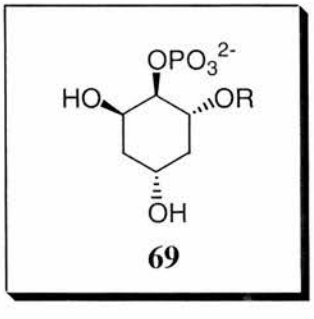

Figure 1.36: *Generic structure of targets for IMPase inhibitors.*

In conjunction with on going work in the research group, a library of compounds of this nature were to be synthesised using our POSAM™ technology. This methodology and the attempted synthesis is discussed further in Section 2.1.

CHAPTER TWO

RESULTS AND DISCUSSION

2.1. POSAM™ (Permutational Organic Synthesis in Addressable Microreactors) in solid-phase organic synthesis.[154, 155]

One of the major problems in the synthesis of combinatorial libraries on solid-phase is the deconvolution of the synthesised compounds in order to identify the compound that shows the desired biological activity, or any other required property. When the library is produced as a mixture, as is very common, this deconvolution process requires the partial re-synthesis and re-screening of the library, until the active compound is identified. This method is both time consuming and very costly, so other methods of identification are very attractive. Another problem commonly encountered in solid-phase synthesis is the ability to check the efficiency and the purity of the synthetic sequence that is being carried out. This problem arises due to the small amounts of compounds that are produced. In a 'one bead, one compound' synthesis, the amount of synthesised material is usually in the region of a few nanomoles, which makes it very difficult to check the efficiency and purity of the reaction. In a highly sensitive biological screening assay, this could be a serious problem, as it may be an impurity that gives a positive result. The logical way to overcome this problem is to perform the synthesis on a much larger scale, making the characterisation and analysis of the compounds much easier. The ability to side step these problems, and carry out synthesis where the purity, efficiency and deconvolution are not considered problematic, is a very attractive option, and work has been carried out to try and achieve this. The methodology that we developed, POSAM™, has tried to overcome these problems, and this will now be discussed.

With the considerations set out above in mind, three boundary conditions were set when developing the new methodology. These were;

(i) To synthesise single, discrete compounds.

(ii) To work on a scale allowing full characterisation of any library member.

(iii) To use inert materials for any components in contact with solvents/reagents.

These boundary conditions then directed the project towards four operational requirements. These are;

(i) To contain supported compounds.

(ii) To have the ability to label contained compounds.

(iii) To react library members in parallel.

(iv) To reorganise library members for subsequent reactions.

To be able to contain the supported compounds comprising the library, microreactors were designed that would be used with the system. At this time, the use of microreactors had been described in solid-phase synthesis,[114, 115] but these were constructed from polypropylene. When the polypropylene microreactor described by Nicolaou *et. al.* was stirred in refluxing toluene, the microreactor dissolved, then a polypropylene mass was formed when the heat was removed and the solvent allowed to cool. As we required the ability to carry out reactions using quite harsh conditions, one of the design features of the POSAM™ was that all the wettable parts of the apparatus would be made from inert materials, namely glass or PTFE. Frit glass microreactors of various size, shape and frit porosity were constructed and then tested. This testing was carried out by filling the microreactor reaction well with preloaded *N*-Fmoc-(2*S*)-leucine Wang resin ester, swelling the resin in DMF, deprotection of the amine, then subsequent reaction with PyBOP® activated *N*-Fmoc-(2*S*)-phenylalanine, to give the resin bound dipeptide, within the microreactor reaction well. The microreactor design that was chosen for use in the POSAM™ apparatus is shown in Figure 2.1.

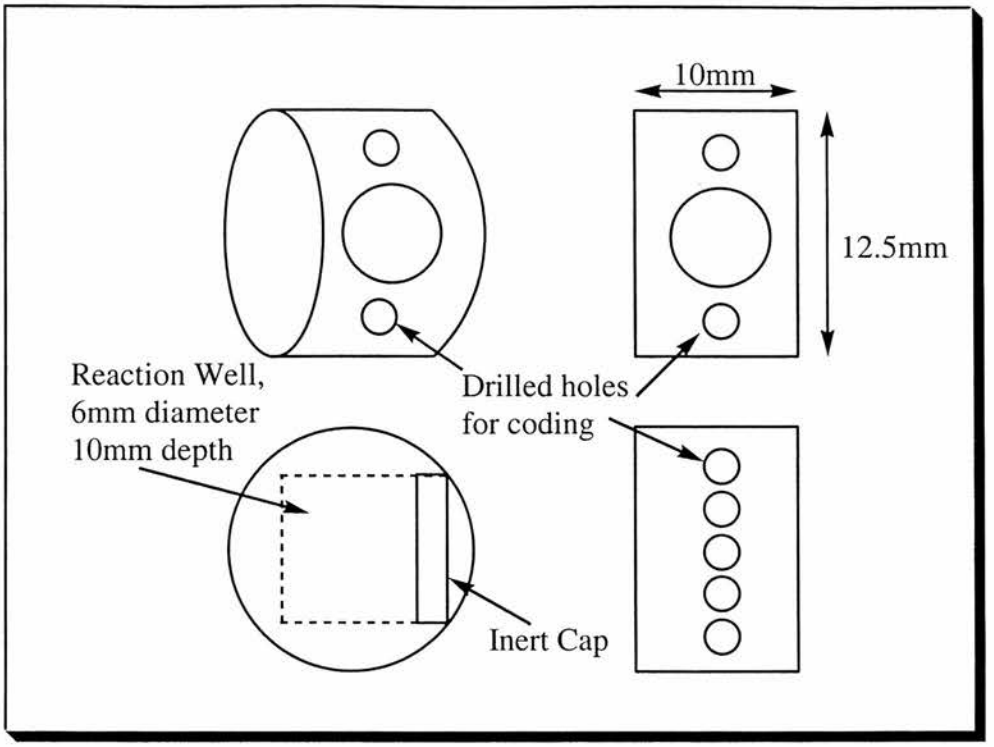

Figure 2.1: *Microreactor design for use in POSAM™ apparatus.*

The microreactor shown in Figure 2.1 is constructed from high density sintered (frit) glass, with a pore size of 40μm or less. The inert cap has two designs. The original format was constructed from silicon rubber, and is a push fit cap that fits tightly into the reaction well, leaving room for the resin to both swell and move in the well. The second design is a PTFE grub screw, which fits into a threaded reaction well opening, sealing the resin inside. This second design fits in with the original operating parameters that we set ourselves regarding the components of the apparatus. The coding holes that are shown on the microreactor hold coloured PTFE pegs, a different colour corresponding to a reaction that the microreactor and its contents have undergone. The entire microreactor, when fitted with the PTFE screw cap, is resistant to 2.5M BuLi in hexanes for longer than 72 hours, when stirred at 30°C.

In order to be able to expose more than one solid-supported component to any given reagent solution, so that concurrent parallel syntheses may be carried out, apparatus that enables the stacking of the microreactors in a column was looked at.

Jacketed vessel tubes, with an internal diameter of 13mm were constructed from glass tubing, then these jacketed reaction chambers were fitted with a sinter at one end, the bottom. The reaction chambers were made as jacketed vessels, thus enabling a wide range of chemistry that requires either low or high temperatures to be carried out. It was envisaged that it would possible to carry out reactions in the temperature range of -78 to 200°C. This, coupled with the chemically inert nature of all the components used in the apparatus, means that virtually every organic reaction can be carried out in the apparatus. The only problem with this is the instability of the solid support used in the reaction at elevated or reduced temperatures. The length of the reaction chambers is variable, thus enabling different numbers of microreactors to be stacked in the column. The smallest one in use holds three microreactors, while the largest holds around forty. The length of reaction chamber that is most frequently used is one that holds nine microreactors. The uppermost microreactor in the column is held in place by placing a PTFE coated spring on top. This is then held in place by a screw fit top, thus minimising any vertical movement of the microreactors in the reaction vessel when the system is subjected to filling and draining under nitrogen pressure, which could prove to be problematic. A simplified version of the POSAM™ apparatus is shown in Figure 2.2.

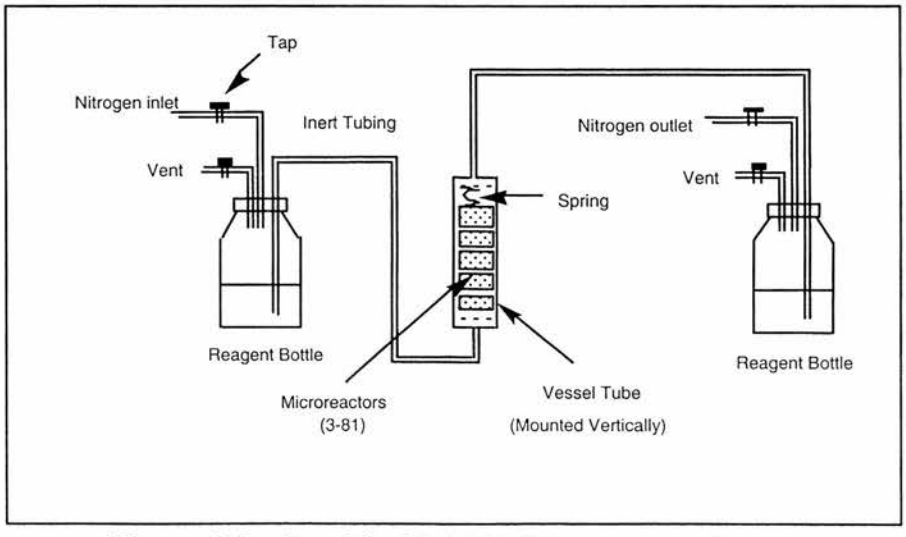

Figure 2.2: *Simplified POSAM™ apparatus design.*

The initial work with this system was carried out on the coupling of an amino acid, phenylalanine, to a resin bound amino acid, leucine, to form a solid-supported dipeptide. Although the chemistry is very well established, it was the proof of concept that was the important factor in this work. When the concept had been shown to work, then more interesting work could be carried out using the POSAM™ apparatus.

2.1.1. Development and optimisation of POSAM™ methodology for solid-phase organic synthesis.

The initial work with this apparatus was carried out on the attachment of an amino acid, phenylalanine, to a preloaded resin bound *N*-Fmoc protected amino acid, leucine. The resin was dry weighed into a microreactor, and placed in the reaction chamber, along with two others, giving three microreactors stacked in a column. DMF was then passed through the reaction chamber in order to swell the resin in the microreactor, then the resin bound amino acid was deprotected by treatment with 20% piperidine/DMF solution. After deprotection, the resin in the microreactors was washed by flushing DMF through the reaction chambers, and then the resin bound amino acid was reacted with a solution of PyBOP® activated amino acid in an NMM/DMF solution, as shown in Scheme 2.1.

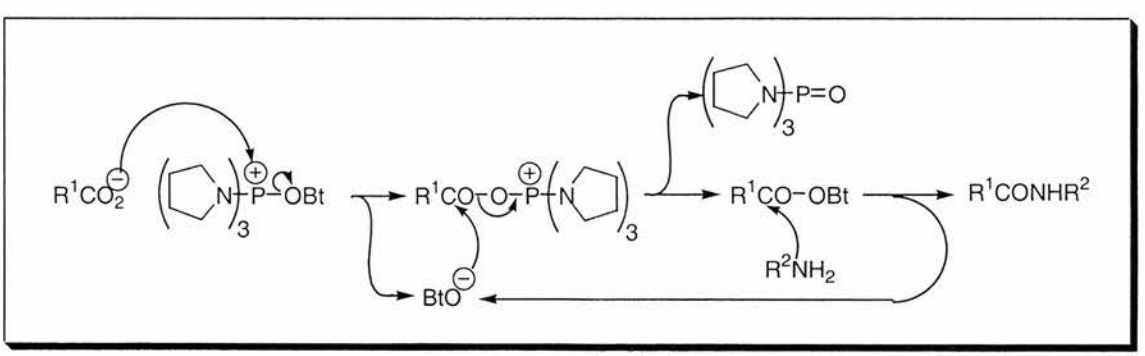

Scheme 2.1: *PyBOP® activated amino acid coupling reaction.*

Further deprotection, followed by cleavage from the resin using a 95:2.5:2.5 TFA:TES:H_2O mixture should afford the desired free dipeptide product. However, this

did not prove to be the case. With the POSAM™ apparatus set up in its initial configuration, Figure 2.3, the synthesis did not work.

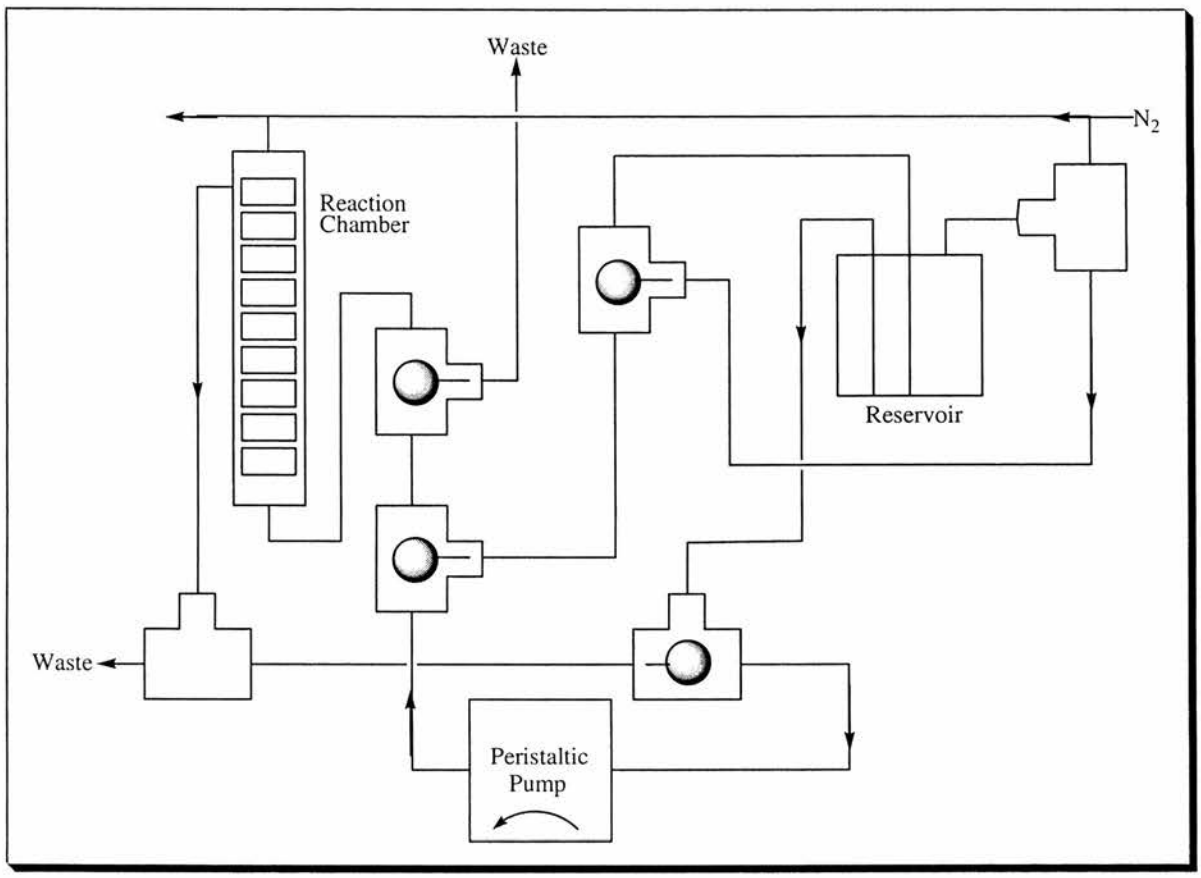

Figure 2.3: *Set-up of POSAM™ apparatus.*

In this configuration, solvents and reagents are pumped from the reservoir, through the tubing to the reaction chamber, through the microreactors, and then circulated around the system using the peristaltic pump. When draining was required, the action of the peristaltic pump was reversed, so solvents and reagents were returned to the reservoir. However, when draining the system, to completely remove all solvents and reagents, the system was pumped with no solvents in the tubing. However, the PTFE tubing used in the peristaltic pump was not designed for use under dry conditions, so on every occasion, failure of the tubing in the pump was observed. This led to leaks of solvents and reagents, and exposure to air. This was a major problem, so a different method for passing solvents and reagents through the POSAM™ apparatus and the reaction chambers, containing the microreactors, was sought.

In order to develop this method, a new reaction chamber, capable of holding only five microreactors was designed. Instead of the peristaltic pump passing solvents and reagents through the system, the solvents and reagents are introduced into the reaction chamber from the bottom, *via* a syringe, under an inert atmosphere of nitrogen, as shown in Figure 2.4.

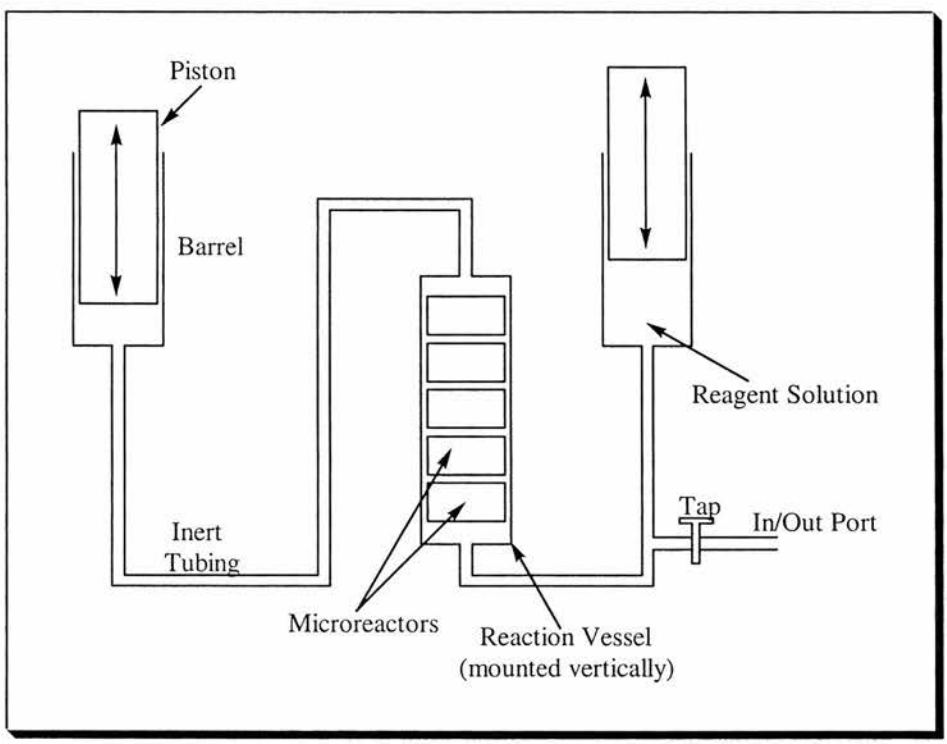

Figure 2.4: *Apparatus set-up used for 'little' POSAM™.*

To drain the reaction chamber of reagents, the plunger of the syringe is pulled out, bringing the contents back into the syringe, with everything still under an inert atmosphere. With this new apparatus set-up, the coupling of the resin bound leucine to phenylalanine was attempted again, this time using only one microreactor in the reaction chamber. Initial NMR results of the material cleaved from the solid support in this reaction indicated that coupling of the two amino acids had occurred. However, comparison of the ratio of the integrals for the CH_3 signal associated with leucine and the aromatic protons of the phenylalanine ring did not show the expected 6:5 ratio, but a

6:1.3 ratio. This data was consistent with a 26% conversion of the resin bound amino acid to the desired dipeptide product. The reaction was repeated under the same conditions, however, this time three microreactors were placed in the reaction chamber, to observe if the coupling across a number of microreactors was uniform. After washing, cleavage and NMR analysis, the material from the first microreactor, the one nearest to the source of reagents and solvents, showed a lower level of conversion than when only one microreactor was used. The observed ratio of phenylalanine aromatic protons to the methyl protons of leucine was 6:0.7, or approximately 12% coupling. A significant decrease in the coupling of the two amino acids was observed as distance from the reagent source increased, with microreactor 2 showing a 1.9% coupling, and microreactor 3 showing 1.8%. However, after all the previous attempts, this was the first time that any degree of coupling of the amino acid to the resin bound amino acid contained in the microreactor had been observed, albeit, only in a low percentage conversion.

The next step in the design process was to try and improve the percentage conversion in the bottom microreactor, and also to achieve a respectable degree of conversion in the other microreactors in stacked in the reaction chamber. As the observed coupling was incomplete, this indicated that one or more of the steps in the synthetic procedure using POSAM™ were causing the problem. Scheme 2.2 shows the synthetic sequence to produce the dipeptide.

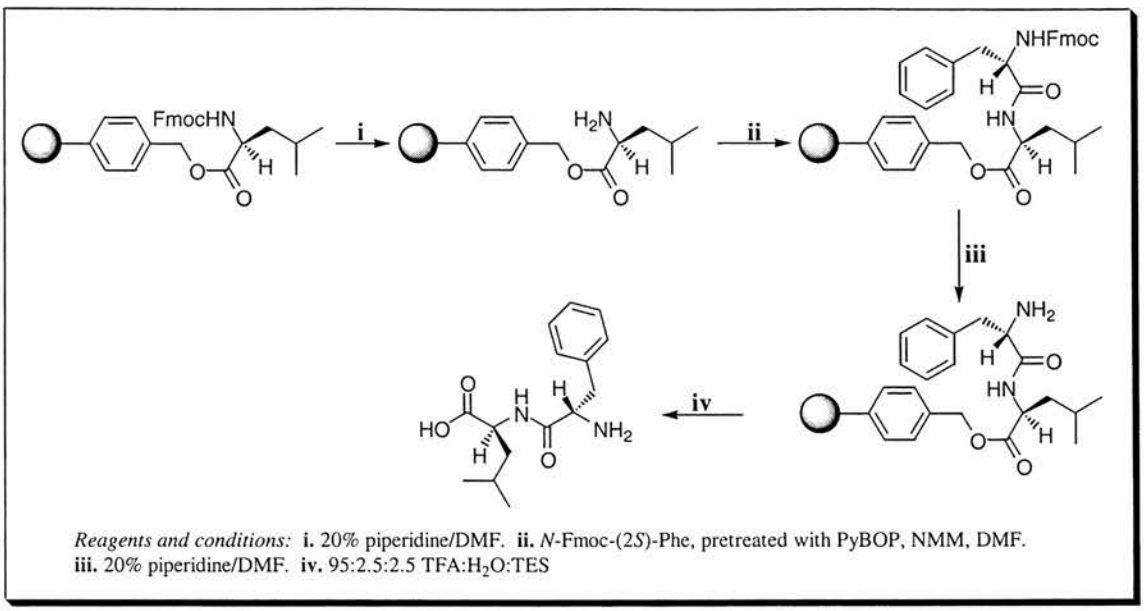

Reagents and conditions: **i.** 20% piperidine/DMF. **ii.** *N*-Fmoc-(2*S*)-Phe, pretreated with PyBOP, NMM, DMF. **iii.** 20% piperidine/DMF. **iv.** 95:2.5:2.5 TFA:H_2O:TES

Scheme 2.2: *Synthesis of Dipeptide on solid-phase using POSAM™ apparatus.*

To determine which step, or steps, in the synthesis was causing problems, giving low conversion of the amino acids to the dipeptide, each step was examined in detail. Examination of the NMR spectrum of the material cleaved from the solid support after all the synthetic steps should determine which of the steps was causing problems, as the distribution of the products in the cleaved material will indicate where the problem lies. If *N*-Fmoc-leucine were detected in the ^{1}H NMR spectrum of the cleaved material, after exposing the loaded resin to each of the steps **i-iii** in Scheme 2.2, then it would be conclusive that the deprotection step, step **i**, was not working. This could indicate that the piperidine solution was either not reaching the resin contained in the microreactors, or was not reacting efficiently with the resin. Detection of free leucine would indicate that either, step **i** had worked and the peptide coupling step, step **ii**, had not, or it could indicate that step **i** had not worked, but step **iii** had. The presence of *N*-Fmoc-phenylalanylleucine in the ^{1}H NMR spectrum would show that steps **i** and **ii**, the first deprotection and the amino acid coupling, had worked, but that step **iii** had not worked. The presence of phenylalanylleucine in the NMR spectrum would indicate that steps **i-iii** had worked, and the desired dipeptide product had been formed in the

microreactors. In the reaction previously mentioned where 26% conversion of the resin bound amino acid to the dipeptide was observed, the ratio of the leucine CH_3 to the phenylalanine aromatic protons indicated the presence of free leucine. However, no signals corresponding to the Fmoc protecting group were observed in the spectrum, indicating that the deprotection step was working, and the piperidine was getting into the microreactors, and hence to the resin bound amino acid. From this result, it was determined that either the initial Fmoc deprotection step, step **i**, was only partially successful, with the second deprotection step, step **iii**, removing all of the protecting groups, or that the peptide coupling step, step **ii**, was somehow being undermined by the presence of piperidine, which may have been left over from step **i**, in the solvent gel surrounding the resin beads in the microreactor reaction well. After the deprotection steps, the microreactors are washed with a fresh DMF solution. This is achieved by introducing DMF into the system, then passing the solvent back and forth over the microreactors for 30-40 minutes. This step is then repeated, using another portion of fresh DMF. Another reason for the coupling step having a low percentage conversion to the dipeptide product could be the presence of piperidine in the solvent gel that surrounds the resin beads. This is still present due to insufficient washing of the microreactors, or drainage of the system. The piperidine could then be reacting with, or affecting the PyBOP® activated amino acid, that is added to the reaction chamber for the coupling step, decreasing the amount available to react with the resin bound amino acid. This would then result in the reduced levels of conversion of the resin-bound amino acid to dipeptide product, as were being observed. The most practical way to remove this residual piperidine was to add another washing step to the synthesis protocol, and see if this was the problem step. Although this adds another 40-60 minutes to the deprotection cycle, if it leads to complete or near 100% conversion of the resin bound amino acid to the desired dipeptide product, then it would prove to be a

very important step. The synthesis of the dipeptide was repeated again, using the same apparatus as before, however, this time, washing the microreactors with three portions of DMF after every deprotection step with 20% piperidine/DMF solution. In this case, NMR analysis indicated quantitative (>97%) conversion of the resin bound amino acid to the dipeptide product from the integral ratio of the leucine CH_3 protons to the phenylalanine aromatic protons. However, as had been shown to be the case with previously attempted syntheses, a decrease in the percentage conversion of the resin bound amino acid to dipeptide product was observed with increasing distance from the source of the solvent/reagents, 4.8% in the second and 4.4% in the third microreactor. From these observed levels of conversion to the product, it would appear obvious that the flow of reagents and solutions into the microreactors is being hindered during the amino acid coupling step. To try and improve this diffusion of reagents through the microreactors, the reaction was carried out again, this time using an ultrasonic probe, inserted into the POSAM™ reaction chamber through a seal at the top. Ultrasound has previously been used as a method of agitation to enhance the rate of reactions on solid-phase.[156] The acceleration of the rate of the peptide coupling and cleavage steps in SPPS has been observed.[157, 158] It was thought that this method could be used to increase the percentage conversion in the coupling step of the dipeptide synthesis. When the reaction chamber had been completely filled with reagents, the ultrasonic probe was immersed in the solution, and turned on for 10 minutes. The chamber was then drained, refilled, and the process repeated. After completion of the synthetic sequence, and cleavage from the support, NMR analysis showed results comparable to previous reactions, with a 73% conversion in the first microreactor, 4.5% conversion in microreactor 2 and 5.1% in microreactor 3. The increase in the level of conversion in microreactor 3 is interesting to note, as this had never been previously observed. This would seem to indicate that the ultrasonic probe had caused an effect in the coupling

reaction, but only on the microreactor situated nearest to it in the reaction chamber. As the use of the ultrasonic probe had not given any improvement in the conversion of the resin-bound amino acid to the dipeptide product across three microreactors, methods of improving the coupling reaction were further investigated. This began by looking at the arrangement of the microreactors within the reaction chambers.

As was stated before, the reaction chambers are constructed from 13 mm diameter glass tubing, into which the 12.5 mm microreactors are inserted. The microreactors are randomly placed in the reaction chamber, giving the set-up shown in Figure 2.5.

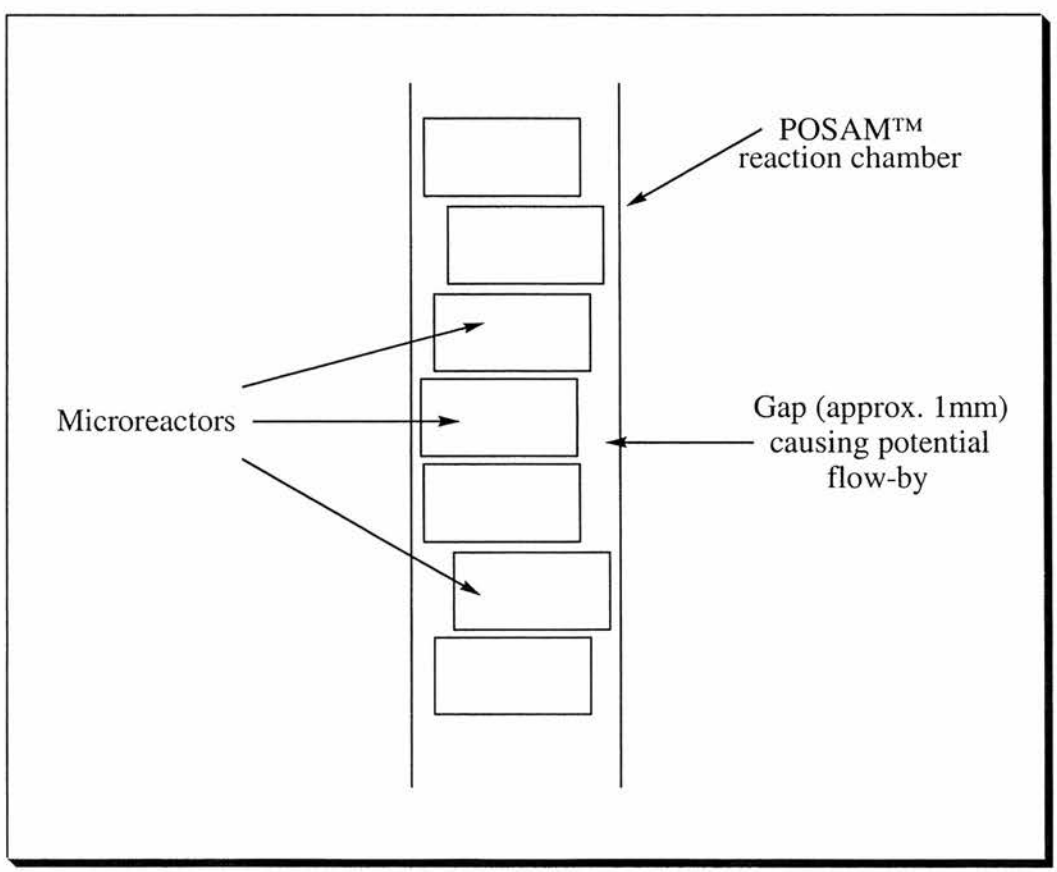

Figure 2.5: *Random arrangement to microreactors in the POSAM™ reaction chamber.*

Considering the dimensions of the constructed POSAM™ reaction chambers, and the microreactors, it can be seen that there is a significant difference of approximately 1 mm in their respective diameters. This void between the edges of the

microreactor and the reaction chamber walls. Arranging the microreactors in a random manner is intended to minimise any solvent flow-by that may occur. Due to the presence of the void, a basic explanation of the motion of fluids in a system such as the reaction chamber is required.

Fluid flow can be very complex, but in some situations can be represented by relatively simple idealised models. An ideal fluid is one that is incompressible (does not change density) and has no internal friction (viscosity). The path of an individual particle in a moving fluid is called a flow line. If this overall flow line does not change with respect to time, then the flow is known as steady flow. In steady flow, everything passing through the same point follows the same flow line. Figure 2.6,[159] shows patterns of fluid flow around a variety of obstacles, and also through a channel of varying cross section.

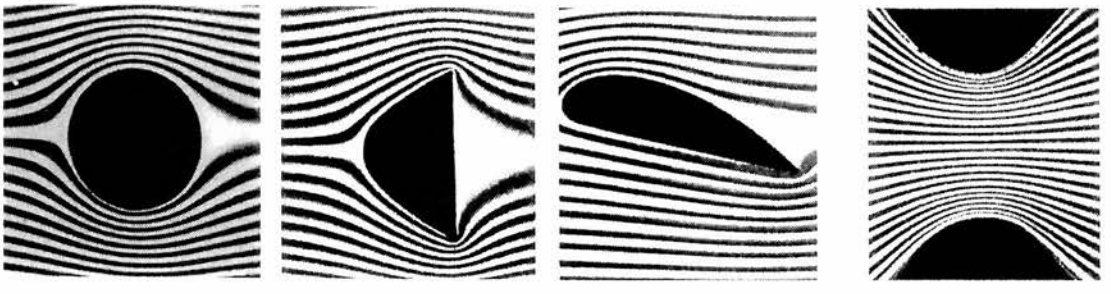

A **B** **C** **D**

Figure 2.6: *Examples of Laminar flow in fluid systems.*

(from University Physics by Young and Freedman, Copyright 1996, reprinted by permission of Addison Wesley Educational Publishers)

The images in Figure 2.6 were produced by injecting dye into water flowing between two closely spaced glass plates. The patterns produced are patterns indicative of laminar flow, where adjacent layers of fluid slide smoothly past each other and the flow is steady. At high flow rates, the flow can become irregular and chaotic. This is termed turbulent flow, and in this state there is no steady state pattern as the flow is changing continuously. If we consider **A** in Figure 2.6, the fluid flows around the

circular object in a smooth motion. If we consider this object to be one of our microreactors sitting in the reaction chamber with solvent being introduced from the bottom of the chamber, then although our microreactor is porous, and the object in the picture is not, the majority of the liquid being introduced into the system will flow around the sides of the microreactor, and straight up the reaction chamber walls. In this case, the fluid is flowing along the path of least resistance. This path will always be followed, as it is the direction of flow that requires the least energy. As the fluid flows between the microreactor and the reaction chamber wall, flow lines are formed, as the flow is steady. These flow lines then form a flow tube as shown in Figure 2.7.

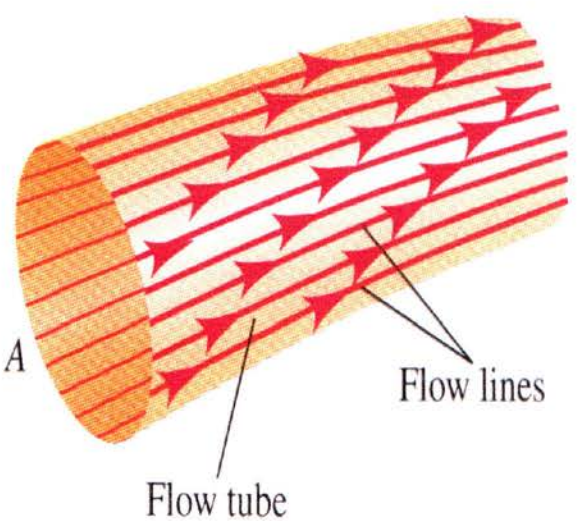

Figure 2.7: *A flow tube formed during the steady flow of a fluid.*

(from University Physics by Young and Freedman, Copyright 1996, reprinted by permission of Addison Wesley Educational Publishers)

From the very definition of a flow line, if the fluid is in steady state flow, then no fluid can cross the sidewalls of a flow tube, so the fluids in different flow tubes cannot mix. In our system, we can consider this phenomenon, and say that as the fluid is flowing between the microreactors and the reaction chamber walls, the fluid will continue flowing with the same velocity and direction until such a time as the microreactors are no longer in its path. There will be no movement of fluid from the flow tube into the microreactors in a sideways manner.

If it were possible to reduce the size of the gap between the walls of the POSAM™ reaction chamber and the microreactor, then the laminar flow would be reduced too, causing the solvents and reagents to travel through the microreactors, not around the sides. The first attempt at reducing this gap was tried with ordinary PTFE tape. The microreactors were charged with preloaded resin, and then the PTFE tape was wrapped around the surface of the microreactor, approximately 5 times, but not covering the top or bottom faces. The microreactors were then stacked on top of each other as would normally happen, and the attempted synthesis of the dipeptide was carried out. After cleavage, ^{1}H NMR analysis of the residue showed that the PTFE tape had reduced the percentage conversion to the dipeptide. This could be because that with the sides of the microreactor enclosed in PTFE tape, reagents such as piperidine could not be sufficiently washed out of the microreactors after the cleavage step. This is then giving the same end result of low percentage conversions as previously observed. However, very close to uniform coupling had been observed across the series of microreactors, with 7.5%, 3.2%, 8.7% and 9.1% detected from the first microreactor up the POSAM™ reaction chamber. This effect could be due to the PTFE tape having the desired effect, restricting laminar flow and directing the solvent flow through the microreactors. As enclosing the microreactors in PTFE tape had not had the absolute desired effect, a different approach was tried in order to improve the percentage conversion of the resin bound amino acid to the dipeptide product. Again, we considered the arrangement of the microreactors in the reaction chamber. The increased levels of conversion had only been observed in the first microreactor, at the bottom of the stack in the reaction chamber, nearest to the source of the solvents and reagents. Considering this microreactor showed that this position had a unique feature when compared to the positions of the other microreactors in the chamber. This feature is that the whole of the bottom face of the microreactor is exposed to the flow of solvents and

reagents. The other microreactors in the chamber only have their sides in contact with the solvent, and as was discussed earlier with respect to flow tubes, no solvent is going to flow in the sides of the microreactors. From this observation, it was deduced that the solvent flows into the first microreactor, reacts with the preloaded resin in the microreactor reaction well, and then passes through into the second microreactor, but the amount of solvent and reagents passing thorough is decreasing, as the solvent tends to take the path of least resistance, and flow between the microreactors and the reaction chamber walls. The only other microreactor that bears a resemblance to the bottom microreactor is the top one. This too has a full face open to solvents and reagents, but in this case, they are not being forced into the microreactor, but are flowing from around the sides, and filling the reaction chamber above the microreactor. Any reagents that get inside the microreactor in this position do so by some method of diffusion, not by direct motion.

By considering all this information, it seemed logical that the way to achieve 100% conversion of the resin bound amino acid to dipeptide product throughout the reaction chamber would be to make the bottom face of every microreactor available to the flow of solvents and reagents. After considering available options, it was decided that the best way to do this was to produce a washer that could be placed between each microreactors in the reaction chamber. The washers would be made from an inert material, so would still be inside the restraints of the original POSAM™ design criteria. Materials such as PTFE or silicon rubber, commonly used in many commercially available peptide synthesisers, were considered. The first washer developed was made from silicon rubber. Each washer is approximately 14 mm in diameter, slightly larger than the reaction chamber, with a 6 mm hole in the centre. The reasoning behind making the washer slightly bigger that the reaction chamber was to ensure a tight fit between the walls of the reaction chamber and the washer. This would then allow no

solvent to flow up the sides, but would direct the solvent flow through the hole in the middle, directly onto the reaction well of the microreactor, as shown in Figure 2.8. For clarity, the microreactor is drawn in white, above the black washer.

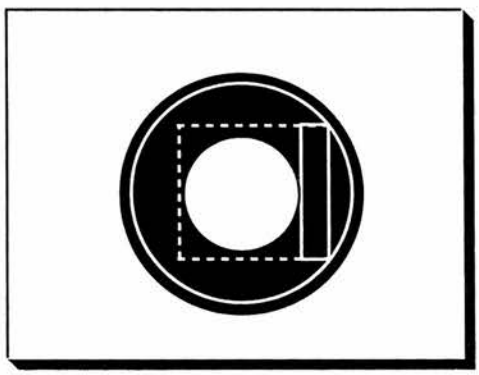

Figure 2.8: *POSAM™ microreactor and silicon washer.*

In order to test the washers under reaction conditions, three microreactors were charged with preloaded resin, and then inserted into the POSAM™ reaction chamber. However, in this experiment, a silicone washer separated each of the microreactors, as shown in Figure 2.9.

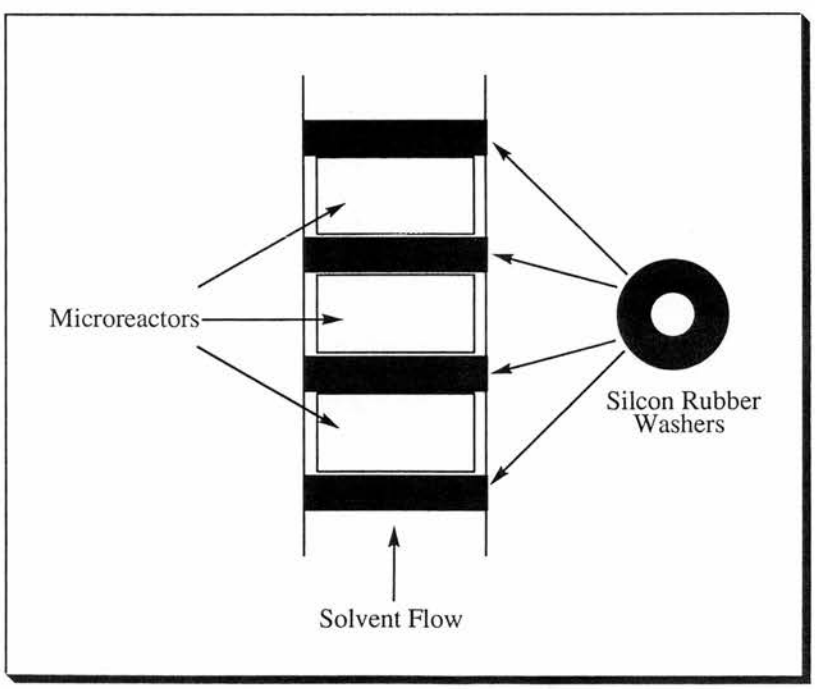

Figure 2.9: *Arrangement of silicon washers in POSAM™ reaction chamber.*

When inserting the washers into the reaction chamber, they were positioned using a glass rod, indicating that they were the required tight fit. This would then make it virtually impossible for any solvent to flow up the sides of the reaction chamber, by-passing the microreactors. The reaction was then carried out, including the extra washing step in the deprotection step that was shown to be required earlier. After all of the reaction steps, the material was cleaved from the solid support, and analysed by ^{1}H NMR. In the bottom microreactor, the one nearest to the solvent source, ratios of the signals in the NMR spectrum indicated 90.5% conversion of resin bound leucine to phenylalanylleucine. In the second microreactor, quantitative conversion was observed, and this was also the case when the third microreactor was analysed. By inserting the washers into the reaction chamber, between the microreactors, the flow-by of solvents and reagents had been stopped. This had solved the problem that was occurring of non-uniform coupling across a range of microreactors.

The original POSAM™ design was intended for use with larger numbers of microreactors in a reaction chamber, in order to produce large libraries of compounds. To show that the design would fulfil the design parameters, the concept of the washers had to be shown to work over a larger range of microreactors in the reaction chamber. For this experiment, the reaction chamber that holds nine microreactors was used, as this arrangement was considered to be the most frequently used POSAM™ reaction chamber in any experiment. The reactors were all charged with preloaded resin, and stacked on top of each other in the reaction chamber, all separated by silicon washers. The first step of the synthesis is passing DMF around the system through the microreactors, so that the resin within the microreactor reaction well can swell. When carried out with no washers in the system, solvents were transported around the system using the syringe arrangement. However, with the silicon washers separating the microreactors, the use of a syringe to pump solvent was very difficult. This was due to

restrictions in the system causing a build up of internal pressure. To try and overcome this problem, a new apparatus set up was developed. This new set-up utilised a solvent reservoir as previously outlined in one of the POSAM™ designs. Instead of using a peristaltic pump to pass solvent through the microreactors, a constant and regulated flow of an inert gas, nitrogen or argon, at a pressure ranging from 0.4 to 0.7 atmospheres was used. A schematic diagram of the new POSAM™ apparatus set up is shown in Figure 2.10.

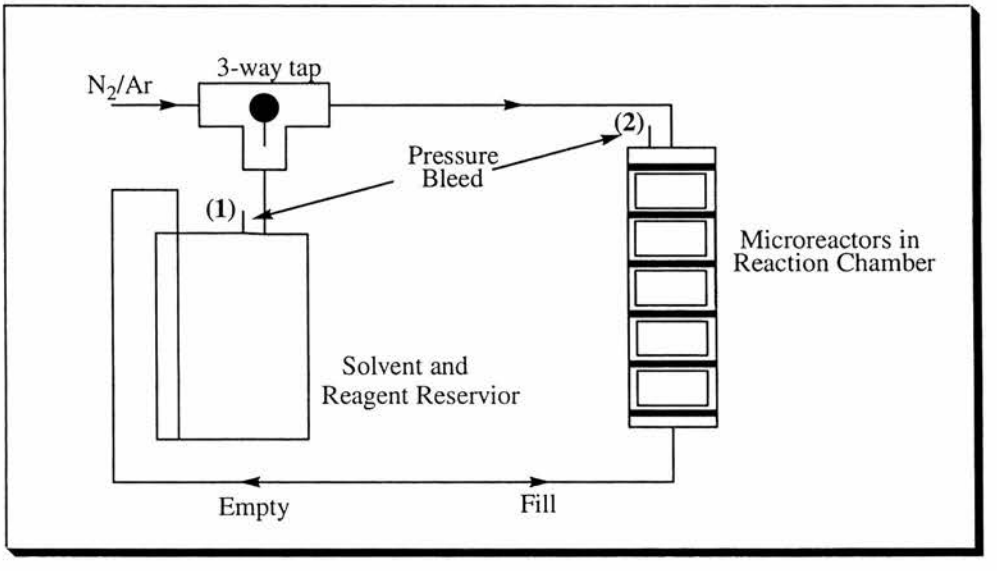

Figure 2.10: *Schematic of new POSAM™ apparatus arrangement.*

When using this new POSAM™ apparatus arrangement, the inert gas flow was also causing movement of the microreactors and silicon washers vertically in the reaction chamber, due to the restrictions caused by the washers. This was a potential problem, as if the microreactors are not positioned directly on top of the silicon washer in the reaction chamber, then the conversion of the resin-bound amino acid to product could be reduced, as the problem of solvent and reagent flow-by could appear again.

To fill the reaction chamber with solvent from the reservoir, pressure bleed **2** is opened, and the solvent flows freely. When the solvent front has passed above all of the microreactors in the reaction chamber, pressure bleed **2** is closed, and pressure bleed **1** is now opened. At this point, the position of the 3-way-tap is also changed, so that the

inert gas flow into the solvent reservoir, which is making the solvent flow around the system, is stopped. By moving the 3-way-tap, the gas flow now goes through the reaction chamber, and forces the solvent to flow in the opposite direction, back into the reservoir. When the first experiment using this new set up was carried out, it was observed that when filling the reaction chamber with solvent, the microreactors were wetting from the inside. The solvent was then passing through the sides of the microreactors, before passing onto the next microreactor in the stack. This would appear to show that the solvents and reagents were flowing into the microreactor reaction well, which contained the preloaded resin. It was also noticed that when the position of the 3-way-tap was moved, and the solvents returned to the reservoir, the microreactors returned to their original state and colour, indicating that they were completely dry and drained. This would seem to show that the washing and rinsing procedures followed in the synthesis would now be more effective, as all of the excess reagents were being forced out of the system by the flow of inert gas. For the synthesis of the dipeptide, all the normal washings, coupling and deprotection steps were carried out, as for the other POSAM™ reactions. After removal from the reaction chamber, the microreactor nearest to the solvent source (1), the microreactor in the middle of the reaction chamber (5), and the uppermost microreactor (9), were removed, and the material cleaved from the solid support and analysed by ^{1}H NMR. The results were as good as those seen in the case of three microreactors, with 100% conversion of the resin bound amino acid to the dipeptide observed in microreactor 1, 100% conversion in microreactor 5 and 97% conversion in microreactor 9. On the basis of these results, it was assumed that there was a uniform coupling across all nine microreactors present in the POSAM™ reaction chamber. The quantitative conversion of the resin-bound amino acid to dipeptide product had now been observed across a range of nine microreactors. The experiments described are represented graphically below, showing the percentage

conversion of the resin-bound amino acid to dipeptide product, relative to the position of the microreactor in the POSAM™ reaction chamber.

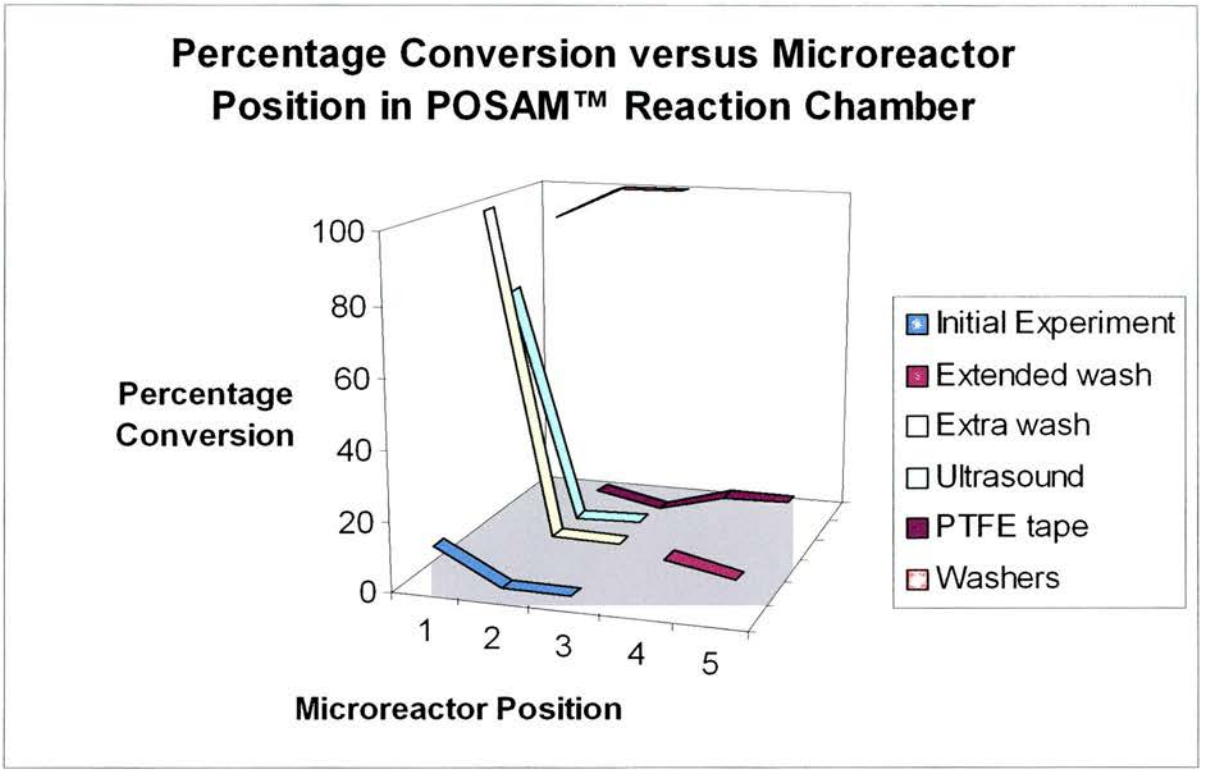

Graph 2.1: *Percentage Conversion versus Microreactor Position in POSAM™ Reaction Chamber.*

2.1.2. Synthesis of a tripeptide library using POSAM™ methodology.

Now that the POSAM™ apparatus and method had been optimised for the coupling of an amino acid to a resin-bound amino acid to form a dipeptide, the extension of this method to the production of a library of compounds was carried out. A library of tripeptides, consisting of all possible combinations of phenylalanine, alanine and valine, twenty-seven compounds in all, was to be produced. Nine microreactors were charged with 25 milligrams of *N*-Fmoc-phenylalanine-Wang resin ester, nine microreactors with 25 milligrams of *N*-Fmoc-valine-Wang resin ester and another nine charged with 25 milligrams of *N*-Fmoc-alanine-Wang resin ester, and the microreactors were then sealed and labelled appropriately. The microreactors were then assembled in three POSAM™ reaction chambers as shown in Figure 2.11.

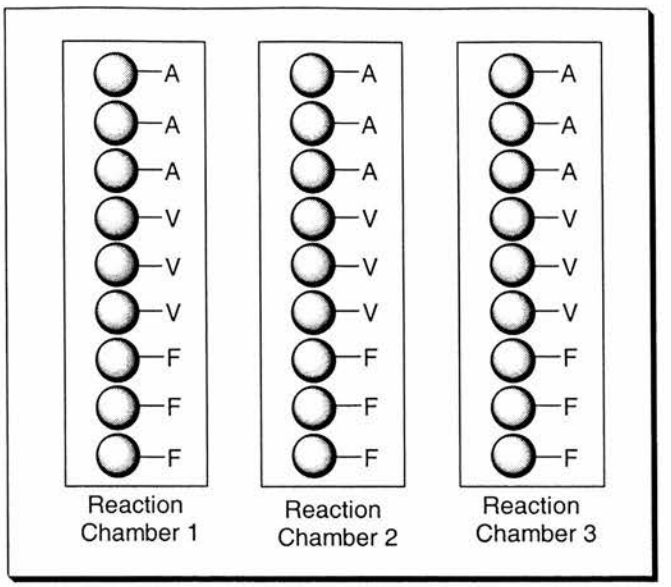

Figure 2.11: *Arrangement of microreactors in POSAM™ reaction chambers.*

The reaction chambers were first treated with DMF in order to swell the resin contained in the microreactors, followed by Fmoc deprotection using 20% piperidine in DMF solution. After washing with DMF to remove all traces of piperidine from the resin gel, each of the reaction chambers were treated with a 40 fold excess of PyBOP® activated amino acid dissolved in a 0.4 M solution of NMM in DMF. The amino acids used were phenylalanine in reaction chamber 1, valine in reaction chamber 2 and alanine in reaction chamber 3. This solution was passed over the microreactors for 1 hour, and then the microreactors were left standing in the solution overnight. After draining and washing with DMF, the methanol was passed through each of the reaction chambers, to contract the resin in the microreactors. This was carried out to eliminate any problems that may arise during the next step in the synthesis, the 'split and mix' step.

The microreactors were removed from the reaction chambers and reassembled such that each reaction chamber now contained one full set of nine dipeptides, Figure 2.12.

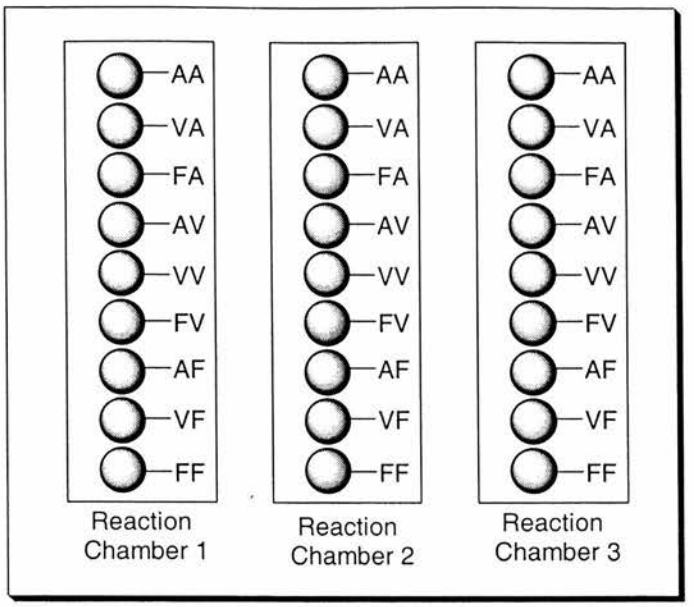

Figure 2.12: *Arrangement of microreactors in POSAM™ reaction chambers after 'split and mix' step of synthesis.*

The reaction chambers were again treated with DMF first to swell the resin in the microreactors, followed by Fmoc deprotection. After washing and draining the reaction chambers were treated with a 40-fold excess of a PyBOP® activated amino acid solution, the same amino acid combinations described earlier, for 1 hour. The microreactors were then allowed to stand in the solution for 8 hours, drained and washed to give a library of twenty-seven, resin-bound *N*-Fmoc protected tripeptides. Final Fmoc deprotection and washing gave the product tripeptide library arranged in the microreactors as shown in Figure 2.13.

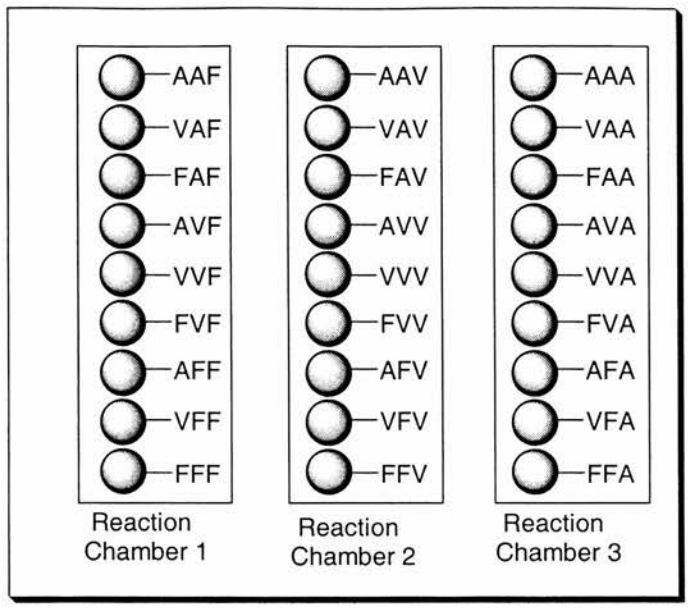

Figure 2.13: *Arrangement of tripeptide products in POSAM™ reaction chambers.*

Methanol was then passed through each of the reaction chambers to contract the resin in the microreactors and then the reaction chambers were drained and dried under a stream of nitrogen for 1 hour. The microreactors were removed from the reaction chambers and placed into twenty-seven separate premarked vials. The free products were obtained through the separate hydrolytic cleavage of the resin functionalised materials with a 95%:2.5%:2.5% mixture of TFA:H_2O:TES. The resin was removed from the cleavage mixture by filtration, and then the mixture was concentrated under reduced pressure. To progress to this stage in the synthetic procedure, from having charged the microreactors with resin had taken approximately 30 hours in total.

To determine the quality of the tripeptide library, several of the twenty-seven residues were taken and dissolved in deuterated water, then analysed by ^{1}H NMR spectroscopy to calculate the overall efficiency of the synthesis. This was determined by the comparison of specific regions in the ^{1}H NMR of each compound, these being the aromatic protons of compounds containing phenylalanine, the signal of the two CH_3 methyl groups of valine and the CH_3 methyl group of alanine. Based on the integrals

from these regions, the efficiency of the synthesis was judged to be greater than 95% in each of the library members investigated.

2.1.2. Synthesis of IMPase Inhibitor Library.

The POSAM™ methodology was utilised to prepare a library of potential inhibitors of IMPase, which had been identified from molecular modelling studies carried out in the group. To be able to prepare the library using our POSAM™ methodology, resin immobilised epoxide, **80**, had first to be prepared. This was done by carrying out the synthetic procedure shown in Scheme 2.3, as reported by Shultz *et. al.*[160]

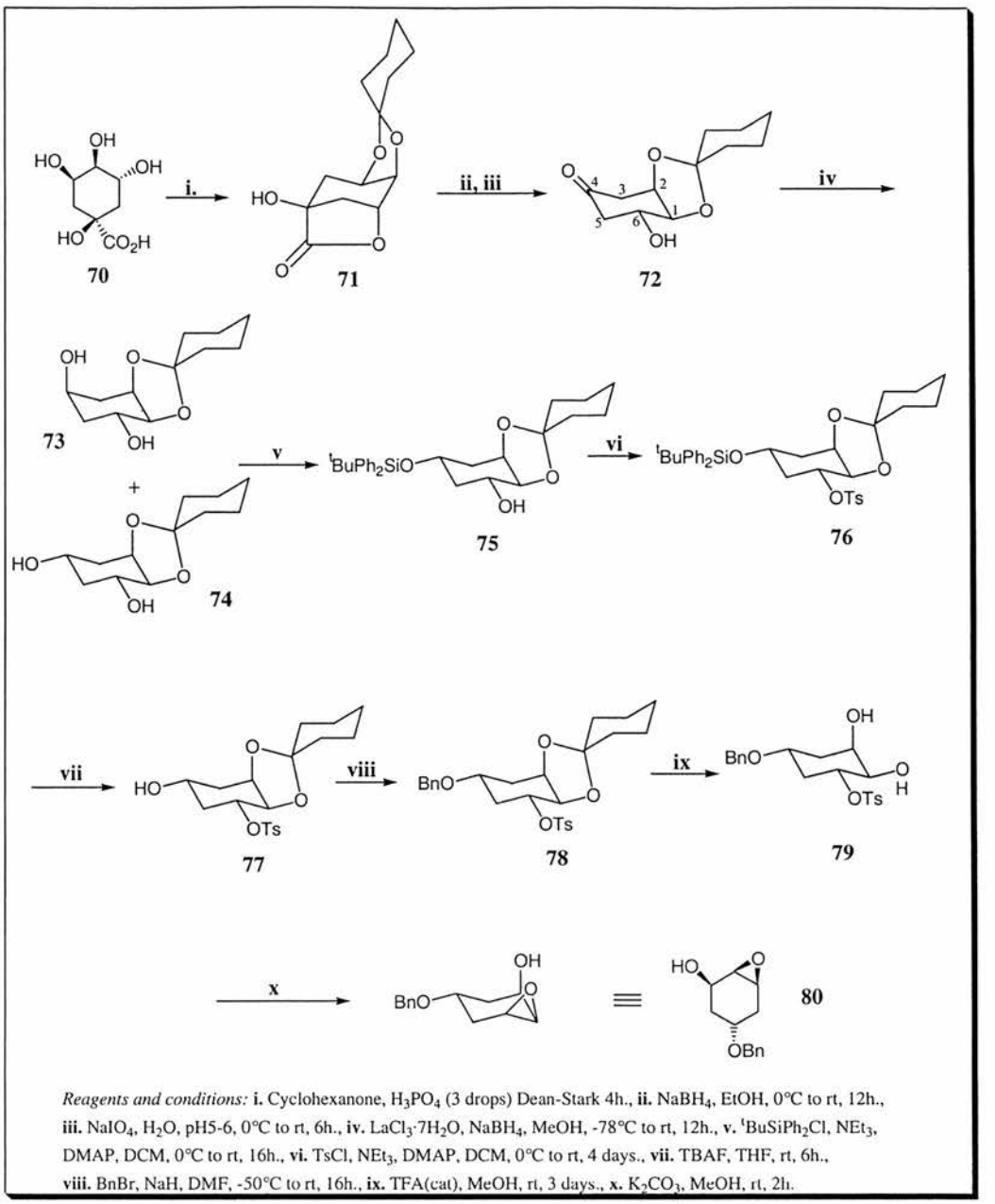

Scheme 2.3: *Synthesis of epoxide used in synthesis of IMPase inhibitors.*

After the epoxy alcohol had been synthesised, the next step was the attachment of this to solid support. The epoxide was firstly treated with sodium hydride in DMF and then added to a stirring suspension of Merrifield resin in DMF. The mixture was stirred overnight at room temperature to give the polymer-supported epoxide, **81**, Scheme 2.4.

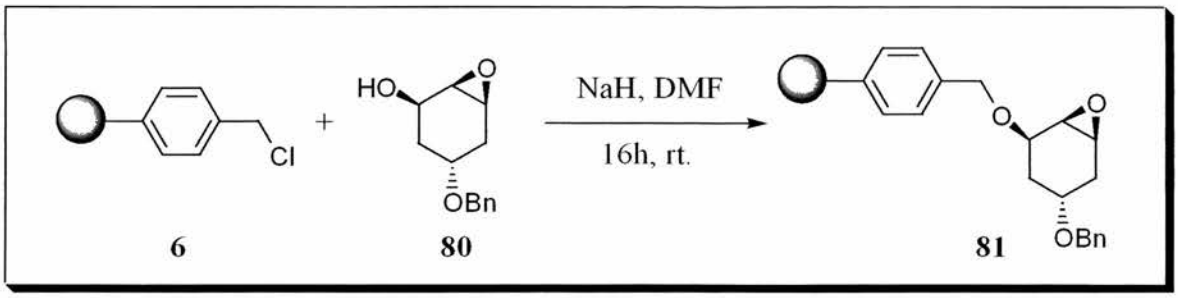

Scheme 2.4: *Immobilisation of epoxide for IMPase inhibitor synthesis.*

Previous work on the opening of this epoxide in the solution-phase had already been carried out in the group, and so the optimum conditions for opening the epoxide had been established.[160] This method had also been successfully applied within the group to open the epoxide when supported on Merrifield resin. This method and subsequent phosphonylation, to produce a library of potential IMPase inhibitors, is shown in Scheme 2.5.

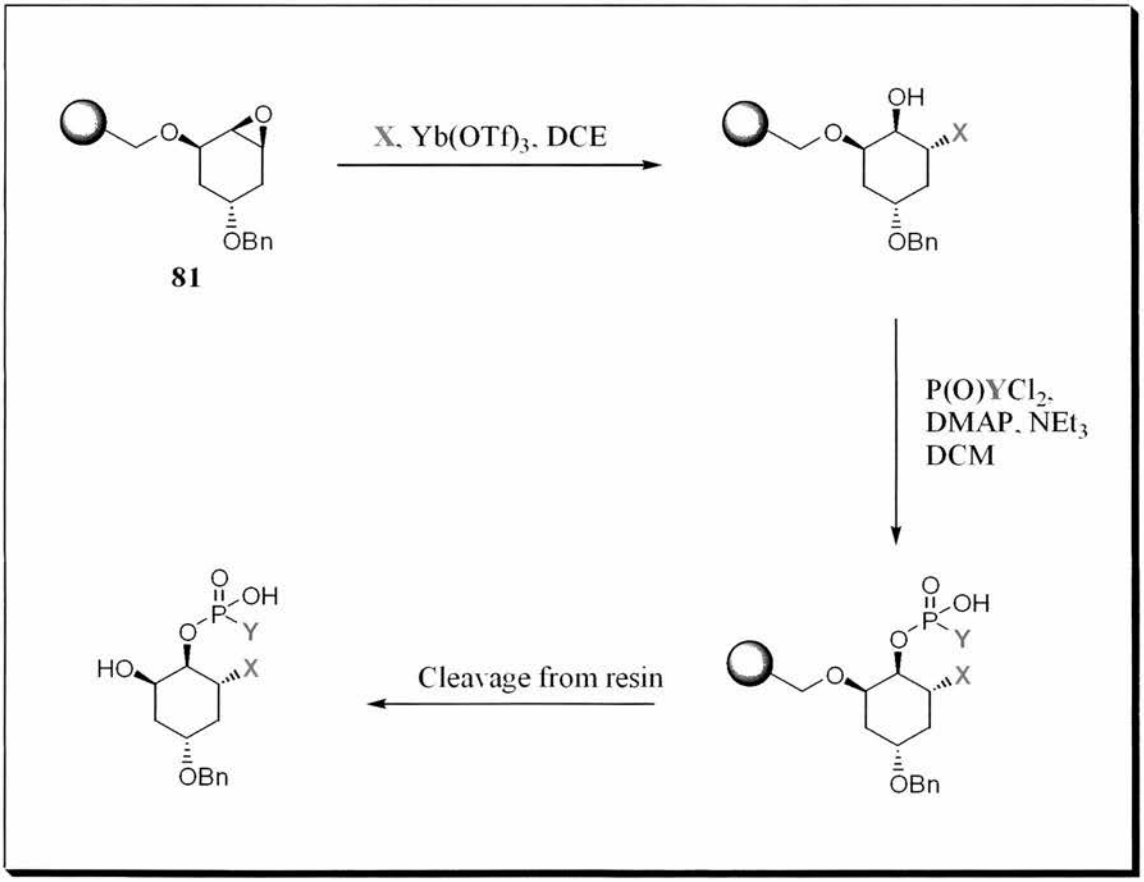

Scheme 2.5: *Opening and Phosphonylation of Support bound epoxide* **81**.

In Scheme 2.5, diversity is introduced into the library during the epoxide ring-opening step, with the introduction of X. A further degree of diversity is then introduced in the phosphonylation step, with the introduction of Y. A target library of 18 compounds was the aim for this synthesis, with six different compounds, methanol, benzyl alcohol, phenethyl alcohol, butylamine, propylamine and phenethylamine, used to open the epoxide. In the phosphonylation step, three compounds were to be used, methylphosphonic dichloride, ethylphosphonic dichloride, and propylphosphonic dichloride. This gives the library of compounds shown in Figure 2.15. The rationale behind chosing these compounds comes from previous work carried out in the group. During previous syntheses of IMPase inhibitors, the compounds **82** and **83**, Figure 2.14, have been identified as substrates when tested with the enzyme.

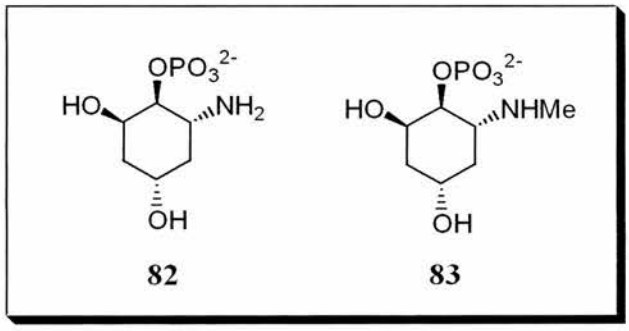

82 **83**

Figure 2.14: *Substrates of IMPase.*

As the inhibitors of IMPase previously produced had contained an oxygen atom attached at the C-6 position, this work lead to the belief that a nitrogen atom could instead replace this oxygen atom. It was also expected that the resulting amine functionality would be protonated at physiological pH, resulting in an overall charge decrease on the molecule. It would also make the compounds less polar, helping them to cross the blood-brain barrier. Modelling work previously carried out on this project has shown that one of the oxygen atoms on the phosphate group is free, and is directed towards a known lipophilic pocket in the enzyme, made up of Leu-42, Val-140 and

Ser-165. With the inclusion of side chains at the C-6 position, it also seems reasonable to believe that these sidechains would be able to fit into the same lipophilic pocket.

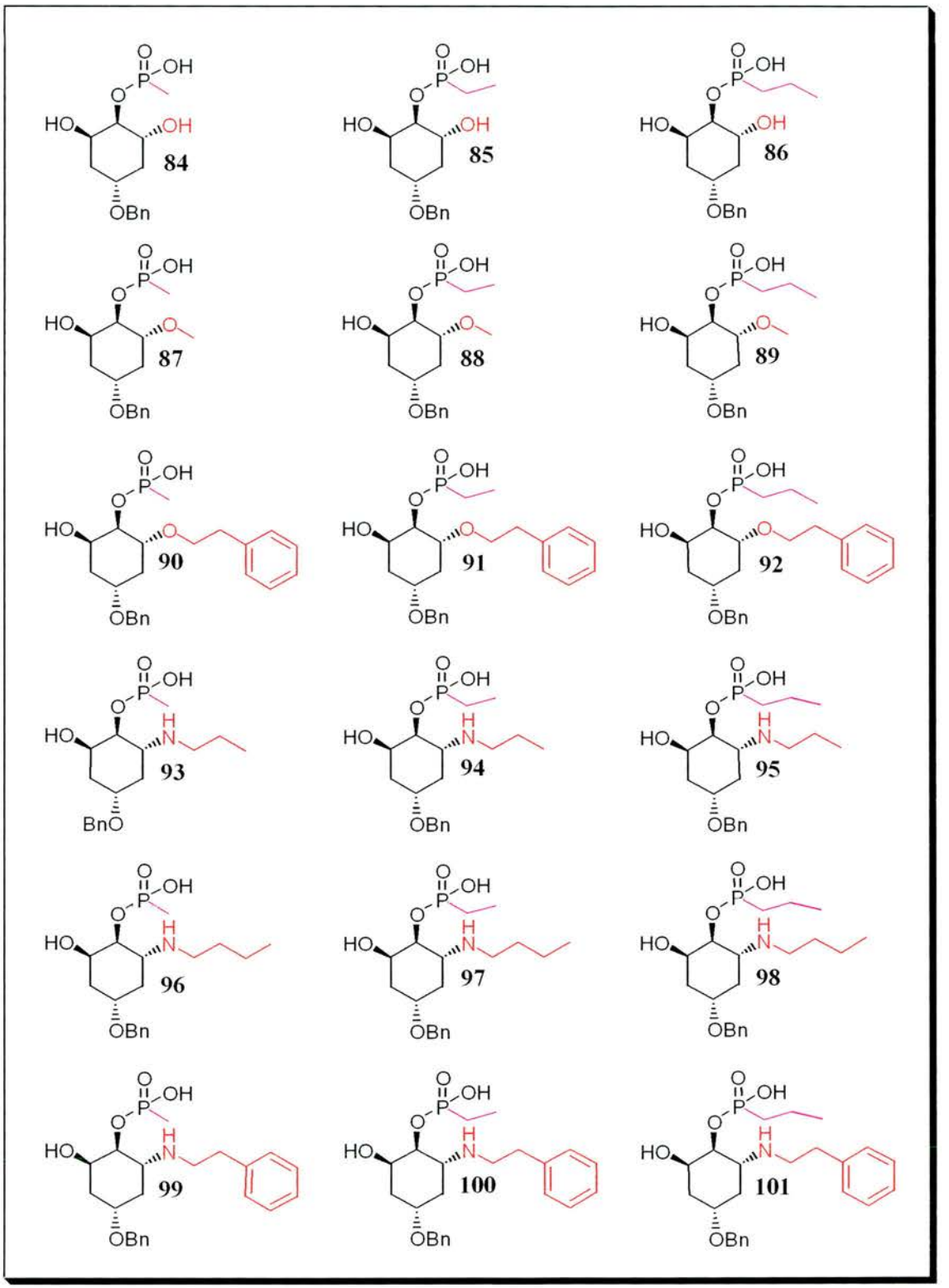

Figure 2.15: *Proposed library of potential IMPase inhibitors.*

Simultaneous replacement of one of the oxygen groups on the phosphate, with an alkyl group, to give a phosphonate, or an alkoxide group, giving a phosphodiester, should allow these side chains to be directed straight through the lipophilic pocket, making the binding tighter, thus giving better enzyme inhibition. This also gives a further reduction in the overall charge on the molecule.

Considering the above synthetic strategies, two classes of compounds were chosen for the proposed library synthesis. These were aminophosphonates, and aminophosphodiesters. The attempted synthesis of aminophosphonates is discussed in this work. It was hoped that these compounds would be neutral in overall charge at physiological pH, and so they would offer much improved bioavailability *in vivo*.

The attempted synthesis of the compound library outlined in Figure 2.15, was carried out using our POSAM™ technology previously discussed. In the opening of the epoxide on solid support, the dry resin was first suspended in 1,2-dichloroethane, then ytterbium (III) trifluoromethanesulfonate (triflate) and the alcohol or amine were added to the resulting suspension. In the corresponding solution-phase reaction, the mixture is then stirred at reflux. The design of the POSAM™ apparatus supports the use of a wide range of reaction temperatures, -78 to 200°C, however, a method of applying heating or cooling to the system had never been investigated. The apparatus set-up for the synthesis of the library of IMPase inhibitors consisted of six POSAM™ reaction chambers, each with nine microreactors containing solid-supported epoxide. There are two methods available for carrying out the reaction at an elevated temperature, which are;

(1) To heat the solvent reservoir prior to the solvent and reagents entering the POSAM™ reaction chamber, so that the elevated temperature has already been reached.

(2) To heat a liquid medium, such as water or oil, depending on the temperature required, and then to pass this heated liquid through the jacketed POSAM™ reaction chambers, and heating the solvents and reagents through the vessel walls.

In method one, the solvent reservoir would have to be suspended in a heated source, such as a water or oil bath, and the solvent then passed through the microreactors under inert gas pressure as normal. Using this method would require a large elevated temperature bath, introducing risks into the method. There could also be problems with differences between the temperature of the reagent mixture leaving the solvent reservoir and the temperature of the mixture when it passes through the microreactors. Due to these two problems, method one was abandoned, and method two further investigated. In method two, a relatively large heated source is still required, but the solvent reservoirs are not being placed into this, so one element of risk is eliminated. It would seem that the best way to heat the jacketed vessels would be to use some form of pump to pass the heated medium through the reaction chamber jackets, with either an internal or external heating source. However, the problem of differences in temperature between the jacketed vessels still exists. In the initial set-up of the apparatus, the six reaction chambers were assembled with the heating jackets connected in series, as shown in Figure 2.16, and heated water was passed through the reaction chamber jackets using a heating water pump. The water was re-circulated from a single source.

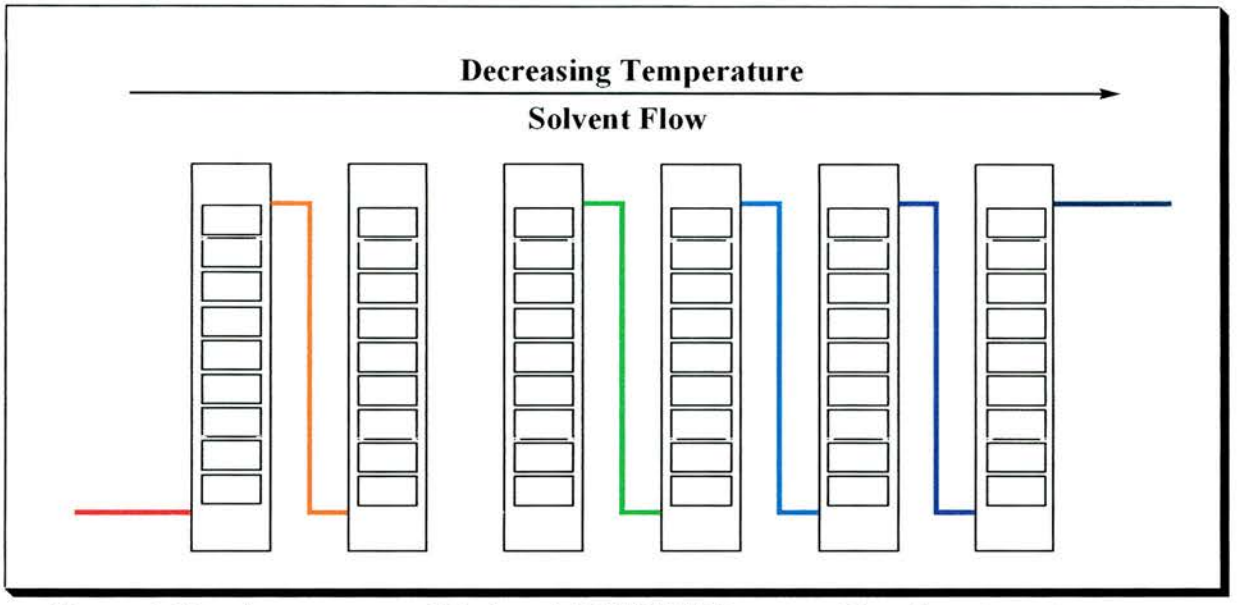

Figure 2.16: *Arrangement of Jacketed POSAM™ Reaction Chambers in series.*

Although never investigated, if a change in the temperature of the heat source occurs, *i.e.* cooling in and between the reaction chambers, then differences in the temperature of the heating jacket will also occur. This will then give non-uniform reaction conditions across the series of POSAM™ reaction chambers. There would appear to be two methods to solve this problem. Firstly, the tubing between each of the reaction chambers could be insulated. This may still result in a slight temperature reduction in the heating jacket of the first reaction chamber relative to the final reaction chamber in the series, but this difference would be significantly reduced. The other available solution is to take the POSAM™ reaction chambers out of series, and apply heat to each one individually. To achieve this, a device that diverts the flow of the heating medium to each of the reaction chambers had to be designed and tested. The first piece of apparatus tested was a six-armed distillation head. The distillation head was attached to tubing from the water heater, and to this were added six further pieces of tubing, each one connected to the POSAM™ reaction chamber heating jackets. The water exiting the heating jackets was then returned to the water source and the water re-circulated through the system. When the set-up was tested, constant water flow was only observed through three of the pipes. All attempts at removing air bubbles and

voids in the tubing did not improve the situation. So, three of the arms of the distillation head were blocked. This gave, in effect, a three-way splitter, resulting in three constant flows of water. When the reaction chambers had been assembled in series, reduction in medium temperature between the first and last reaction chamber had been considered a problem. Now, rather than six reaction chambers in series, two chambers were connected together. Although the temperature would probably change between the two chambers as outlined previously, the difference would not be significant. When measured, the temperature difference between the water flowing out of the heater, and the water flowing out reaction chamber heated jacket was found to be 2°C. The heated water pump was then tested to determine the temperature that could be reached. It was found that at 50°C, the heater and pump had an automatic cut-off. As this was the case, then reaction was carried out at 45°C, a temperature that could easily be controlled, but not high enough to carry out the reaction under reflux conditions. The solid-supported epoxide, **81**, was weighed into a series of twenty-seven microreactors, which were then placed into the POSAM™ reaction chambers in columns of nine. The ytterbium (III) triflate was weighed into reagent bottles, ready for pumping through the system, and then dissolved in DCE. At this point it was noted that the ytterbium (III) triflate was of limited solubility in DCE, and would not all dissolve. This was a major concern for the work to be carried out, as any residual particulate material in the solution could lead to blocking of the sinters in the POSAM™ apparatus. Alternatively, it could also lead to blocking of the pores in the microreactors. If this occurred, then the flow of solvents and reagents into the microreactors, would be hindered, and so would prevent any reaction occurring. In order to dissolve all traces of ytterbium (III) triflate, and remove the possibility of any blockages, a two solvent system was investigated, by adding a second solvent to the mixture. Initially, acetonitrile was found to dissolve the ytterbium (III) triflate that would not go into solution, and so a 2:1 DCE/acetonitrile solvent

mixture was used in the reactions. The resin-bound epoxide, **81**, was then reacted with the corresponding alcohols. Scheme 2.6 shows the set up of the microreactors in the reaction chambers, and the reactions that were carried out.

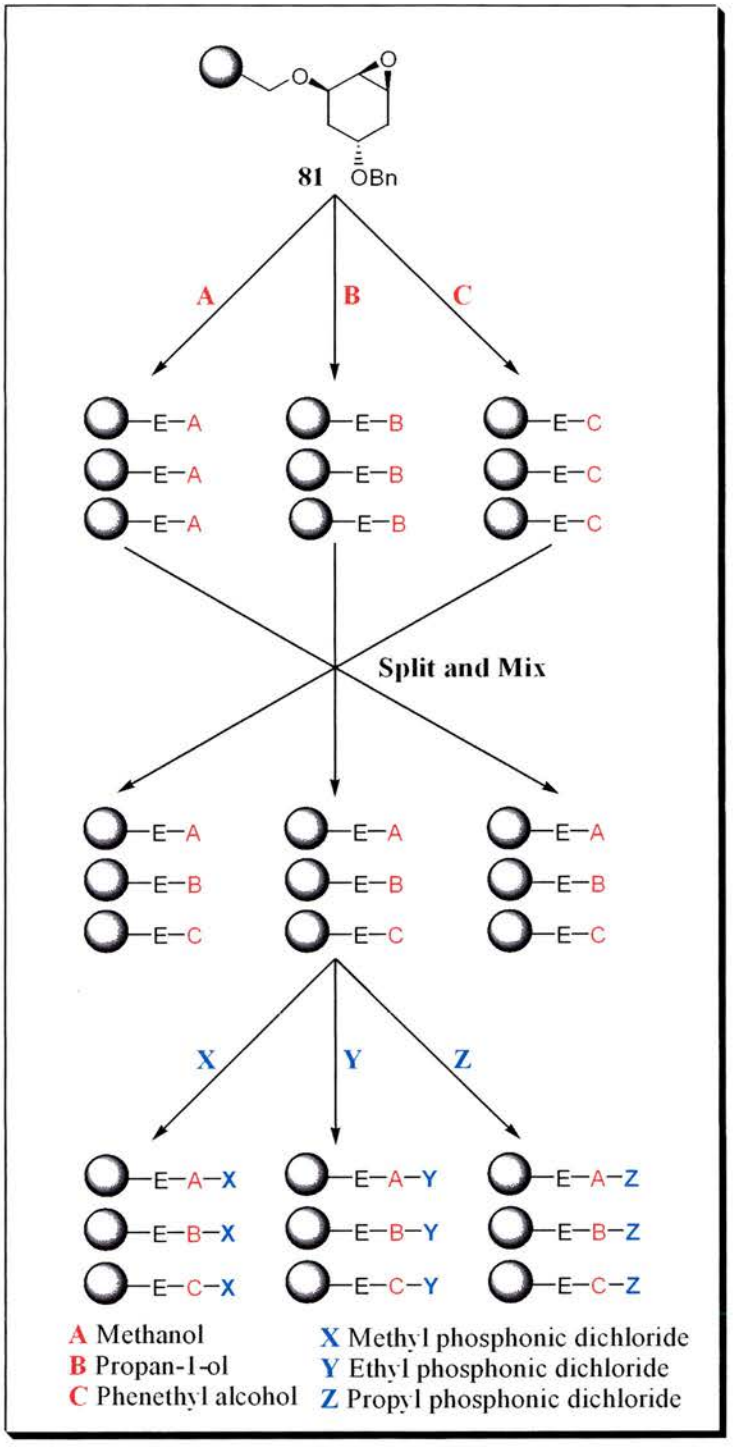

Scheme 2.6: *Arrangement of Microreactors in POSAM™ reaction chamber for epoxide opening.*

The reagents and solvents were pumped through the POSAM™ reaction chambers using nitrogen pressure, alternating the flow of gas to fill then empty the reaction chambers in 30 minute cycles. At the same time as filling and emptying, the jacketed reaction chambers were heated to 45°C by water being pumped from the water pump. The reagents were pumped through the reaction chambers for 12 hours, then the chambers were completely filled, and left to stand at 45°C overnight. After this period, pumping of the reagents and solvents was started again and continued for another 12 hours. The chambers were then drained of all reagents and solvents under nitrogen pressure, and the microreactors were washed with DCE. This was carried out in order to remove all traces of excess reagents that may have been trapped in the polymer or still present in the system. After washing, the microreactors were then washed with methanol, to contract the resin inside the microreactors. This was carried out, as problems had been previously encountered when transferring microreactors between reaction chambers in the 'Split and Mix' part of the synthesis. If the resin has not been contracted, there is an outside chance that the still swollen resin may force the stopper from the hole in the microreactor. If this happens, then the resin-bound compound is lost from the microreactor. The microreactors were then removed from the reaction chambers, and redistributed into the arrangement shown in Scheme 2.6 after the 'Split and Mix' step. The microreactors were then washed with DCM, to re-swell the resin inside them, and then treated with the designated phosphonylation agent. The solvent and reagents were again pumped through the system under nitrogen pressure for 12 hours, then left in the reaction chamber overnight. This was repeated, then all the excess reagents were washed away with fresh DCM. The resin inside the microreactors was then contracted with methanol for the reasons outlined earlier, and then dried under a flow of nitrogen. The microreactors were then removed from the reaction chambers

for analysis of the synthesised compound on the solid support. However, the analysis of these compounds was never carried out.

The next step in the library preparation was the synthesis of the aminophosphonate sub-library. As discussed earlier, the addition of acetonitrile to the DCE solution had solved the problem of the solubility of the ytterbium (III) triflate catalyst. For the preparation of the aminophosphonate library, it was thought that the same conditions could be used, and would not present any problems, either technical or synthetic. However, when the amines used, butylamine, propylamine and phenethylamine, were added to the solution of ytterbium (III) triflate catalyst, crystallisation occurred. The time it took for crystallisation to occur ranged from instantly to 2 hours. Heating of the solution to 60°C, or to reflux temperature (81-83°C) did not dissolve the crystals that had formed. Similarly, neither did the addition of further solvent to the mixture. This phenomenon had never been observed before in the research group, when opening the epoxide with amines. However, previously, the opening of the epoxide with an amine had only been carried out with the epoxide in the solution-phase, not the solid-supported epoxide. This would appear to be a classic example of when solution-phase synthetic methodology is transferred straight to solid-phase, and the transition is not as easy or smooth as would be hoped.

To try and determine what was happening in this system, some experiments were carried out with the model epoxide used for previous inositol work in the research group, cyclohexene oxide, **102**, Figure 2.17.

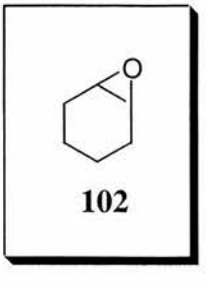

102

Figure 2.17: *Cyclohexene oxide, model epoxide used in IMPase inhibitor work.*

Firstly, cyclohexene oxide was added to one of the solutions in which crystals had formed, to determine whether the crystals disappeared or decrease in number. Although the crystals were still present, analysis by mass spectrometry showed the presence of phenethylamine, **103**, the model epoxide and also the ring opened compound, **104**, at 220 a.m.u., Figure 2.18.

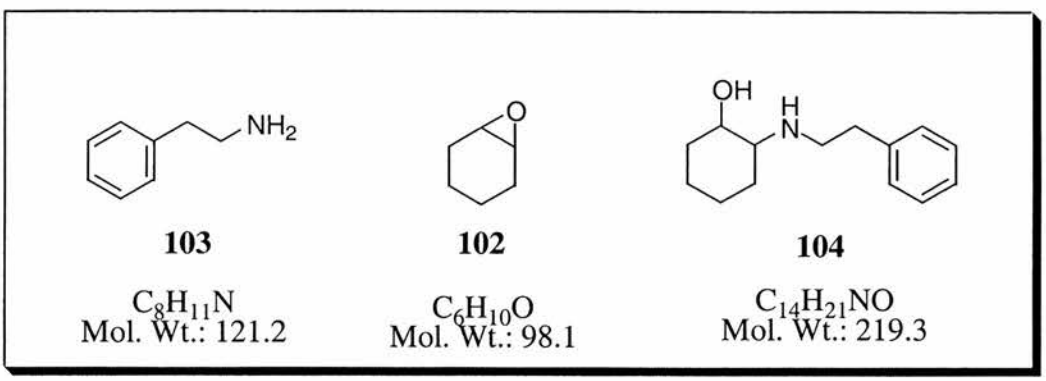

103 $C_8H_{11}N$ Mol. Wt.: 121.2

102 $C_6H_{10}O$ Mol. Wt.: 98.1

104 $C_{14}H_{21}NO$ Mol. Wt.: 219.3

Figure 2.18: *Products observed in mass spectrum of isolated crystals.*

There was no signal in the mass spectrum corresponding to ytterbium (III) triflate at 620 a.m.u., however, there were a series of signals in the spectrum at 561, 589 and 607 a.m.u, which could correspond to various ytterbium products or complexes. Also present in the mass spectrum was a signal at 275 a.m.u., which could also correspond to a product of reaction between the catalyst and amine. A possible product is shown in Figure 2.19.

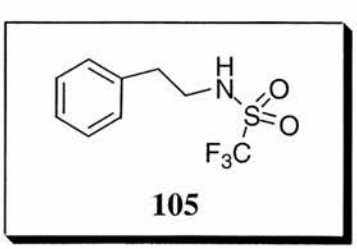

105

Figure 2.19: *Possible reaction product between Ytterbium (III) triflate and phenethylamine.*

Further work is required on the synthesis of the aminophosphonate library for identification of the compound forming the crystals. Additionally, work can be carried out to develop reaction conditions that do not promote crystal growth.

2.2. Quantification of resin loading by ^{19}F Gel-Phase NMR Spectroscopy.

Monitoring reactions on solid supports, and characterising solid-supported compounds is one of the most difficult procedures associated with solid-phase chemistry. Work was carried out to investigate loading levels of the solid-supports using ^{19}F gel-phase NMR, used previously to monitor the progress of solid-supported reactions,[79, 81] as discussed in Section 1.4.1.1.2.

This work began with the immobilisation of 2-fluorophenol, **106**, onto Merrifield resin, **6**. Through having a fluorinated compound attached to the solid support, it was hoped that both the attachment step could be monitored, and also that the final resin bound compound could also be analysed. Following the treatment of 2-fluorophenol with sodium hydride in DMF, the generated fluorophenoxide ion, **107**, is then added to a suspension of Merrifield resin, **6**, in DMF and stirred at 60°C, Scheme 2.7.

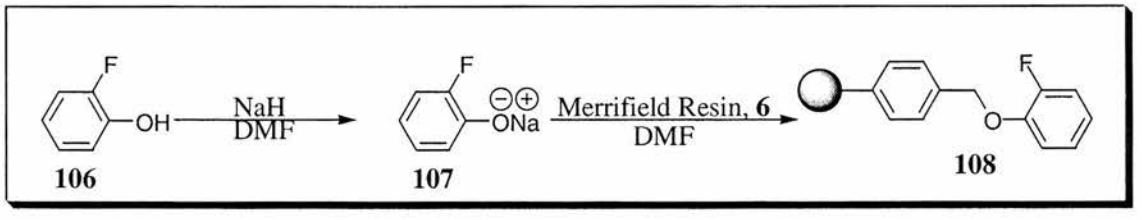

Scheme 2.7: *Substitution of Merrifield resin with 2-fluorophenol.*

After washing and drying, the solid-supported compound is ready for analysis. Previous work in this area,[79, 81] had shown that the solvent used in the gel-phase NMR experiments should facilitate the swelling of the resin backbone. To this end, deuterated benzene had been shown to give satisfactory results.[81] The reaction shown in Scheme 2.7, when analysed by ^{19}F gel-phase NMR, gave a signal in the spectrum at –134.5 ppm

(internally referenced). The broadness of this signal would be consistent with a fluorine atom bound to the solid support, rather than one that is free in solution. As this result was encouraging, the next compound attached to the solid support was a different isomer of fluorophenol, 4-fluorophenol. This was carried out in a manner analogous to 2-fluorophenol, Scheme 2.7, giving the resin-bound compound **109**, Figure 2.20.

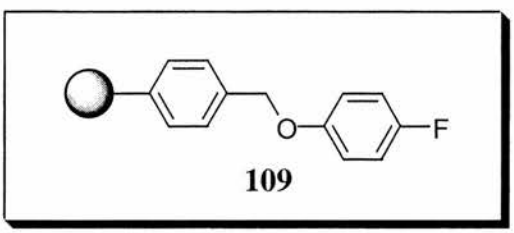

109

Figure 2.20: *Solid-supported 4-fluorophenol,* **109**.

Upon analysis by ^{19}F gel-phase NMR, a broad signal was again observed, at -124.6 ppm. Again, this is consistent with a resin-bound fluorine atom. However, there was also a sharp intense signal at –125.7 ppm. This sharp signal is indicative of fluorine free in solution, from residual 4-fluorophenol. The residual 4-fluorophenol probably became trapped in the polymer backbone after the resin was contracted with methanol, and then subsequently released upon re-swelling with deuterated benzene.

We now had two species attached to the solid support, both of which had significantly different chemical shifts. These two resin-bound compounds could now be investigated together. A series of reactions were carried out in order to try and determine the optimum time required for the attachment of 2-fluorophenol onto Merrifield resin. In the reaction series, the length of time that the 2-fluorophenolate ion, **107**, was allowed to stir with Merrifield resin was varied, with all other reaction conditions kept consistent. After the desired time period for stirring had elapsed, water was added to the reaction, and after filtering and washing, the resin was treated with 4-fluorophenolate ion, **110**, and left to stir overnight. The reaction mixture was left

overnight as this is longer than is required to achieve maximum substitution. After filtering and drying, this gives a mixed sample of the resins **108** and **109**, Scheme 2.8.

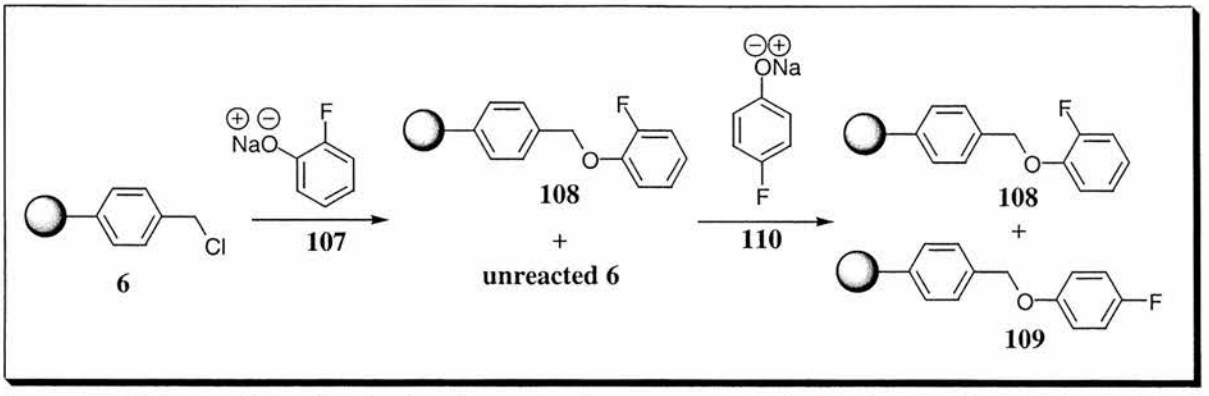

Scheme 2.8: *Synthesis of samples for reaction optimisation studies.*

The resins were then analysed by ^{19}F gel-phase NMR, to compare the integrals of the resin-bound fluorine peaks. The results are shown in Table 2.1.

Table 2.1: *Integral Ratio of resin-bound 2-fluorophenol,* **108** *to 4-fluorophenol,* **109**.

Reaction Number	Stirring Time @ 60°C (minutes)	Ratio of signal integrals 2-fluorophenol:4-fluorophenol
1	15	2:1
2	30	4:1
3	60	14:1
4	120	Exclusively 2-fluorophenol

In reaction 1, broad signals were obtained in the ^{19}F gel-phase NMR spectrum for both of the resin-bound species. Integration of these two signals gave a 2:1 ratio of the solid-supported 2-fluorophenol to the 4-fluorophenol. After 30 minutes stirring, reaction 2, this ratio had increased as would be expected, to 4:1. This indicates that more of the available reaction sites on the solid support have been taken up by the first reacting species. In reaction 3, 60 minutes stirring, the ratio had increased significantly, showing very little 4-fluorophenol substituted onto the solid support. Finally, after 120 minutes stirring with 2-fluorophenolate, no 4-fluorophenol had been substituted onto the solid support. This indicates that all of the reaction sites on the solid support have been occupied by the first reacting species, the 2-fluorophenolate ion **107**, leaving none available for reaction with 4-fluorophenol. This method could now be utilised as one for determining the degree of a reaction on solid-phase. This may be achieved by removing a small amount of the solid support, at any point during a reaction. This portion of resin is then further reacted to determine the extent of the reaction. The major drawback of this, and the majority of other techniques used for analysing solid-phase reactions, is that they only provide qualitative, not quantitative, information about the reaction(s) being carried out. It therefore seemed logical that the method could be applied to the quantitative analysis of resin-bound compounds. This was the next step in the investigation.

At first, it was unknown as to whether it would be possible to find the necessary conditions where a fluorine containing compound, present in the solution-phase at a known concentration, could be used as an internal reference for a suspended gel-phase resin sample, also containing fluorine. The concentration of fluorine bound to the solid support can then be calculated from the integrals of the two fluorine signals present in the ^{19}F gel-phase spectrum. To determine if this was actually possible, experiments were set up to determine the spin lattice relaxation time constants, T_1, for

solid-supported 2-fluorophenol, **108**. However, before these experiments could be carried out, a suitable, and improved, sample preparation protocol had to be developed.

When the previous ^{19}F gel-phase NMR experiments had been carried out, deuterated benzene had been used as the lock solvent, as this solvent has shown good polystyrene swelling properties.[81] However, we had seen that when this solvent was used, the resin sample suspended in the solvent tended to descend to the bottom of the NMR tube in a very short space of time (>10 minutes). This is problematic, as when the resin sinks, the sample no longer remains homogeneous in the RF receiver coils of the NMR machine. The buoyancy of the resin was then examined by suspending it in deuterated chloroform. In this case, the resin tended to rise to the surface of the solvent, in a similar time period to that previously observed for the deuterated benzene system. With the knowledge of how the resin behaved in these two solvents, it seemed feasible to expect that the resin would be of neutral buoyancy, or very close, in a 1:1 mixture of the two solvents. When this was tried, using deuterated chloroform and benzene, the resin was solvated and suspended in a homogeneous fashion in the NMR tube, within the RF receiver coils of the instrument. This homogeneous suspension lasted for a period of greater than 30 minutes, which give an adequate time frame in which to carry out the NMR experiments. A solution-phase reference standard had now to be included in the NMR solvent mixture. The most favourable choice for this reference standard would be one that gave a signal in the NMR spectrum significantly different from the two broad resin-bound product signals. For this reason, fluorobenzene, having a signal at –112 ppm in the NMR spectrum was chosen. The new solvent mixture of 50% deuterated chloroform, 49.8% benzene and 0.2% fluorobenzene was the NMR solvent used for all subsequent ^{19}F gel-phase NMR experiments. The fluorobenzene standard was included at such a low level in the solvent mixture so that the broad signals of the resin-bound fluorine atoms would not be swamped by the solvent signal. This 0.2%

fluorobenzene in the solvent mixture provided a concentration of 21.3×10^{-3}M (12.8×10^{-6} moles fluorine in 0.6 cm^3 of the NMR reference solvent). As the NMR solvent system had now been optimised, the next step was the determination of the spin lattice relaxation rate for the resin-bound fluorine atom.

2.2.1 Determination of Spin Lattice Relaxation Rates (T_1) for gel and solution-phase samples.

The most common method for measuring spin lattice relaxation rates is known as the Inversion Recovery pulse sequence, Figure 2.21.[161]

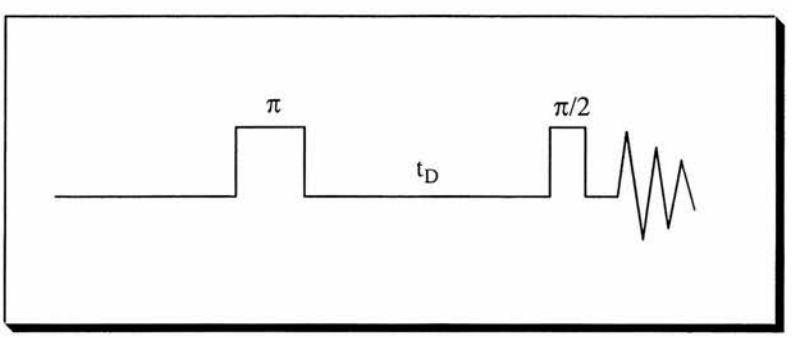

Figure 2.21: *Inversion Recovery Pulse Sequence.*

In this experiment, a pulse is first applied along the z-axis. This pulse is sufficiently long enough to rotate the magnetisation through 180°, or π radians. This pulse inverts the magnetisation from equilibrium, M_o, to - M_o. If this pulse is exactly 180°, then the magnetisation becomes exactly -M_o, giving no magnetisation along the xy-axis, hence no signal in the NMR spectrum. The magnetisation then begins to return from -M_o to equilibrium, at the spin lattice relaxation rate, T_1. In order to monitor the relaxation of the magnetisation, some component must appear in the xy-plane. This is achieved but applying a 90° pulse (π/2 radians), which rotates any z magnetisation into the xy-plane, producing a signal. The experiment can be best described as a vector diagram, shown in Figure 2.22.

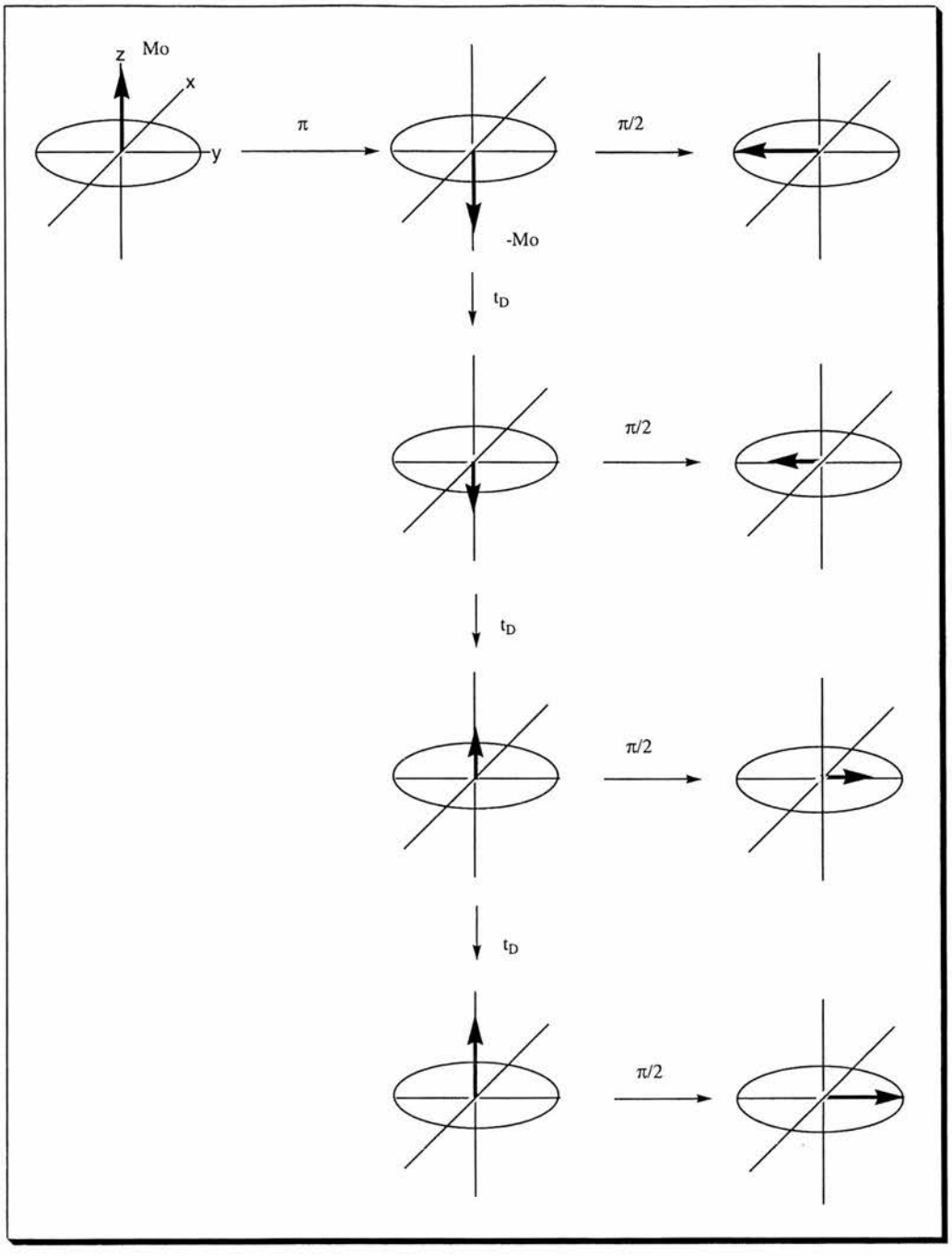

Figure 2.22: *Vector Diagram for the Inversion Recovery Pulse Sequence*

These diagrams show both the effect of the pulses on the spin system, and demonstrate the behaviour of the spin system as it evolves during a delay. If a long time is allowed to pass between the 180° and the 90° pulses, then the magnetisation will return to M_o before the 90° pulse is even applied, therefore the amplitude of the produced signal would be the same as if no 180°pulse had ever been applied to the system. Alternately, if there is only a very short delay, then the magnetisation will still

be along the –z-axis before the second pulse is applied. This will have the overall effect of inverting the produced signal, making it 180° out of phase. The experiment was repeated with different time delays, and the signal amplitude at any given time increases from - A_∞ to $+A_\infty$. The inversion recovery experiment was carried out on the sample of fully reacted, 100% loaded 2-fluorophenyl Merrifield ether, **108**, suspended in the solvent system previously described.

From the experiments, the T_1 value for the 2-fluorophenyl Merrifield ether signal was calculated to be 4.2±0.6 s, while the fluorobenzene solution reference had a T_1 value of 0.91±0.14 s. To accurately quantify the fluorine concentrations from the obtained NMR data, the interpulse relaxation delay has to be set to at least five times the magnitude of the T_1 value, so this was set to 25 s. When the samples were run, good spectra with adequate signal-to-noise ratios could be obtained within 30 minutes, on a conventional spectrometer fitted with a standard high-resolution probe tuned for ^{19}F detection under these conditions.

Upon examination of the spectrum of the sample used in the initial experiment, integration of the two ^{19}F signals that appeared at –113 ppm and -134 ppm, due to the solution-phase and solid-supported fluorine atoms respectively was carried out. The integration gave an excellent correlation between the expected fluorine content, (92.2×10^{-3}M) and the observed fluorine content (88.2×10^{-3}M). As this method had worked for this sample, the possibility of using the method to quantify the substitution levels of what were essentially 'blind' samples was investigated. In the 'blind' samples, portions of the 100% fully loaded 2-fluorophenyl-Merrifield ether, **108**, were blended with unfunctionalised Merrifield resin, **6**. This was done to give samples with varying amounts of fluorine attached to the solid support, altering the concentration of fluorine attached to the solid-phase. The 'blind' samples are outlined in Table 2.2.

Table 2.2: *Table of samples prepared for quantification of resin-bound fluorine.*

Loaded Resin (mg)	Unloaded Resin (mg)	Expected ratio (bound:solution)	Observed Ratio (bound:solution)
30.1	0	4.33:1	4.51:1
23.5	6.9	3.38:1	3.11:1
18.1	11.5	2.60:1	2.93:1
2.6	27.5	0.37:1	0.40:1

These blended samples were suspended in the NMR solvent, and ^{19}F gel-phase NMR spectra were acquired under the conditions already discussed. Graph 2.2 shows the plot of the theoretical resin-bound fluorine concentration against the experimentally observed resin-bound fluorine concentration in the 'blind' samples prepared. The spectra were recorded in 32 transients, over 30 minutes. The solid line represents unit gradient.

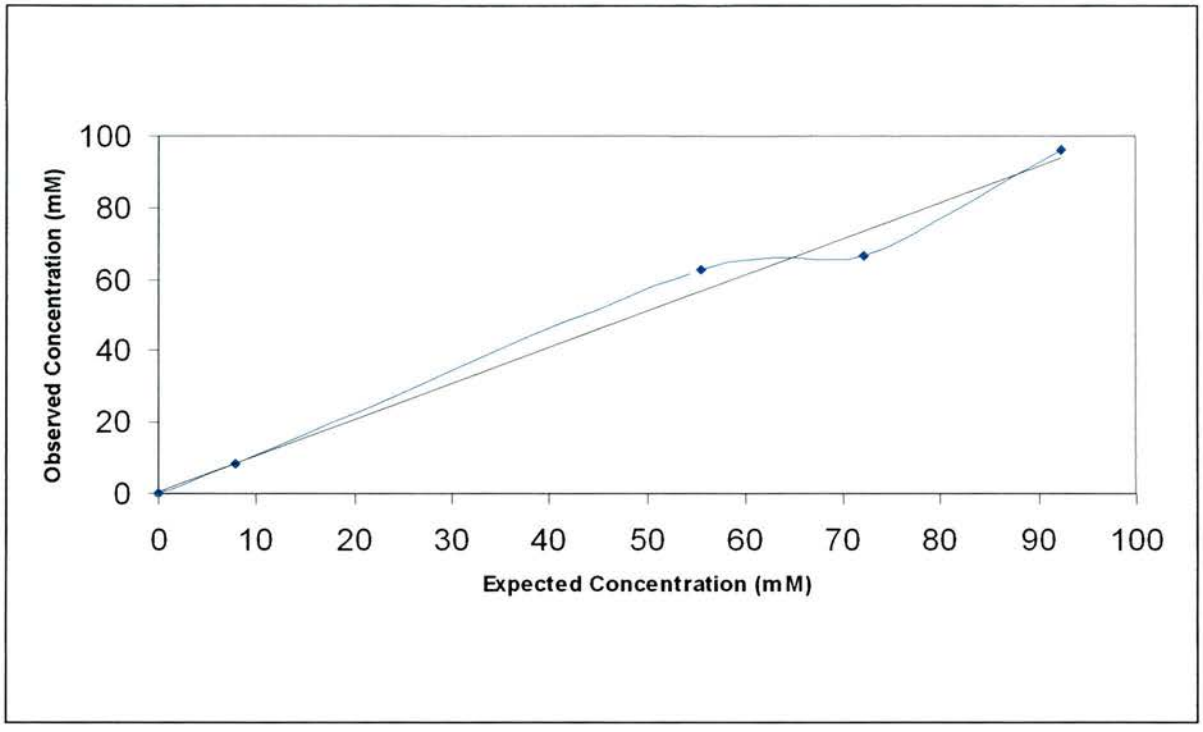

Graph 2.2: *Correlation of observed resin-bound fluorine concentration to theoretical concentration using ^{19}F Gel-Phase NMR Spectroscopy.*

This excellent correlation between the theoretical and experimentally determined fluorine content provided us with a high level of confidence in our ability to monitor solid-phase reactions, where it is suitable to use ^{19}F labelling. It also gave confidence in quantifying the number of available reaction sites that are still available on the solid support, for a reaction to take place.

An interesting point to note is that the fluorobenzene reference sample appeared to bind to the Merrifield resin and its derivative through a non-specific interaction. This was evidenced by the appearance in the spectrum of a new, slightly broader signal. This signal appeared approximately 0.2 ppm upfield of the sharp reference signal, as a shoulder on the sharper solvent signal. This signal increased in intensity, relative to the reference signal, in samples that contained larger amounts of resin. One reason for this second peak comes from initial work in the 1960's on mixtures of benzene and hexafluorobenzene. This work showed that benzene and hexafluorobenzene form a

1:1 co-crystal, when mixed together at low temperatures.[162] The crystal structure of the co-crystal is shown in Figure 2.23.

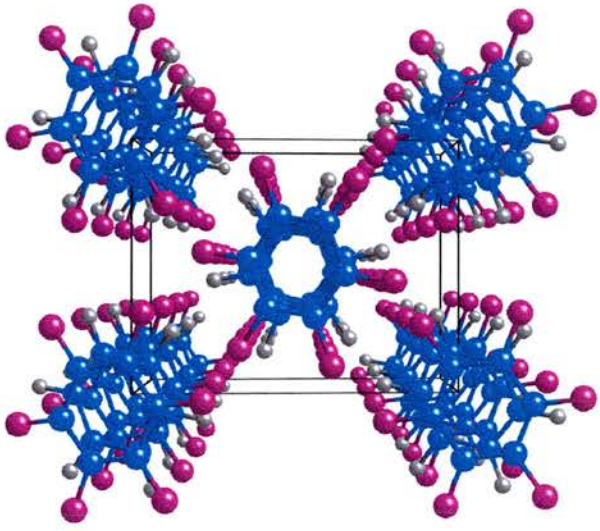

Figure 2.23: *Crystal Structure of 1:1 co-crystal of benzene/hexafluorobenzene at low temperature.*

As can be seen from the crystal structure, the aromatic rings, alternating benzene and hexafluorobenzene, stack on top of each other. Harris and co-workers at the University of Birmingham have shown, in similar work carried out on hexafluorobenzene/tri-o-thymotide (TOT) co-crystals, that more than one fluorine environment exists within their crystal.[163] This has been observed through the presence of two signals in the solid-state ^{19}F NMR spectrum for that system. The second signal appears as a shoulder on the major fluorine signal. The appearance of this second signal is possibly due to the aromatic pi-stacking of the hexafluorobenzene ring with the aromatic rings of tri-o-thymotide, while the major fluorine signal is from hexaflurorobenzene that is not contained within the environment of the co-crystal. This example could be directly related to our system of resin-bound fluorophenol attached to

Merrifield resin, where we observe a slightly broader signal upfield of the main fluorobenzene solvent signal. This broader signal would appear to correspond to fluorobenzene that is stacking between the aromatic rings of the polystyrene polymer backbone. For the purposes of quantifying the extent of the reactions by the ^{19}F gel-phase method, the integrals for both of these signals were combined, and compared to the resin bound fluorophenyl moieties.

2.3 Imine and Carbon-Carbon bond formation on solid supports.

As originally stated in the POSAM™ apparatus design parameters, all the wettable components were constructed from the chemically inert materials glass or PTFE. The original target for the POSAM™ apparatus was the ability to perform carbon-carbon bond forming reactions, through Grignard reactions on resin-bound species. The resin-bound species to be used was an imine, formed from a resin-bound aldehyde, **111**, Scheme 2.9.

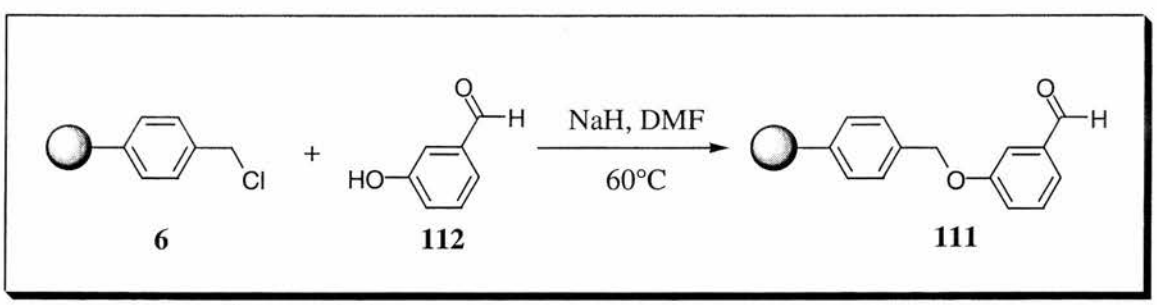

6 **112** **111**

Scheme 2.9: *Synthesis of resin-bound aldehyde,* **111**.

Attachment of 3-hydroxybenzaldehyde, **112**, to Merrifield resin gave the supported aldehyde **111**, which showed characteristic IR stretches at 1259 cm^{-1} and 1702 cm^{-1}, for ethers and carbonyls respectively. This polymer-supported aldehyde was the base resin used in all the reactions to form polymer-supported imines.

The proposed synthesis of the resin-bound imines is outlined in Scheme 2.10. Solution-phase synthesis of imines would normally be carried out under conditions that allow the azeotropic removal of water formed during the reaction. This removal of

water drives the reaction to completion, and eliminates the possibility of hydrolysis of the formed imine back to starting materials. However, solid supports based on a polystyrene backbone, such as Merrifield resin, are not stable to elevated reaction temperatures. As this was the case, another method had to be found to remove water from the reaction mixture.

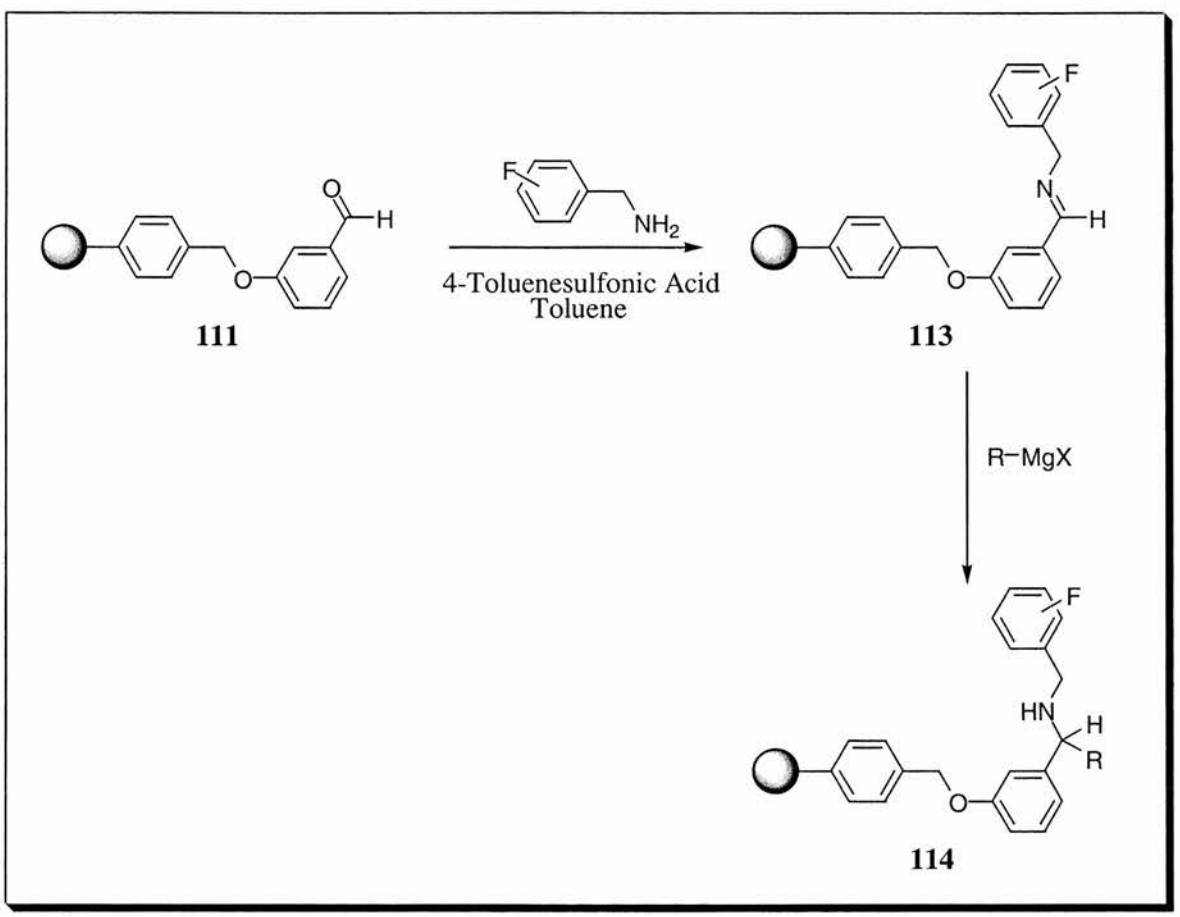

Scheme 2.10: *Proposed imine formation and subsequent Grignard reaction.*

The synthesis outlined in Scheme 2.10 was first attempted under non-POSAM™ conditions. To remove any water formed, a microreactor containing sodium sulfate (Na_2SO_4) was placed in the reaction vessel. This was then stirred along with the reaction mixture. However, the silicon stopper of the microreactor became dislodged during stirring, and the Na_2SO_4 contaminated the resin sample. A second attempt was made at the reaction, this time using 4Å molecular sieves to remove water formed during the reaction. However, these proved to be prone to mechanical damage and

disintegrated when stirring in the reaction mixture, leaving a clay residue on the resin sample and affecting the measurement of any mass increase.

Both of the methods of removing water formed during the condensation reaction had led to contamination of the resin sample. Previously, the use of trimethylorthoformate, **115**, as an effective and inexpensive dehydrating reagent in the formation of both solution-phase and resin-bound imines had been reported.[78, 164]

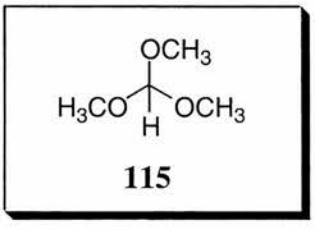

115

Figure 2.24: *Dehydrating reagent used in imine synthesis.*

In the reported solid-phase imine synthesis, the authors carried out the condensation of an aldehyde with a resin-bound amine in a solution of trimethylorthoformate (TMOF). Where the solubility of the aldehyde in TMOF was poor, co-solvents such as THF or acetonitrile had been used. The authors did try the corresponding reaction with resin-bound aldehyde and amine free in solution, but stated that this reaction proceeded much slower, and often required a second treatment of the partially converted polymer-supported aldehyde with amine to drive the reaction to completion. The synthesis of a number of resin-bound imines was then performed using TMOF as the solvent, Scheme 2.11.

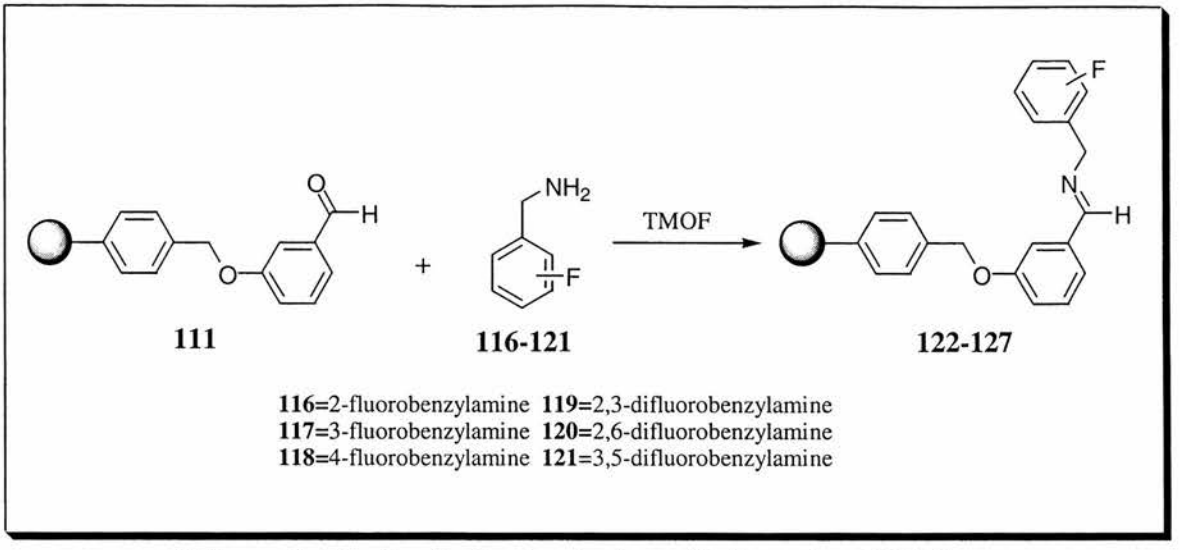

Scheme 2.11: *Synthesis of resin-bound imine using TMOF.*

After washing and filtration, IR analysis of the resin-bound compound showed the complete disappearance of the carbonyl stretch of the aldehyde resin at 1702 cm^{-1} and the appearance of a new stretch at around 1645 cm^{-1}. It should be noted that this was achieved without the addition of a second portion of amine to the resin-bound aldehyde, but with overnight stirring.

This resin-bound imine was then taken and reacted with a Grignard reagent, vinyl magnesium bromide, in THF at room temperature. Unfortunately, analysis by IR spectroscopy gave no meaningful results, as the spectrum was very noisy. Nothing in the spectrum could be distinguished from the polymer backbone. This feature proved to be a problem in many of the Grignard reactions carried out on the immobilised imine. The reaction was repeated, however this time, the reaction mixture was lowered to -78°C prior to addition of the Grignard reagent. After stirring for 4 hours with the temperature rising to room temperature, IR analysis still showed the presence of the imine peak at 1645 cm^{-1}, but also the presence of a new sharp peak at 3700 cm^{-1}. The experiment was then repeated, however, this time, the temperature was allowed to warm slowly to –40°C, and was stirred at that temperature for 6 hours. IR analysis of the resin from that reaction showed the presence of the peak at 1645 cm^{-1}, but no peak at 3700 cm^{-1}. As neither of these reactions had appeared to work, we began to wonder

whether we did have the resin-bound imine, or a different species that could not react with the nucleophilic Grignard reagent. To determine if the resin-bound species was the imine, a sample of the resin was taken and to it was added water. As stated earlier, the polystyrene-based polymer supports do not have good swelling properties in water, so an equal quantity of THF was added to the mixture. The resin was then stirred at high speed, to ensure good mixing, for 30 minutes. After washing with THF and drying, IR analysis of the resin-bound compound showed the original peak at 1645 cm^{-1} and the appearance of a new peak, at 1699 cm^{-1}, corresponding to the resin bound aldehyde, **111**.

This incomplete hydrolysis of the resin-bound compound indicates that we do have the imine immobilised on the solid support.

To achieve a reaction on the resin-bound imine, different approaches had to be taken. One of these methods was the reaction of imine **124** with a reducing agent, to form the secondary amine, Scheme 2.12.

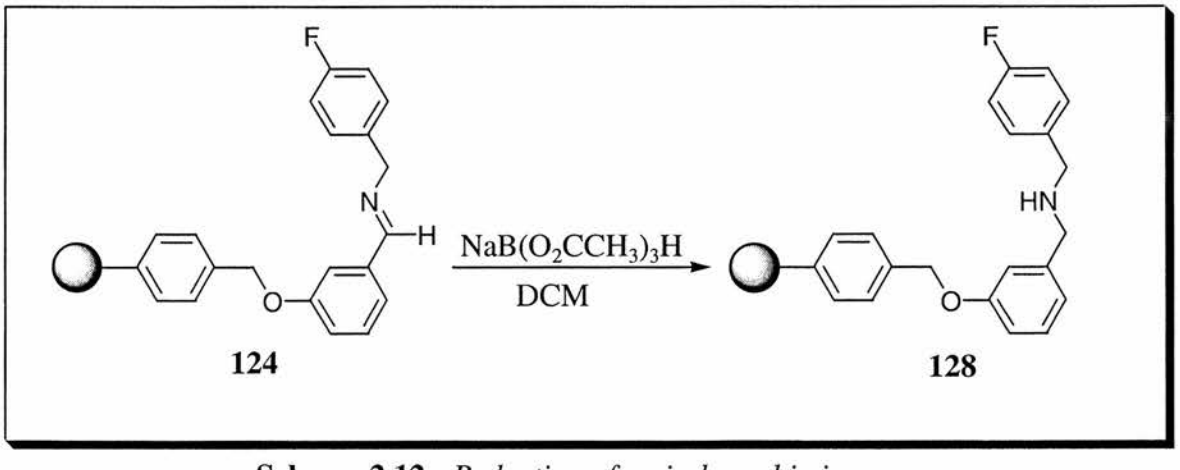

124 **128**

Scheme 2.12: *Reduction of resin-bound imines.*

The resin-bound imine was suspended in DCM and to this was added sodium triacetoxyborohydride over a period of 10 minutes. After washing and drying under vacuum, analysis of the resin by IR showed the disappearance of the peak at 1645 cm^{-1}, but no new peaks in the spectrum. Analysis by ^{19}F gel-phase NMR spectroscopy

showed the signal from the starting imine at -112.6 ppm together with a new signal at -112.5 ppm, corresponding to the reduced resin-bound species, **128**.

As the resin-bound imine had been reduced to the secondary amine, substitution of the imine with a different nucleophile other than a Grignard reagent was attempted. The imine was reacted with trimethylsilylcyanide (TMS-cyanide), Scheme 2.13.

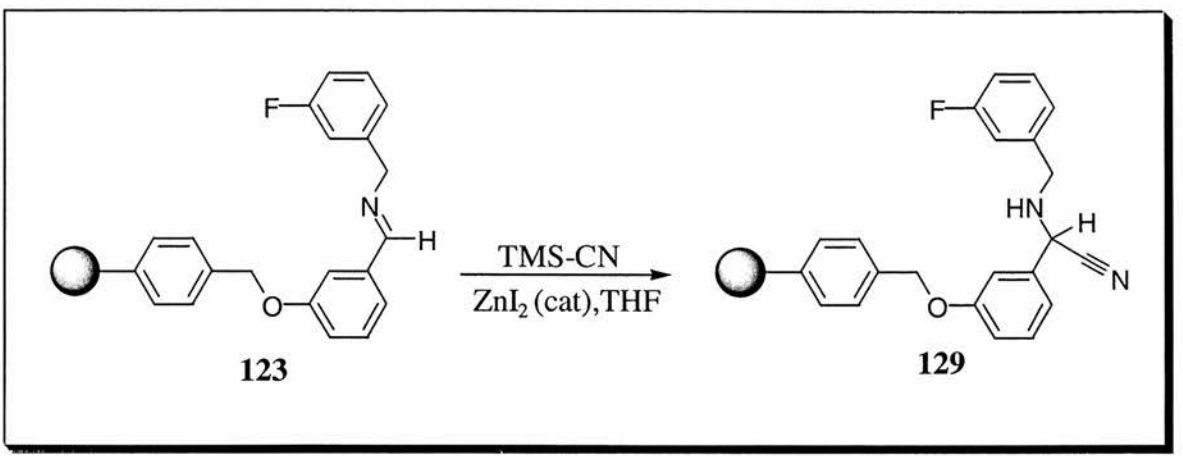

123 **129**

Scheme 2.13: *Reaction of resin-bound imine with TMS-cyanide.*

IR analysis of the product from the catalysed reaction outlined in Scheme 2.13 showed the disappearance of the imine stretch at 1645 cm^{-1} and the appearance of a new, sharp peak at 2217 cm^{-1}. This new peak corresponds to the C-N stretch of the nitrile functionality incorporated into the resin-bound compound, **129**. We had now observed two reactions with the resin-bound imine, so this led us back to a finding a method to react the imine with Grignard reagents.

Work by Chenera *et. al.* investigating the traceless silicon based linker, **34**,[60] Section 1.3.3, had investigated the reaction of Grignard reagents with resin bound imines. In this work they used a 1:1 mixture of diethyl ether and toluene as the solvent for the reaction, and reported smooth addition of the Grignard reagent to the imine. This method was adopted for the synthesis using our resin-bound imine, Scheme 2.14.

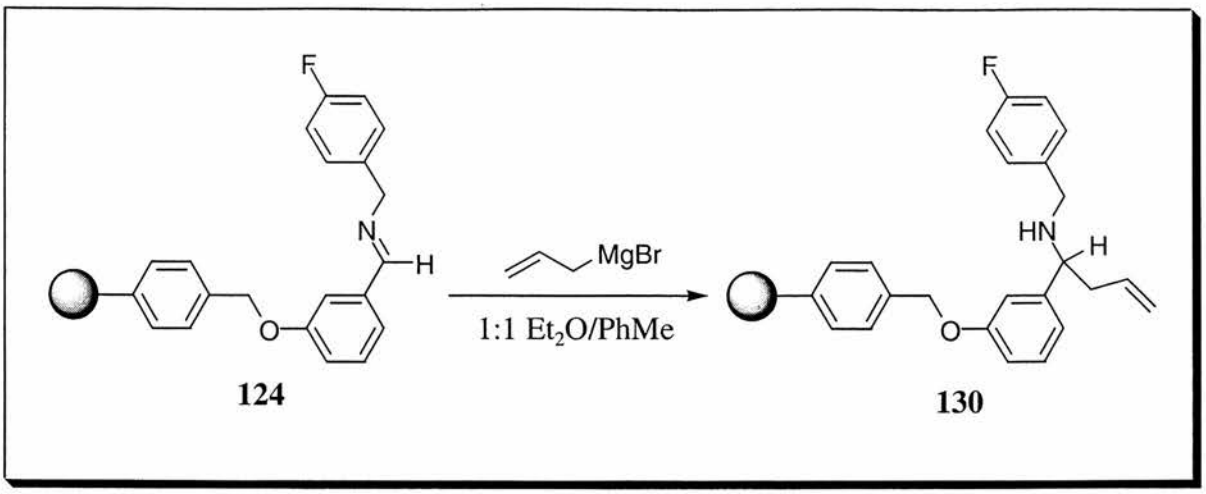

124 **130**

Scheme 2.14: *Reaction of Grignard reagent with resin-bound imine in 1:1 toluene/diethyl ether mixture.*

After washing and drying the resin-bound material after the synthesis, the first point to note was the pronounced colour change between the starting resin and the resin post-reaction. The colour had altered from a light fawn colour to deep yellow. Analysis of the resin by IR spectroscopy showed the disappearance of the imine C-N stretch at 1645 cm^{-1}. The spectrum also showed the appearance of a sharp peak at 3696 cm^{-1}, possibly resulting from the N-H stretch of a secondary amine, and also a weaker peak at 1637 cm^{-1}, corresponding to the C=C stretch of the allyl group from the Grignard reagent.

2.4 Resin-Bound Transition Metal Complexes as catalysts.

Many important processes in all sectors of the chemical industry rely on the efficient use of catalysts in some form or other. These catalysts are often the focus of research projects, as any improvement to a catalyst can lead to savings of millions of pounds per annum for the particular process involved.

A major objective when designing any new catalytic system has to be the efficiency and ease of catalyst removal after the reaction. This both minimises the cost of the catalyst, and also reduces the chances of contamination of the end product.[165] To

try and achieve this, a very attractive approach is to investigate the immobilisation of transition metal complexes, often used in the chemical industry as catalysts, onto suitable solid supports. Previous work in this area has detailed the use of porous solids,[165] including zeolites[166] or organic polymer supports.[167]

Unfortunately, there are often many problems with supported compounds, mainly associated with the partial or total degradation of the supported material, or the leaching away of the transition metal from the solid supports under the often hard forcing reaction conditions that are common in many industrial processes. To overcome these problems, we began looking at the possible use of polymer supports where the atoms donated to the transition metal centre are both redox stable, and are also positioned such that they are tightly bound to the transition metal complex. This was done through the design and then synthesis of structural analogues of dirhodium tetraacetate. In these analogues, two of the adjacent μ-bridging acetate groups are covalently linked to each other through a linker group, which is also attached to a polymeric support.

Dinuclear rhodium (II) complexes have been shown to catalyse a rich diversity of hydrogenation, carbonylation and cycloadditon reactions.[168-170] In most of these processes, phosphines are added to generate a catalytic rhodium (I) species, however there is evidence to suggest that rhodium (II) species can be used to catalyse the same chemistry. Dirhodium tetraacetate, **131**, is obtained as a crystalline solid from methanol. It is a particularly good source of rhodium (II) as it is both easy to prepare and is also air stable, Figure 2.25.

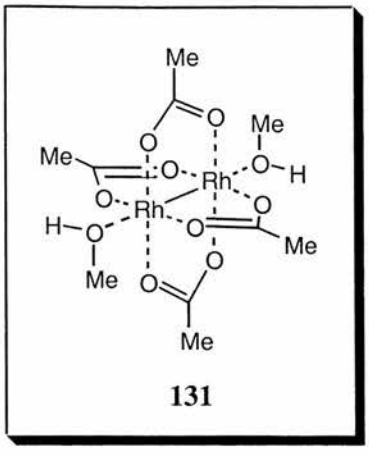

131

Figure 2.25: *Dirhodium tetraacetate.*

The structure of dirhodium tetraacetate is interesting because the four carboxylate groups all form μ-bridges, such that each donates an oxygen atom to the two metal centres. It occurred to us that if two of the carboxylate ligands could be replaced with a templated, solid-supported dicarboxylate unit, then this would deliver each of the carboxylate ligands in a similar position to adjacent carbonyls in the tetraacetate complex, as shown by complex **132** in Figure 2.26.

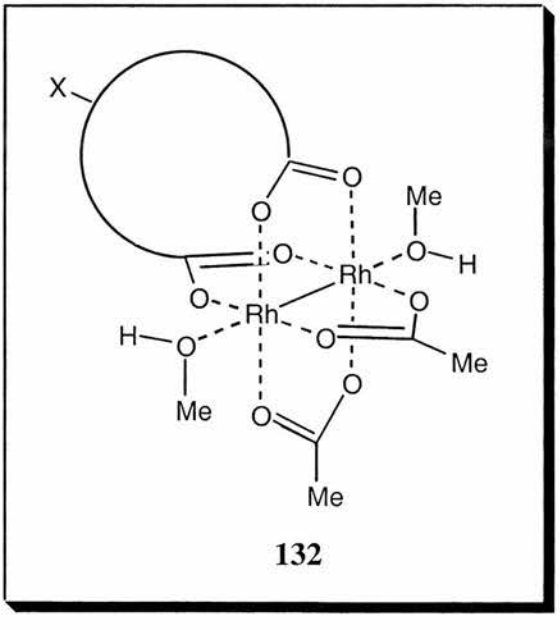

132

Figure 2.26: *Replacement of two acetates with a templated dicarboxylate.*

If the two templated carboxylic ligands can be delivered in this way, then tight binding to the complex should be observed. Also, if the template is suitably

functionalised through a spacer group of some description, it should also be possible to anchor the dinuclear transition metal complex onto a polymeric support, such as Merrifield resin, **6**. Compounds that were found to cause little, or no perturbation in the position of the carboxylate groups in the dirhodium complex, from molecular modelling studies, were chosen first. From these compounds, *meta*-disubstituted benzenes, which are capable of forming two μ-coordinated eleven or twelve membered rings, were found to be good choices. With this in mind, complex **133** was chosen as the first initial target molecule, Figure 2.27, where Y is solvent.

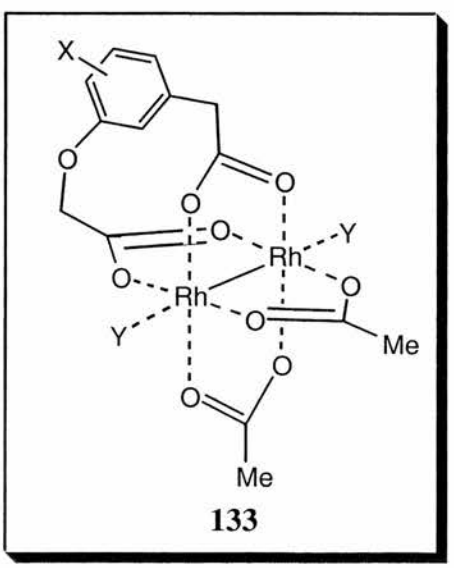

133

Figure 2.27: *Initial target for resin-immobilised catalyst.*

In order for the compound to be covalently linked to a solid support, a third area of functionality also had to be introduced into the molecule, represented by X in Figure 2.27. The trifunctionalised 3,4-dihydroxyphenyl acetic acid was identified as a starting point for the synthesis. However, problems arose through regioselectivity problems that are inherent to this molecule, giving a mixture of the templates **134** and **135**, Figure 2.28.

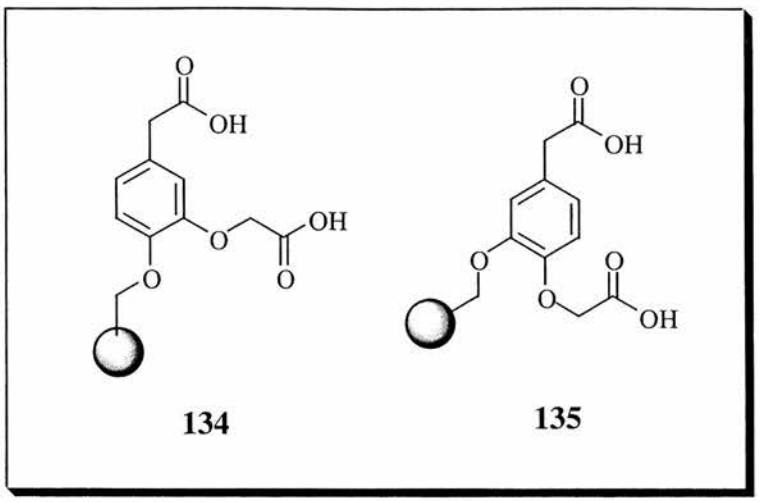

Figure 2.28: *Solid-supported ligands from 3,4-dihydroxyphenylacetic acid.*

To overcome these problems, methyl-3,5-dihydroxyphenylacetate, **136**, was identified as a better starting material for the synthesis, as due to the C2-symmetry of the compound, the attachment of *tert*-butyl acetate is not affected by regioselectivity problems. The synthesis of the supported catalyst is shown in Scheme 2.15.

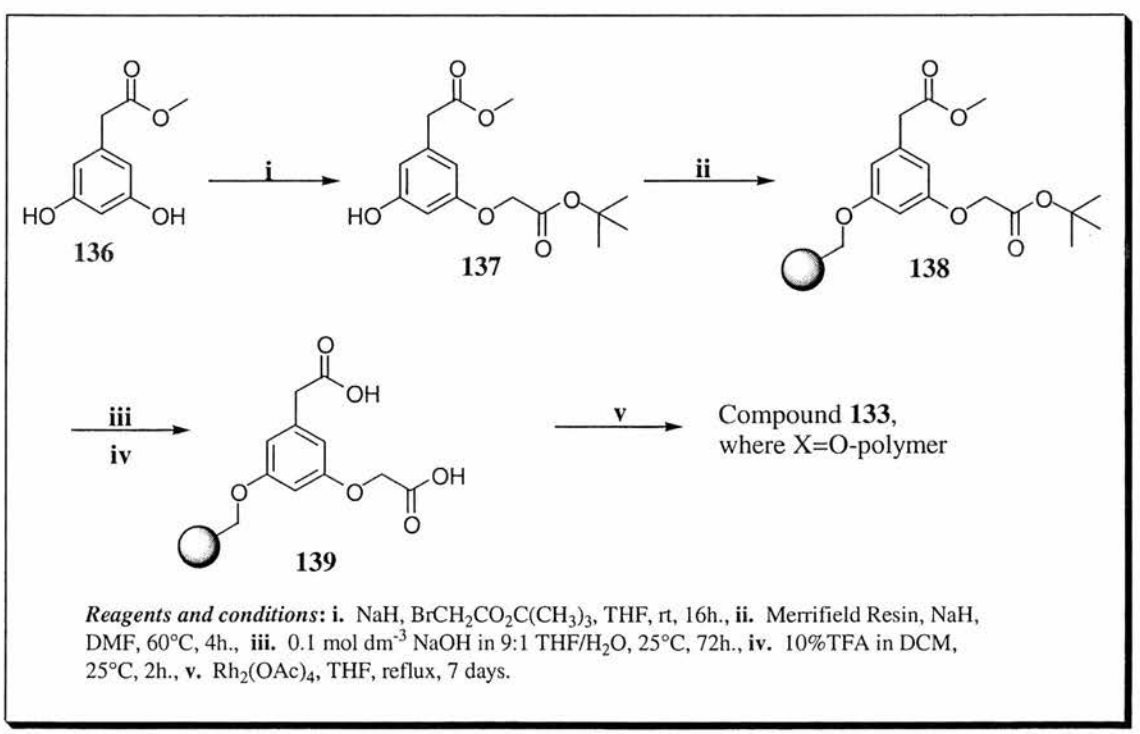

Scheme 2.15: *Synthesis of solid-supported rhodium catalyst.*

After mono-*O*-alkylation of methyl-3,5-dihydroxyphenylacetate, **136**, the isolated phenolic diester is treated with sodium hydride to form the phenoxide ion. This was then stirred with a suspension of Merrifield resin to give resin immobilised *bis*-carboxylic ester, **138**, which displayed the expected strong carbonyl absorbance in the IR spectrum. Hydrolysis of the ester functionalities gave the resin bound diacid, **139**. The diacid was then treated with dirhodium tetraacetate, **131**, under reflux conditions for seven days. At varying time points, small portions of the resin were removed from the reaction mixture and analysed by IR spectroscopy. It should also be noted that the resin had under gone a colour change from light brown to a distinct green colour, the same colour as dirhodium tetraacetate.

After 72 hours, the IR spectra of the resin-immobilised catalyst were consistent, with no differences between time points. At this stage it was assumed that the uptake of dirhodium tetraacetate onto the solid support was complete. At the same time as the preparation of the solid-supported catalyst, underivatised Merrifield resin, **6**, was refluxed with dirhodium tetraacetate, to act as a control reaction. In this case, no uptake of rhodium was observed by IR spectroscopy.

The dark green coloured resin, along with the other supported catalysts prepared from 3,4-dihydroxy acetic acid, **134** and **135**, Figure 2.25, was passed on to the research group of Dr. J-A. Andersen, who performed testing of the supported catalysts for activity in the hydroformylation, isomerisation and hydrogenation of olefinic substrates, shown in Scheme 2.16.

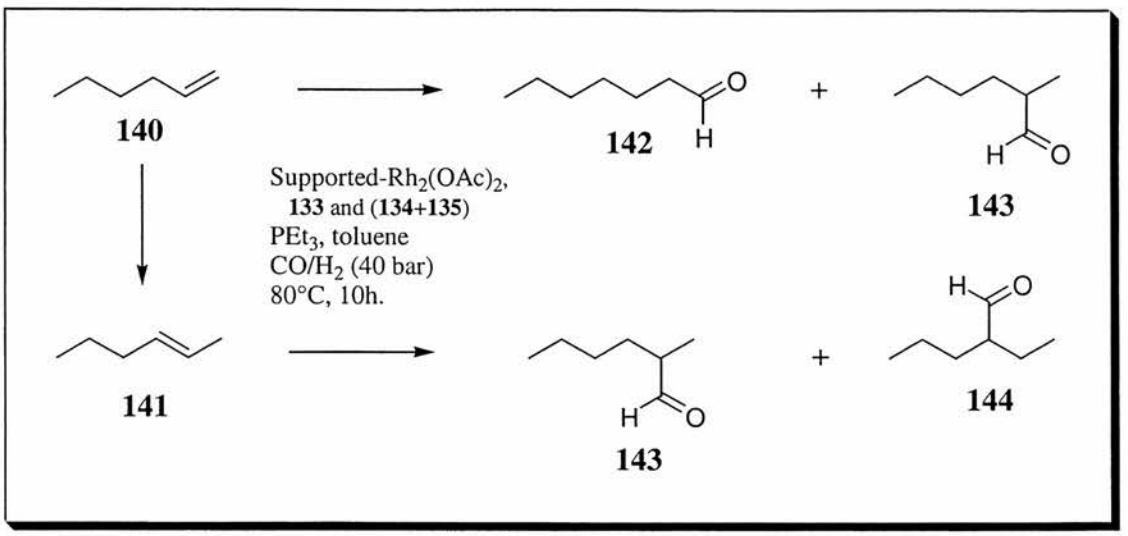

Scheme 2.16: *Catalytic reactions using supported rhodium catalysts.*

Catalytic hydroformylation of 1-hexene **140** was performed with the supported catalysts at 80°C using synthesis gas. Quantitative conversion to the heptanal isomers **142** and **143** was observed, along with 2-ethylpentanal **144**, formed after the initial isomerisation of 1-hexene, **140** to 2-hexene **141**, was observed after 10 h, with a linear to branched chain ratio of approximately 1:1. Table 2.3 shows the results from the catalytic testing for both supported catalysts.

Table 2.3: *Hydroformylation of 1-hexene using polymer-supported catalysts.*

Ligand bound to $Rh_2(OAc)_4$	**T (°C)**	**Reaction Time (h)**	**Pressure (bar)**	**% reaction**	**% 2-hexene**	**% Aldehydes**	**Aldehyde Ratio (142:143:144)**	**Ratio (*n*:*iso*)**
134+135	80	10	40	100	0	100	4.3:3.3:1	1:1
134+135	120	4	40	50	50	5	5.9:3.7:1	1.3:1
135	80	10	40	100	0	100	5:3.3:1	1.1:1
Recovered **134+135**	80	10	40	68	37	63	3.9:1:0	3.9:1
Recovered **135**	80	10	40	45	13	87	2.7:1:0	2.7:1

The results obtained from the solid-supported catalysts compare well with catalytic systems based on Rh (I). In addition, this new system of supported catalysts displayed several superior properties in selectivity, compared to the control homogeneous catalyst derived from dirhodium tetraacetate. An example of this is that the isomerisation of 1-hexene, **140** to 2-hexene, **141**, by the mixture of polymer-supported catalyst **134** and **135**, was eliminated at higher temperatures. Another example is the hydrogenation of the product aldehydes, **142**, **143** and **144** to the corresponding alcohols. This process does occur with the parent catalyst, but when the supported catalysts were employed in the reaction, it was completely suppressed. Interestingly, this observation is in accordance with reactions carried out using the parent catalyst supported within zeolites.[171] However, the rates of reaction for the polymer-supported catalysts **133** and the mixture, **134** and **135** were much higher than those for the zeolite systems. Therefore, for the hydroformylation reaction, it is evident that the polymer-supported system is an excellent catalyst in supporting higher rates of reaction, and also catalysing cleaner chemistry than the parent catalyst. The system also

offers the additional, highly desirable advantage over conventional homogeneous systems in that its physical form also makes removal of the catalyst from the reaction mixture easier, by simple filtration of the reaction mixture.

2.5 Immobilisation of perfluorinated compounds onto PTFE.

Work began in conjunction with different projects in the research group investigating the ability to immobilise perfluorinated compounds onto a fluoropolymer backbone, namely polytetrafluoroethylene, PTFE, through fluorophilic interactions. The PTFE backbone provides a very stable environment for reactions at high temperatures and high pressures, and would therefore provide a very stable platform for immobilising catalysts used in industrial process under these conditions. Initial work began with the attempted immobilisation of perfluorinated acids onto the polymer backbone, using the method shown in Figure 2.29. The perfluorinated compounds were predissolved in solvent and then passed through the column of PTFE polymer contained in the column. The polymer used in all the reactions, unless stated, was FLUON® CD076, obtained from ICI Fluoropolymers. The polymer is a macroporous co-polymer of tetrafluoroethene and 0.1% hexafluoropropene. Microscope pictures of the PTFE polymer are shown in Appendix 1.

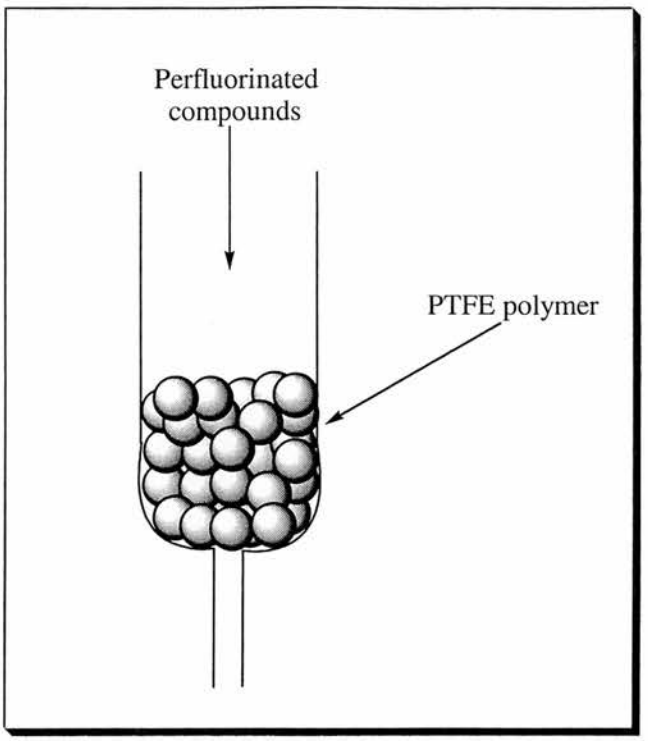

Figure 2.29: *Immobilisation of perfluorinated compounds onto PTFE.*

The first experiment carried out was the immobilisation of perfluorododecanoic acid, (C12) **145**, onto the polymer, to give the immobilised acid **145a**, Scheme 2.17.

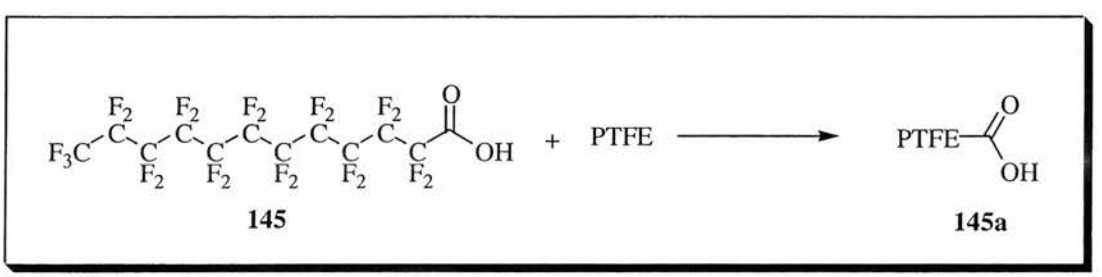

145 **145a**

Scheme 2.17: *Immobilisation of perfluorododecanoic acid onto PTFE.*

The perfluorinated acid was dissolved in diethyl ether and passed through the column a number of times. After passing through the column, the column was washed with diethyl ether, and all the ethereal washes were combined. After removal of the solvent under reduced pressure, an 8.8% loss of the acid was observed from mass measurements. Analysis by IR spectroscopy showed the appearance of a peak at 1640 cm^{-1}, possibly due to the carbonyl stretch of the acid, incorporated into the polymer backbone. The series of reactions were then carried out, with varying amounts

of acid dissolved in equal aliquots of diethyl ether, to determine whether different concentrations of acid resulted in greater incorporation into the polymer. The results are shown in Table 2.4. In each experiment, 500 mg of the PTFE polymer were used.

Table 2.4: *Percentage immobilisation of perfluorododecanoic acid on PTFE.*

Experiment Number	Perfluorododecanoic acid added (mg)	Perfluorododecanoic acid recovered (mg)	% change
1	301	284.8	5.4
2	250	247	1.2
3	202	189.2	6.3
4	151.3	146.3	3.3
5	100.7	98.9	1.8
6	75	73.7	1.7
7	26	25.8	0.8

As shown in the results in Table 2.4, there is a trend of lower incorporation as the amount of perfluorododecanoic acid used in the reaction decreases. This may indicate that a highly concentrated solution is required in order to immobilise the acid on the internal surfaces of the PTFE polymer. The experiment was next attempted with the PTFE polymer and the perfluorinated acid stirred at room temperature for 24 hours. After washing the PTFE and removing the solvent, 100% of the starting acid was recovered, giving no incorporation into the polymer. Since stirring had offered no improvement to the level of incorporation, the polymer was refluxed with the perfluorinated acid. Again, after filtering and washing, the recovered mass of acid was consistent with an incorporation of 8.9% of the acid onto the polymer. To try and improve the immobilisation of the perfluorinated acid on the polymer, a fluorinated solvent was used in the reaction. It was thought that this would both aid the dissolution

of the perfluorinated acid and would also penetrate the macroporous framework of the PTFE polymer matrix. To the perfluorinated acid in diethyl ether was added perfluorodecalin, **146**, Figure 2.30.

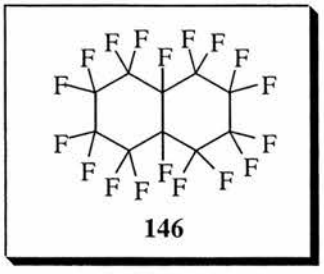

146

Figure 2.30: *Perfluorodecalin used to improve immobilisation of perfluorinated acid on PTFE.*

After stirring the reaction mixture at room temperature for 48 hours, the PTFE was washed and dried. Analysis by IR spectroscopy showed no new peaks in the spectrum. This reaction was then repeated, substituting FLUON® CD123, a PTFE homopolymer containing no hexafluoropropene, for FLUON® CD076. However, this did not alter the result, with no new peaks observed in the IR spectrum. Although the perfluorodecalin could be aiding the perfluorinated acid solutions movement into framework of the polymer, it could also be aiding the solubilisation of the acid, and washing away any acid incorporated into the polymer matrix.

When the reactions using the pipette arrangement were repeated, the immobilisation of the perfluorinated acid was not observed. In an attempt to achieve immobilisation of the acid, the reaction was carried out with THF as the solvent. After refluxing for 4 hours and washing with THF, the spectrum showed a peak at 1780 cm^{-1}, as well as a less intense peak at 1700 cm^{-1}. The peak at 1700 cm^{-1} corresponds to the carbonyl stretch of the unbound acid. To try and remove this unbound acid, the polymer was washed again with THF. Analysis of the polymer after this washing step showed the disappearance of these peaks in the spectrum. One reason for the poor incorporation into the polymer could be due to the chain length of the perfluorinated

acid being immobilised. To investigate this, perfluorooctanoic acid (C8), **147** and perfluorohexadecanoic acid (C16), **148** were immobilised, giving polymer-supported C8 acid, **149** and polymer-supported C16 acid, **150**. The perfluorooctanoic acid, **147**, dissolved in THF was refluxed with the PTFE polymer for 24 hours, then washed and dried. IR analysis at this stage showed a peak at 1683 cm^{-1}. The sample of PTFE was then taken and washed with a further portion of THF, and reanalysed by IR spectroscopy. The IR spectrum still contained the peak at 1683 cm^{-1}, but this peak was less intense than before the second washing step. When the immobilisation of perfluorohexadecanoic acid, **148**, was carried out, the acid was found to be only sparingly soluble in THF at room temperature, however the solubility did increase with increasing temperature. After stirring the perfluorinated acid and PTFE at reflux for 24 hours. After removing heat, the perfluorinated acid in the solution crystallised, forming a layer on the polymer. The acid crystals were removed by decanting off the supernatant liquid, then adding THF until all crystals had been dissolved. Washing and drying of the PTFE followed by analysis by IR showed the presence of a peak at 1778 cm^{-1}. A portion of this sample was then taken and washed with further THF. When analysed by IR spectroscopy, the peak at 1778 cm^{-1} was still present, but as seen before, the intensity of his peak had decreased. The second portion of the PTFE polymer, **150**, was taken and reacted with dirhodium tetraacetate, **131**, in order to try and form a catalyst immobilised on PTFE, **151**, Scheme 2.18.

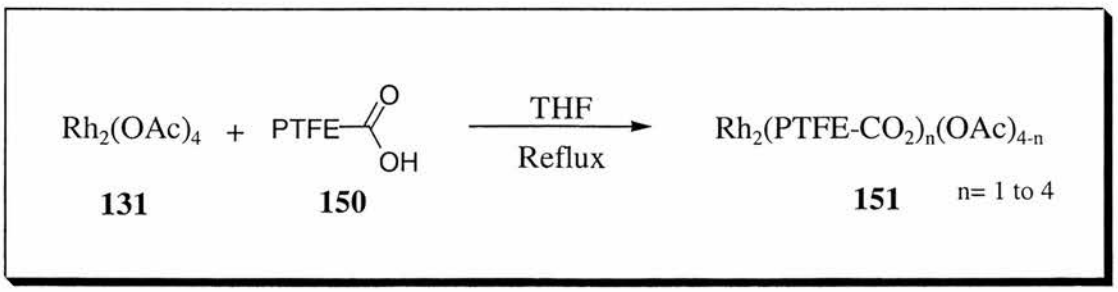

Scheme 2.18: *Formation of a PTFE immobilised catalyst.*

The polymer-supported acid, **150** and dirhodium tetraacetate, **131** were refluxed in THF for 45.5 hours, when a sample of the polymer was removed. Analysis by IR showed the peak at 1778 cm^{-1} was still present. Also, a new peak at 937 cm^{-1} had appeared in the spectrum. This peak corresponds to one in the IR spectrum of dirhodium tetraacetate at 943 cm^{-1}. Heat was reapplied, and the polymer refluxed for a further 52 hours, making 97.5 hours in total. After washing with THF and drying, further IR analysis of the polymer showed that the peak at 937 cm^{-1} was still present. The polymer had also slightly changed colour from white to light green, which is the colour of dirhodium tetraacetate in THF.

CHAPTER THREE

EXPERIMENTAL

3 Experimental.

NMR spectra were recorded on a Varian 300 (300 MHz, ^{1}H NMR; 298 MHz, ^{19}F NMR and 75.4 MHz, ^{13}C NMR), a Bruker AC-300 spectrometer (300 MHz, ^{1}H NMR; 75.4 MHz, ^{13}C NMR; 298 MHz, ^{19}F NMR) or a Bruker DRX500 spectrometer (470 MHz, ^{19}F NMR). Both ^{1}H and ^{13}C spectra are described in parts per million (ppm) downfield shift from TMS and are reported consecutively as position (δ_H or δ_C), relative integral, multiplicity (s-singlet, d-doublet, t-triplet, q-quartet, dd-double of doublets, sep-septet, ddd-double of double doublets, m-multiplet, br-broad), coupling constant (*J*/Hz) and the assignment (numbering according to IUPAC nomenclature for the compound). ^{1}H NMR were referenced internally on ^{2}HOH (4.68 ppm), $C^{2}HCl_3$ (7.27 ppm). ^{13}C NMR were referenced internally on $CH_3O^{2}H$ (49.8 ppm) or $C^{2}HCl_3$ (77.0 ppm). ^{19}F NMR were referenced internally on $CFCl_3$ (0 ppm).

IR spectra were recorded on a Perkin-Elmer 1710 f.t. IR spectrometer, or a Nicolet Avatar 360 IR spectrometer. The samples were prepared as KBr discs, nujol mulls, solutions in chloroform or thin films between sodium chloride discs. The frequencies, (ν) as absorption maxima are given in wavenumbers (cm^{-1}) relative to a polystyrene standard. Intensities are recorded as br-broad, w-weak, m-medium, st-strong, vst-very strong.

Mass spectra were recorded on a VG 70-250 SE or a Kratos MS-50. Fast atom bombardment (FAB) spectra were recorded using glycerol as a matrix. CI spectra were recorded using ammonia as a reagent. Major fragments are given as percentages of the base peak intensity (100%).

Flash chromatography was performed according to the method of Still *et al.*[172] using Fluka C60 (40-60 μm mesh) silica gel. Analytical thin layer chromatography (tlc) was

carried out on 0.25 mm pre coated silica gel plates (Macherey-Nagel SIL g/UV_{254} or Whatman K6F silica gel 60A) and compounds were visualised using UV fluorescence, ethanolic phosphomolybdic acid or ninhydrin.

Solvents used were either distilled, or of analar quality. Petroleum ether refers to that portion boiling between 40 and 60°C. Solvents were dried according to literature procedures. Ethanol and methanol were dried using magnesium turnings. Isopropanol, *N,N*-dimethylformamide (DMF), toluene, dichloromethane, acetonitrile, diisopropylamine, triethylamine and pyridine were distilled over CaH_2. THF and diethyl ether were dried over sodium/benzophenone and distilled under nitrogen.

Synthesis of tripeptide library using POSAM™.

Nine POSAM™ microreactors were charged with *N*-Fmoc-phenylalanine Wang resin ester (substitution level 0.41 mmol g^{-1}, 25 mg, 1.025 x 10^{-5} mol, 9.23 x 10^{-5} mol in total), nine charged with *N*-Fmoc-valine Wang resin ester (substitution level 0.38 mmol g^{-1}, 25 mg, 9.5 x 10^{-6} mol, 8.55 x 10^{-5} mol in total) and nine charged with *N*-Fmoc-alanine Wang resin ester (substitution level 0.52 mmol g^{-1}, 25 mg, 1.3 x 10^{-5} mol, 1.17 x 10^{-4} mol in total). The microreactors were then sealed and assembled in the POSAM™ reaction chambers, such that three of each were present in each reaction chamber. Into each reaction chamber was then passed DMF (40 cm^3) for 20 minutes to swell the resin. The reaction chambers were drained and then the microreactors were reacted with 20% piperidine in DMF solution (40 cm^3). The solution was passed over the microreactors for 30 minutes, then drained under nitrogen pressure. The microreactors were then washed with DMF (3 x 40 cm^3) and drained. The microreactors contained in reaction chamber 1 were then reacted with *N*-Fmoc-phenylalanine (1.521 g, 3.93 mmol) and PyBOP® (2.046 g, 3.93 mmol) dissolved in a 0.4 M solution of NMM in DMF (50 cm^3). Reaction chamber 2 was treated with *N*-Fmoc-valine (1.332 g, 3.93 mmol) and PyBOP® (2.046 g, 3.93 mmol) dissolved in a 0.4 M solution of NMM in DMF (50 cm^3). Reaction chamber 3 was treated with *N*-Fmoc-alanine (1.224 g, 3.93 mmol) and PyBOP® (2.046 g, 3.93 mmol) dissolved in a 0.4M solution of NMM in DMF (50 cm^3). After passing the amino acid solutions over the microreactors for 1 hour, the microreactors were allowed to stand in the solution overnight. After this time, the solutions were passed over the microreactors for a further 1 hour, then drained from the reaction chambers under nitrogen pressure. The microreactors were then washed with DMF (3 x 40 cm^3), and methanol (40cm^3) was passed through the reaction chambers to contract the resin. The microreactors were rearranged as shown in Figure 2.12. Treatment of each reaction chamber with DMF

(40 cm^3) gave the re-swollen resin, which was then treated with 20% piperidine in DMF (40 cm^3) for 30 minutes, giving the resin-bound, unprotected dipeptides. Coupling of an amino acid to the resin-bound dipeptide was then carried out, using the same amounts of the amino acids and PyBOP® in a 0.4 M NMM in DMF solution (40 cm^3) as used for the previous coupling step. After passing the amino acid solution over the microreactors for 1 hour, the microreactors were left to stand in the solution for 8 hours, then the solution was passed over the microreactors for a further 1 hour. After this time, the reaction chambers were drained under nitrogen pressure, and the microreactors washed with DMF (3 x 40 cm^3). Treatment of the reaction chambers with 20% piperidine in DMF (40 cm^3, 30 mins) followed by washing with DMF (3 x 40 cm^3) gave the unprotected resin-bound tripeptide library. The microreactors were then removed from the reaction chambers and placed in twenty-seven pre-marked vials. The resin from the microreactors was treated with a mixture of TFA:H_2O:TES (95:2.5:2.5) to cleave the tripeptides from the solid support. After filtration to remove the solid support, the filtrate was concentrated under reduced pressure. Several compounds were then analysed for reaction efficiency using ^1H NMR spectroscopy.

NH_2-Phe-Val-Ala-OH, Reaction Chamber 1, Microreactor #6.

δ_H (300 MHz, ^2H_2O) 0.84 (3H, d, $^3J_{H\text{-}H}$=6.84, valine CH_3), 0.85 (3H, d, $^3J_{H\text{-}H}$=6.84, valine CH_3) 1.38 (3H, d, $^3J_{H\text{-}H}$=7.42, alanine CH_3), 1.83-1.93 (1H, m, valine β-C*H*), 3.04-3.15 (2H, m, phenylalanine β-CH_2), 4.15-4.27 (2H, m, α-C*H*), 7.12-7.20 (2H, m, Ar-*H*), 7.25-7.35 (3H, m, Ar-*H*).

NH_2-Ala-Ala-Val-OH, Reaction Chamber 3, Microreactor #26.

δ_H (300 MHz, ^2H_2O) 0.88 (6H, d, $^3J_{H\text{-}H}$=6.82, 2 x valine CH_3), 1.32 (3H, d, $^3J_{H\text{-}H}$=7.75, alanine CH_3), 1.45 (3H, d, $^3J_{H\text{-}H}$=7.44, alanine CH_3), 2.04-2.15 (1H, m, valine β-C*H*), 3.95-4.05 (1H, m, α-C*H*), 4.27-4.39 (1H, m, α-C*H*).

NH_2-Val-Ala-Phe-OH, Reaction Chamber 2, Microreactor #16.

δ_H (300 MHz, ^2H_2O) 0.81-0.99 (6H, m, 2 x valine CH_3), 1.26 (3H, d, $^3J_{H\text{-}H}$=7.14, alanine CH_3), 2.00-2.10 (1H, m, valine β-C*H*), 2.90-3.18 (2H, m, phenylanine β-CH_2), 4.23-4.34 (1H, m, α-C*H*), 4.47-4.57 (1H, m, α-C*H*), 7.15-7.33 (5H, m, Ar-*H*).

NH_2-Ala-Phe-Val-OH, Reaction Chamber 3, Microreactor #20.

δ_H (300 MHz, ^2H_2O) 0.76-0.86 (6H, m, 2 x valine CH_3), 1.36-1.45 (3H, m, alanine CH_3), 1.90-2.02 (1H, m, valine β-C*H*), 2.94-3.04 (2H, m, phenylalanine β-CH_2), 3.92-4.01 (1H, m, α-C*H*), 4.03-4.10 (1H, m, α-C*H*), 7.14-7.33 (5H, m, Ar-*H*).

NH_2-Val-Val-Val-OH, Reaction Chamber 2, Microreactor #14.

δ_H (300 MHz, ^2H_2O) 0.82-0.96 (18H, m, 6 x valine CH_3), 1.90-2.01 (1H, m, valine β-C*H*), 2.01-2.19 (2H, m, 2 x valine β-C*H*), 4.06-4.14 (3H, 3 x α-C*H*).

NH_2-Val-Ala-Val-OH, Reaction Chamber 2, Microreactor #17.

δ_H (300 MHz, ^2H_2O) 0.835 (6H, d, $^3J_{H\text{-}H}$=6.87, 2 x valine CH_3), 0.89 (6H, dd, $^3J_{H\text{-}H}$=6.86, 2 x valine CH_3), 1.27 (3H, d, $^3J_{H\text{-}H}$=7.14, alanine CH_3), 1.99-2.15 (2H, m, valine β-C*H*), 4.09-4.14 (1H, m, α-C*H*), 4.29-4.39 (1H, m, α-C*H*).

(+)-(1*S*,2*R*,6*R*)-1,2-Cyclohexylidenedioxy-4-oxocyclohexan-6-ol, 72.[160]

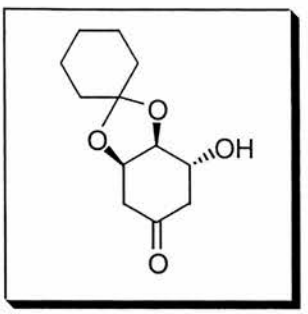

(-)-Quinic acid, **70** (20 g, 104 mmol) and cyclohexanone (30.6 g, 32.3 cm^3, 312 mmol) were treated with conc. orthophosphoric acid and heated under Dean-Stark conditions until all the water had been removed. The reaction mixture was then allowed to cool to room temperature whereupon it solidified. The solid was recrystallised from ethyl acetate/petroleum ether to remove most of the cyclohexanone and the crude lactone, **71** was filtered off. The crude lactone **71** (10 g, 39.4 mmol) was dissolved in ethanol (200 cm^3) and the solution cooled in an ice bath. Sodium borohydride (2.27 g, 60 mmol) was added slowly, in four batches, with vigorous stirring, then allowed to warm to room temperature overnight. The solvent was removed under reduced pressure, and the residue then redissolved in water (250 cm^3). The pH of the solution was adjusted to pH 6 by the dropwise addition of conc. orthophosphoric acid. The weakly acidic solution was cooled to 0°C in an ice bath and sodium periodate (9.26 g, 43.3 mmol) was added slowly in batches over 25 minutes. After stirring for 5 hours, the mixture was extracted with diethyl ether (2 x 100 cm^3) followed by ethyl acetate (2 x 100 cm^3). The combined organic phases were dried with $MgSO_4$ and concentrated under reduced pressure. The residual oil solidified upon drying *in vacuo* and the crude solid was recrystallised from ethylacetate/petroleum ether (1:10), giving the product **72** as a white solid (7.0 g, 79 % from lactone **71),** mp 97-98°C (lit.,[160] mp 97-98°C);

ν_{max}/cm^{-1} ($CHCl_3$): 3462 (br st, OH), 2940 & 2863 (st, C-H), 1712 (st, ketone carbonyl), 1448 (st), 1235 (st, C-O-C ether); δ_H (300 MHz; C^2HCl_3) 1.34-1.46 (2H, br s, cyclohexylidene), 1.50-1.70 (8H, m, cyclohexylidene), 2.46 (1H, ddd, $^2J_{H-H}$=17.8, $^3J_{H-H}$=3.7 and 1.84, 5-H), 2.68-2.74 (2H, m, 3-H and 5-H), 2.81 (1H, dd, $^2J_{H-H}$=17.6, $^3J_{H-H}$=3.6, 3-H), 4.26 (1H, br, s, 6-H), 4.29-4.35 (1H, m, 1-H), 4.68-4.74 (1H, m, 2-H). δ_C (75.4 MHz; C^2HCl_3) 23.51, 23.89, 25.12, 33.27, 36.26, 40.25, 41.66 (5 x C secondary of cyclohexylidene, 3-C and 5-C), 68.45 (6-C), 71.75 (2-C), 74.70 (1-C), 109.54 (C quaternary of cyclohexylidene), 207.76 ((4-C); *m/z* (CI) 244 (100%, $[M+H]^+$), 227 (28%, $[M+H]^+$), 116 (14%, $[M+2H-C_6H_8O_2]^+$);

(-)-(1*S*,2*R*,4*S*,6*R*)-1,2-Cyclohexylidenedioxycyclohexane-4,6-diol, 73 and (+)-(1*S*,2*R*,4*R*,6*R*)-1,2-Cyclohexylidenedioxycyclohexane-4,6-diol, 74.[160]

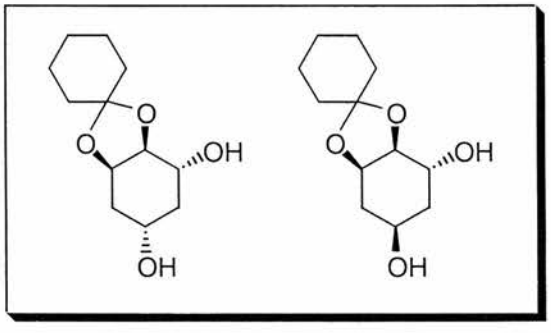

To a stirred solution of the ketone, **72**, (4.22 g, 18.7 mmol) in methanol (300 cm^3) was added $LaCl_3 \cdot 7H_2O$ (6.93 g, 18.7 mmol) and the mixture cooled to –78°C. Sodium borohydride (813 mg, 21.5 mmol) was added in small batches while stirring was continued as vigorously as possible. The mixture was then allowed to warm to room temperature slowly overnight with continued stirring. The solvent was removed under reduced pressure, and the residual oil partitioned between water (100 cm^3) and ethyl

acetate (100 cm^3). The aqueous phase was then further extracted with ethyl acetate (2 x 100 cm^3), the combined organics were dried with $MgSO_4$ and the solvent removed under reduced pressure, to give a mixture of the *cis*- and *trans*- diols as a colourless oil, 3.41 g, 80 %. This mixture was taken on to the next step without separation. ν_{max}/cm^{-1} (KBr): 3427 (m) & 3265 (br m, OH), 2932 & 2868 (st, C-H); δ_H (300 MHz; C^2HCl_3). δ_H (300 MHz; C^2HCl_3) 1.30-1.80 (24H, m, 2 x [10H cyclohexylidene, 3-H, 5-H]), 1.84-2.15 (5H, m, 2 x 3-H, 2 x 5-H, 1 x OH), 2.20-2.34 (2H, m, 2 x OH), 3.21 (1H, d, $^3J_{H\text{-}H}$=4.23, OH), 3.65-3.95 (3H, m, 2 x 2-H, 1 x 6-H), 4.00-4.20 (3H, m, 2 x 4-H, 1 x 6-H), 4.22-4.42 (2H, m, 2 x 1-H). δ_C (75.4 MHz; C^2HCl_3) 23.63, 23.67, 23.99, 24.89, 24.95, 32.97, 35.04, 35.14, 35.73, 37.19, 38.15, 38.42 (2 x [5 x C secondary of cyclohexylidene, 3-C and 5-C]), 65.31 & 66.08 (2 x 4-C), 68.51 & 70.80 (2 x 6-C), 72.68 & 74.03 (2 x 2-C), 79.61 & 80.07 (2 x 1-C), 109.54 & 109.75 (2 x C quaternary of cyclohexylidene); *m/z* (CI) 246 (21%, $[M+H+H_2O]^+$), 229 (100%, $[M+H]^+$);

(-)-(1*S*,2*R*,4*S*,6*R*)-1,2-Cyclohexylidenedioxy-4-(*tert*-butyldiphenylsilyl)-cyclohexan-6-ol, 75.[160]

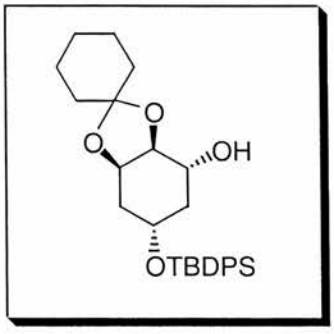

The mixture of *cis* and *trans* diols (3.38 g, 14.8 mmol) was dissolved in dry dichloromethane (50 cm^3) and catalytic DMAP (453 mg, 3.71 mmol) and dry triethylamine (1.545 g, 2.128 cm^3, 15.3 mmol) were added. The mixture was stirred and cooled to 0°C in an ice bath and *tert*-butyldiphenylsilyl chloride (4.197 g, 3.971 cm^3, 15.3 mmol) was added dropwise with vigorous stirring. The mixture was then left to stir overnight at room temperature. The mixture was extracted with water (100 cm^3), then the aqueous phase was further extracted with dichloromethane (3 x 50 cm^3). The combined organic phases were dried with $MgSO_4$, and the solvent removed under reduced pressure. The residual oil was then chromatographed on silica (petroleum ether/ethylacetate; 2:1) to give the silylated product, **75**, as a white sticky foam (3.19 g, 46.3 %); ν_{max}/cm^{-1} (KBr): 3451 (m, OH), 1112 (vst, Si-O). δ_H (300 MHz; C^2HCl_3) 1.06 (9H, s, 'butyl), 1.36 (br s, 1H, 3-H), 1.55-1.60 (10H, m, cyclohexylidene), 1.69-1.78 (1H, m, 5-H), 1.80-1.91 (2H, m, 3-H and 5-H), 3.13 (1H, d, $^2J_{H\text{-}H}$ 6.25, 6-OH), 3.78-3.90 (1H, m, 6-H), 4.02-4.08 (1H, m, 2-H), 4.08-4.18 (1H, m, 4-H), 4.39-4.46 (1H, m, 1-H), 7.30-7.50 (6H, m, $SiPh_2$), 7.60-7.70 (4H, m, $SiPh_2$). δ_C (75.4 MHz; C^2HCl_3) 19.00 ($C(CH_3)_3$), 23.66, 23.97, 24.99 (3 x C secondary of cyclohexylidene), 26.90 ($C(CH_3)_3$),

35.28, 35.74, 36.31, 38.12 (2 x C secondary of cyclohexylidene, 3-C and 5-C), 68.18 (4-C), 69.86 (6-C), 71.69 (2-C), 78.64 (1-C), 109.23 (C quaternary of cyclohexylidene), 127.71, 129.84, 129.90, 135.70, 135.74 (Ar-*C*H and Ar-C quaternary of $SiPh_2$); *m/z* (CI) 467 (100%, $[M+H]^+$), 432 (24%), 388 (47%, $[M+H+H_2O-C_6H_{10}]^+$), 344(30%), 211 (19%, $[M-OSiC_{16}H_{19}]^+$);

(-)-(1*R*,2*R*,4*S*,6*R*)-1,2-Cyclohexylidenedioxy-4-(*tert*-butyldiphenylsilyl)-6-(4'-phenylmethylsulfonyloxy)cyclohexane, 76.[160]

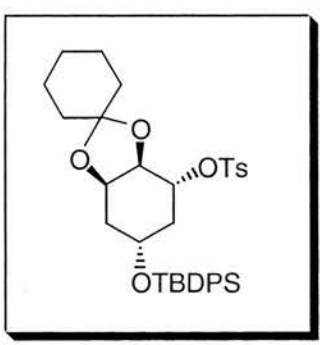

To a stirred solution of the silylated compound **75** (3.23 g, 6.93 mmol) in dry dichloromethane (50 cm^3) was added DMAP (187 mg, 1.53 mmol) and dry triethylamine (608 mg, 838 mm^3, 6.01 mmol). The mixture was then cooled to 0°C in an ice bath and *p*-toluenesulfonyl chloride (1.37 g, 7.19 mmol) was added under vigorous stirring. The mixture was then stirred at room temperature for 4 days, and then water (50 cm^3) was added. The two phases were separated and the aqueous phase extracted with dichloromethane (2 x 50 cm^3). The combined organic phases were dried with $MgSO_4$, and evaporated to dryness. The residual oil was the chromatographed on silica (petroleum ether/ethyl acetate; 10:1), to give the product tosylate, **76**, as a colourless oil, (1.61 g, 62.9 %).

ν_{max}/cm^{-1} (KBr): 2943 & 2858 (st, C-H), 1367 (st, O-SO_2), 1178 (st, C=C), 1104 (O-SO_2); δ_H (300 MHz; C^2HCl_3). δ_H (300 MHz; C^2HCl_3) 1.04 (9H, s, ^{t}butyl), 1.40-1.50 (10H, m, cyclohexylidene), 1.51-1.62 (2H, m, 3-H & 5-H), 2.12-2.26 (2H, m, 3-H & 5-H), 2.42 (3H, s, tosyl CH_3), 3.78-4.01 (2H, m, 2-H & 4-H), 4.08-4.24 (2H, m, 1-H & 6-H), 7.24-7.30 (2H, m, Ar-*H*), 7.35-7.66 (10H, m, Ar-H) 7.73 (2H, d, $^2J_{H-H}$ 8.27, Ar-*H*). δ_C (75.4 MHz; C^2HCl_3) 19.03 ($C(CH_3)_3$), 21.57 (*p*-toluenesulfonyl-CH_3), 23.49, 23.75, 24.90 (3 x C secondary of cyclohexylidene), 26.82 ($C(CH_3)_3$), 34.68, 35.39, 37.26, 38.26 (2 x C secondary of cyclohexylidene, 3-C and 5-C), 65.47 (4-C), 72.94 (2-C), 76.10 (6-C), 81.20 (1-C), 109.45 (C quaternary of cyclohexylidene), 127.62, 127.68, 127.98, 129.54, 129.69, 129.76, 133.61, 133.83, 135.67, 135.67, 144.36 (Ar-*C*H and Ar-C quaternary of *p*-toluenesulfonyl and $SiPh_2$); *m/z* (ES) 643 (100%, [M+Na]), 471 (9%, [M+Na-$C_7H_8SO_3$]);

(-)-(1*R*,2*R*,4*R*,6*R*)-1,2-Cyclohexylidenedioxy-6-(4'-phenylmethylsulfonyloxy)-cyclohexan-4-ol 77.[160]

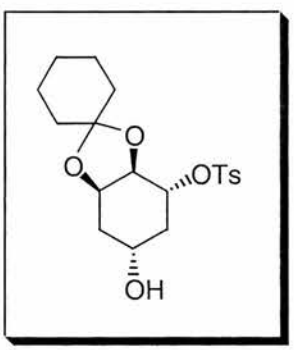

To a stirred solution of the tosylate, **76** (100 mg, 0.16 mmol) in THF (5 cm^3) was added TBAF (500 mm^3 of a 1 mol dm^{-3} solution in THF, 0.5 mmol) and the resulting mixture was stirred at room temperature overnight. The solvent was then removed under reduced pressure and the residual oil chromatographed on silica (petroleum ether/ethyl

acetate; 1:1), to give the product alcohol, **77**, as a white solid (56 mg, 91 %), mp 140-141°C (lit.,[160] mp 140-142°C); ν_{max}/cm^{-1} (KBr): 3394 (st, OH), 2943, 2931, 2919 & 2875 (st, C-H), 1351 (st, O-SO_2), 1188 & 1175 (st, C=C), 1108 (st, O-SO_2); δ_H (300 MHz; C^2HCl_3) 1.22-1.72 (12H, m, cyclohexylidene, 3-H & 5-H), 2.33-2.51 (5H, m, 3-H, 5-H & tosyl-CH_3), 3.94-4.00 (1H, m, 2-H), 4.00-4.11 (1H, m, 4-H), 4.30-4.38 (1H, m, 1-H), 4.40-4.50 (1H, m, 6-H)7.34 (2H, d, J_{H-H} 8.1, Ar-H), 7.84 (2H, d, J_{H-H} 8.3, Ar-H). δ_C (75.4 MHz; C^2HCl_3) 21.60 (*p*-toluenesulfonyl-CH_3), 23.57, 23.84, 24.95, 34.79, 35.09, 37.52, 38.29 (5 x C secondary of cyclohexylidene, 3-C and 5-C), 63.96 (4-C), 73.08 (2-C), 76.17 (6-C), 81.28 (1-C), 109.83 (C quaternary of cyclohexylidene), 128.03, 129.68, 134.05, 144.60 (Ar-CH and Ar-C quaternary of *p*-toluenesulfonyl); *m/z* (ES) 405 (100%, [M+Na]);

(-)-(1*R*,2*R*,4*R*,6*R*)-1,2-Cyclohexylidenedioxy-4-benzyl-6-(4'-phenylmethylsulfonyloxy)-cyclohexane, 78.[160]

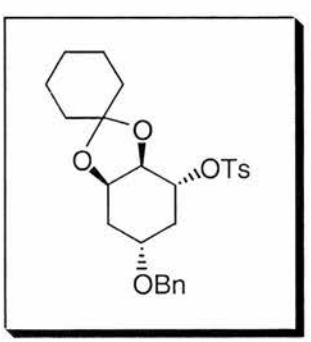

Under an atmosphere on nitrogen, a solution of the alcohol, **77** (340 mg, 0.89 mmol) in dry DMF (20 cm^3) was treated with benzyl bromide (304 mg, 212 mm^3, 1.78 mmol). The solution was cooled to –50°C and sodium hydride (44 mg, 1.11 mmol; 60% dispersion in oil) was added with continuous stirring. The mixture was allowed to warm slowly to room temperature while remaining in the cold bath and then water

($10\ cm^3$) was added with caution. The mixture was extracted with diethyl ether ($2 \times 50 cm^3$) and the combined organic phases dried with $MgSO_4$ and concentrated under reduced pressure. The residual oil was chromatographed on silca (petroleum ether/ethyl acetate; 5:1) to give the benzyl ether, **78** as a white solid (256 mg, 61 %), mp 83-84°C (lit.,[160] mp 83-84°C); ν_{max}/cm^{-1} (KBr): 3059 & 3029 (w, Aryl-H), 2936 (st, C-H), 1364 (st, O-SO_2), 1189 & 1174 (st, C=C), 1110 (st, O-SO_2); δ_H (300 MHz; C^2HCl_3). δ_H (300 MHz; C^2HCl_3) 1.24-1.54 (10H, m, cyclohexylidene), 1.54-1.64 (1H, m, 5-H), 1.66-1.78 (1H, m, 3-H), 2.45 (3H, s, tosyl-C*H*$_3$), 2.48-2.59 (2H, m, 3-H & 5-H), 3.72-3.83 (1H, m, 4-H), 3.95-4.20 (1H, dd, $^3J_{H\text{-}H}$=7.1 & 5.4, 1-H), 4.33-4.39 (1H, m, 2-H), 4.41-4.59 (3H, m, 6-H and OCH_2Ph), 7.29-7.40 (7H, m, Ar-*H*), 7.84 (2H, d, $^3J_{H\text{-}H}$=8.27, Ar-*H*). δ_C (75.4 MHz; C^2HCl_3) 21.61 (*p*-toluenesulfonyl-*C*H_3), 23.54, 23.82, 24.92, 32.61, 34.80, 35.31, 37.50 (5 x C secondary of cyclohexylidene, 3-C and 5-C), 70.79 (O*C*H_2Ph), 71.02 (4-C), 73.03 (2-C), 76.47 (6-C), 81.47 (1-C), 109.73 (C quaternary of cyclohexylidene), 127.52, 127.68, 128.03, 128.44, 129.61 (Ar-*C*H), 133.98, 138.11, 144.52 (Ar-*C* quaternary); *m/z* (ES) 495 (100%, [M+Na]), 323 (14%, [M+Na-$C_7H_8SO_3$]);

(+)-(1*S*,2*R*,4*R*,6*R*)-4-Benzyloxy-1,6-epoxycyclohexan-2-ol, 80.[160]

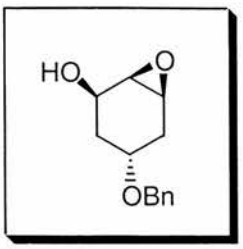

To a stirring solution of the ketal **78** (233 mg, 0.49 mmol) dissolved in methanol (30 cm^3) was added TFA (1 drop). The mixture was then stirred at room temperature for 3-4 days. The solvent was then removed under reduced pressure, and the intermediate diol re-dissolved in methanol (10 cm^3). To this stirring solution, potassium carbonate (135 mg, 0.98 mmol) was added in batches. The thickening reaction mixture was then stirred at room temperature for 1 hour, then filtered, and the residue was washed thoroughly with diethyl ether and ethyl acetate. The combined organic phases were dried with $MgSO_4$ and the solvent removed under reduced pressure. The residual oil was then chromatographed on silica (petroleum ether/ethyl acetate; 1:1), to give the epoxy alcohol **80** as a white solid (80 mg, 78 %), mp 64-66°C (lit.,160 mp 64-65°C); δ_H (300 MHz; C^2HCl_3) 1.50-1.61 (1H, m, 3-H), 1.88-2.12 (4H, m, 2 x 5-H, 3-H & OH), 3.33-3.45 (2H, m, 1-H & 6-H), 3.63-3.73 (1H, m, 4-H), 4.26-4.39 (1H, s, 4-H), 4.44 (1H, A of an AB system, $^2J_{H\text{-}H}$=12, OCH_2Ph), 4.52 (1H, B of an AB system, $^2J_{H\text{-}H}$=12, OCH_2Ph), 7.28-7.39 (5H, m, Ar-*H*). δ_C (75.4 MHz; C^2HCl_3) 29.25, 32.57 (3-C and 5-C), 54.18, 55.51 (1-C and 6-C), 64.91 (2-C), 70.19 (OCH_2Ph), 71.67 (4-C), 127.50, 127.70, 128.48 (Ar-*C*H), 138.31 (Ar-*C* quaternary); *m/z* (ES) 243 (100%, [M+Na]);

Resin-bound (+)-(1*S*,2*R*,4*R*,6*R*)-4-Benzyloxy-1,6-epoxycyclohexan-2-ol, 81.

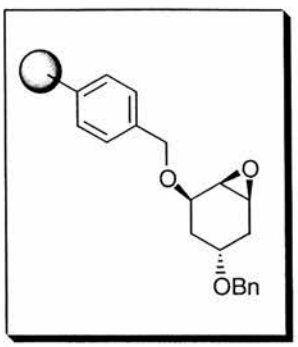

Epoxy alcohol **80** (110 mg, 0.5 mmol) was dissolved in dry DMF (5 cm^3) and added to a suspension of Merrifield resin (substitution level 1.0 mmol g^{-1}, 100 mg, 0.1 mmol) in dry DMF (10 cm^3). To this was then added sodium hydride (20 mg, 0.5 mmol; 60% dispersion in oil) in dry DMF (10 cm^3). The reaction was then stirred at 60°C for 4 hours, then cooled to room temperature when water (10 cm^3) was carefully added. The resin was then filtered and washed with DMF (3 x 25 cm^3), water (3 x 25 cm^3), dichloromethane (3 x 25 cm^3) and methanol (3 x 25 cm^3). The resin was then dried *in vacuo* at 50°C, giving the resin bound epoxide, **81** as a tan coloured solid.

ν_{max}/cm^{-1} (KBr): 1601, 1493, 1452 (st, polystyrene), 1365 (m, C-O-C ether), 1070 (C-O-C ether).

Opening resin-bound epoxide, 81, with propan-1-ol

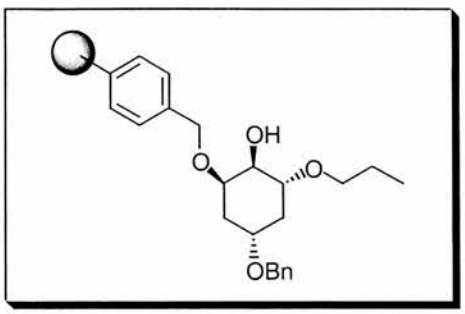

Resin-bound epoxide, **81**, (substitution level 1.0 mmol g^{-1}, 100 mg, 0.1 mmol) was suspended in a 2:1 mixture of 1,2-dichloroethane and acetonitrile (10 cm^3) and stirred. To this suspension was added ytterbium (III) triflate (15 mg, 0.025 mmol) and propan-1-ol (120 mg, 149 mm^3, 2 mmol). The mixture was then stirred at 60°C for 8 hours. The resin was then filtered and washed with dichloroethane and acetonitrile (2 x 25 cm^3 of each), dichloromethane (25 cm^3) and methanol (25 cm^3). The resin was then dried *in vacuo* at 50°C to give the product resin.

ν_{max}/cm^{-1} (KBr): 3420 (st br, OH), 1601, 1493, 1452 (st, polystyrene), 1360 (m, C-O-C ether), 1290 (C-O-C ether), 1236 (C-O-C ether).

Methyl 3-(*tert*-butoxycarbonylmethoxy)-5-hydroxyphenylacetate, 137.

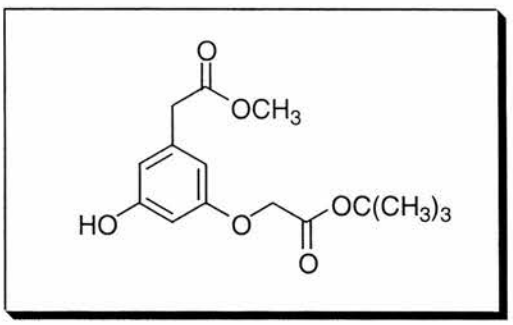

To a stirred suspension of sodium hydride (220 mg, 5.5 mmol; 60% dispersion in oil) in dry THF (10 cm^3) at 5°C was added a solution of methyl 3,5-dihydroxyphenylacetate (1.0 g, 5.5 mmol) and *tert*-butylbromoacetate (1.19 g, 900 mm^3, 6.1 mmol) in dry THF (10 cm^3). The mixture was then stirred whilst slowly warming to room temperature. Water (10 cm^3) was added with care and the solvent removed under reduced pressure. The residual oil was then partitioned between ethyl acetate (50 cm^3) and water (50 cm^3), separated and the aqueous layer extracted with ethyl acetate (2 x 50 cm^3). The combined organic phases were washed with saturated brine (40 cm^3), dried with Mg_2SO_4, then concentrated under reduced pressure. The residual oil was then chromatographed on silica (petroleum ether/ethyl acetate; 1:1) to give **137** as a colourless oil (594 mg, 38.5%); ν_{max}/cm^{-1} (thin film): 3416 (br, st, OH stretch), 2981 (st, C-H stretch) 1736 (vst, carbonyl), 1302 (st, C-O-C ether), 1256 (st, C-O-C ether), 1149 (vst, C-O-C ether); δ_H (300 MHz, C^2HCl_3) 1.46 (9H, s, $C(CH_3)_3$), 3.47 (2H, s, $CH_2CO_2C(CH_3)_3$), 3.65 (3H, s, CO_2CH_3), 4.44 (2H, s, $OCH_2CO_2C(CH_3)_3$), 6.30-6.39 (3H, m, Ar C-*H*), 7.13 (1H, br s, Ar-C-O*H*); δ_C (75.4 MHz, C^2HCl_3) 27.79 ($C(CH_3)_3$), 41.03 ($CH_2CO_2CH_3$), 52.04 (CO_2CH_3), 65.44 ($OCH_2CO_2C(CH_3)_3$). 82.59 ($C(CH_3)_3$), 101.33, 107.11 and 109.99 (Ar *C*-H), 135.87 (quaternary Ar *C*), 157.57 and 159.01 (Ar

C-OH and Ar $COCH_2$), 168.53 (CO_2CH_3) and 172.43 ($CO_2C(CH_3)_3$); *m/z* (CI) 314 (100%, $[M+H_2O]$), 258 (12%, $[M-C_4H_9+H_3O+H]^+$), 200 (10%, $[M-C_6H_{11}O_2+H_2O+H]^+$);

Methyl 3-(*tert*-butoxycarbonylmethoxy)-5-methylpolystyrenephenylacetate, 138.

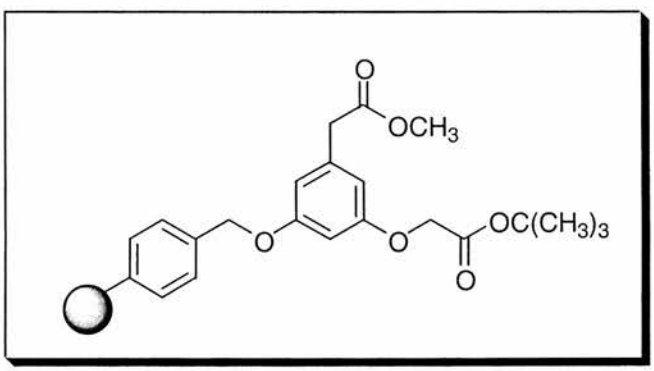

To a stirring suspension of sodium hydride (39 mg, 0.97 mmol; 60% dispersion in oil) in dry DMF (10 cm^3) was added a solution of methyl 3-(*tert*-butoxycarbonylmethoxy)-5-hydroxyphenylacetate, (287 mg, 0.97 mmol) in dry DMF (10 cm^3). After the evolution of hydrogen had ceased, the solution was added to a stirring suspension of Merrifield resin (substitution level 1.03 mmol g^{-1}, 320 mg, 0.33 mmol) in dry DMF (20 cm^3). The mixture was then stirred at 60°C for 4 hours, then at room temperature overnight. After careful addition of water (10 cm^3), the resin was filtered and washed with water (2 x 10 cm^3), DMF (2 x 10 cm^3), dichloromethane (2 x 10 cm^3) and finally methanol (2 x 10cm^3), then dried *in vacuo* at 50°C.

ν_{max}/cm^{-1} (KBr): 1729 (st, carbonyl), 1680 (st, carbonyl), 1600, 1494, 1453 (st, polystyrene), 1257 (st, C-O-C ether), 1147 (st, C-O-C ether).

3-oxyacetic acid-5-methylpolystyrenephenylacetic acid, 139.

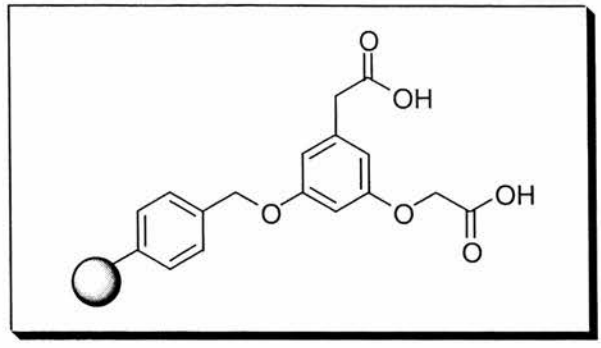

To a stirring mixture of THF (10 cm^3) and sodium hydroxide solution (1 mol dm^{-3} solution, 1 cm^3, 1 mmol) was added methanol, dropwise and with shaking, until the solution became homogeneous. Methyl-3-(*tert*-butoxycarbonylmethoxy)-5-methylpolystyrenephenylacetate, (substitution level 0.82 mmol g^{-1}, 300 mg, 0.25 mmol) was then added and the mixture stirred at room temperature for 24 hours. The resin was filtered and washed with water (3 x 10 cm^3), dichloromethane (2 x 10 cm^3) and methanol (10 cm^3), then dried *in vacuo* at 50°C. When dry, the resin was re-suspended in a 10% v/v solution of TFA in dichloromethane (10 cm^3), and this mixture was stirred at room temperature for 3 hours. The resin was filtered and washed with water, dichloromethane and methanol (3 x 10 cm^3 each) then dried *in vacuo* at 50°C.

ν_{max}/cm^{-1} (KBr): 3389 (br, st OH), 1700 (st, carbonyl), 1600, 1493, 1453 (st, polystyrene), 1255 (m, C-O-C ether).

Bis-rhodium (II)-diacetate immobilised onto ligand 139.

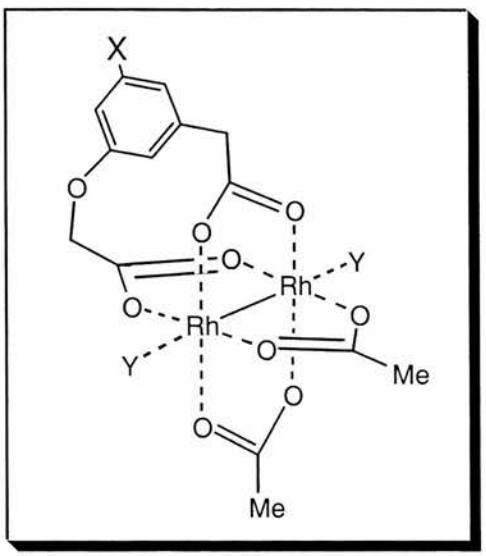

A solution of dirhodium tetraacetate **131** (39 mg, 88 μmol) in dry THF (10 cm^3) was added to a suspension of compound **139** (substitution level 0.88 mmol g^{-1}, 100 mg, 88 μmol) in dry THF (10 cm^3). The mixture was then stirred and heated at reflux for 7 days. After cooling, the resin was collected by filtration, and throughly washed with THF, water, dichloromethane, and methanol (3 x 30 cm^3 each) then dried *in vacuo* at 50°C, to give a distinct dark green coloured resin.

ν_{max}/cm^{-1} (KBr): 1597, 1493, 1453 (st, polystyrene)

2-fluorophenyl Merrifield ether, 108.

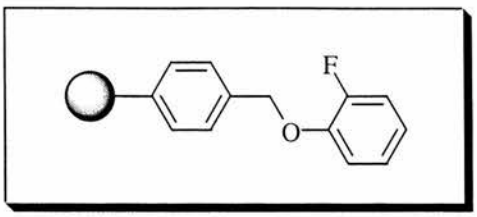

2-fluorophenol, **106** (854 mg, 680 mm^3, 7.6 mmol) was dissolved in DMF (5 cm^3) and added dropwise to a suspension of sodium hydride (304 mg, 7.6 mmol; 60% dispersion in oil) in DMF (10 cm^3). When evolution of hydrogen had ceased, the solution was added to a stirring suspension of Merrifield resin **6** (substitution level 0.76 mmol g^{-1}, 500 mg, 0.38 mmol) in DMF (15 cm^3). The suspension was stirred at 60°C overnight. Water (10 cm^3) was added with care, and the resin filtered and washed with water (20 cm^3) dichloromethane (2 x 20 cm^3) and methanol (20 cm^3). The resin was then dried *in vacuo* at 50°C.

ν_{max}/cm^{-1} (KBr): 1600, 1496, 1450 (st, polystyrene), 1309 (st, C-F), 1195 (m, C-O-C ether).

δ_F (298 MHz; $C_6{}^2H_6$): -134.6

4-fluorophenyl Merrifield resin, 109.

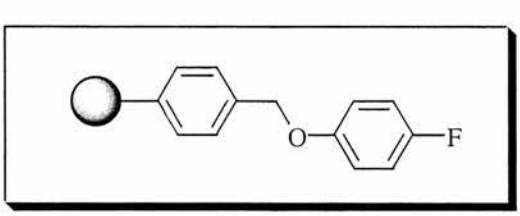

4-fluorophenol (852 mg, 7.6 mmol) was dissolved in DMF (5 cm^3) and added dropwise to a stirring suspension of sodium hydride (304 mg, 7.6 mmol; 60% dispersion in oil) in DMF (10 cm^3). After evolution of hydrogen had ceased, the solution was added to a

stirring suspension of Merrifield resin **6** (substitution level 0.76 mmol g^{-1}, 500 mg, 0.38 mmol) in DMF (15 cm^3). The suspension was stirred at 60°C overnight. Water (10 cm^3) was added with care, and the resin filtered and washed with water (20 cm^3), dichloromethane (2 x 20 cm^3) and methanol (20 cm^3). The resin was then dried *in vacuo* at 50°C.

ν_{max}/cm^{-1} (KBr): 1601, 1493, 1452 (st, polystyrene), 1313 (w, C-F), 1202 (st, C-O-C ether).

δ_F (298 MHz; $C_6{}^2H_6$): -124.6

Investigation into the substitution rates of 2-fluorophenol and 4-fluorophenol onto Merrifield Resin.

The following experiment was carried out four times. 2-fluorophenol (854 mg, 680 mm^3, 7.6 mmol) was dissolved in DMF (5 cm^3) and added dropwise to a stirring suspension of sodium hydride (304 mg, 7.6 mmol; 60% dispersion in oil). After evolution of hydrogen had ceased, the solution was added to a stirring suspension of Merrifield resin **6** (substitution level 0.76 mmol g^{-1}, 500 mg, 0.38 mmol) in DMF (15 cm^3). The suspension was then stirred at 60°C for 15, 30, 60 or 120 minutes. After each time-point, water (10 cm^3) was added, and the resin washed with water (20 cm^3) dichloromethane (2 x 20 cm^3) and methanol (20 cm^3). The resin was then dried *in vacuo* at 50°C. When dry, the resin was re-suspended in DMF (15 cm^3). 4 fluorophenol (852 mg, 7.6 mmol) was dissolved in DMF (5 cm^3) and added to a stirring suspension of sodium hydride (304 mg, 7.6 mmol; 60% dispersion in oil). The solution was then added to the re-suspended sample of Merrifield resin in DMF.

15 minutes stirring:

ν_{max}/cm^{-1} (KBr): 1601, 1493, 1452 (st, polystyrene), 1199 (st, C-O-C ether)

δ_F (298 MHz; $C_6^2H_6$): -124.8 (4-fluorophenyl Merrifield ether, 1F), -134.6 (2-fluorophenyl Merrifield ether, 2F).

30 minutes stirring:

ν_{max}/cm^{-1} (KBr): 1601, 1493, 1452 (st, polystyrene), 1199 (st, C-O-C ether).

δ_F (298 MHz; $C_6^2H_6$): -124.6 (4-fluorophenyl Merrifield ether, 1F), -134.5 (2-fluorophenyl Merrifield ether, 4F).

60 minutes stirring:

ν_{max}/cm^{-1} (KBr): 1601, 1493, 1452 (st, polystyrene), 1199 (st, C-O-C, ether)

δ_F (298 MHz; $C_6^2H_6$): -124.3 (4-fluorophenyl Merrifield ether, 1F), -134.1 (2-fluorophenyl Merrifield ether, 12F).

120 minutes stirring:

ν_{max}/cm^{-1} (KBr): 1601, 1493, 1452 (st, polystyrene), 1199 (st, C-O-C ether).

δ_F (298 MHz; $C_6^2H_6$): -134.2 (2-fluorophenyl Merrifield ether).

3,5-difluorophenyl Merrifield ether, 155.

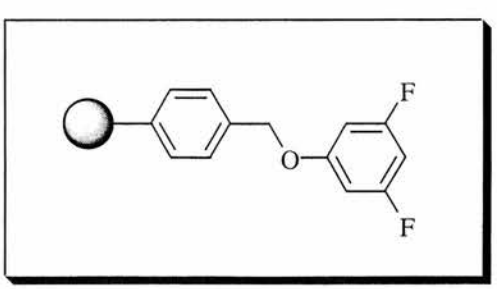

This was carried out in a manner analgous to the substitution of 2- and 4-fluorophenol, using 3,5-difluorophenol (1.0 g, 7.6 mmol).

ν_{max}/cm^{-1} (KBr): 1598, 1493, 1451 (st, polystyrene), 1347 (m, C-O-C ether), 996 (m, C-F).

δ_F (298 MHz; $C_6{}^2H_6$): -110.0.

Attachment of 3-hydroxybenzaldehyde to Merrifield resin, 111

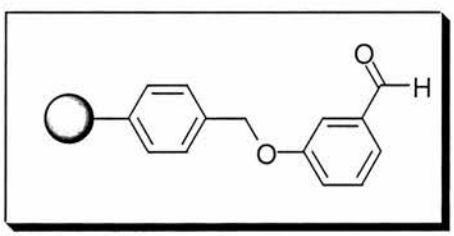

3-hydroxybenzaldehyde, **110** (928 mg, 7.6 mmol) was dissolved in dry DMF (10 cm^3) and added to a stirring suspension of sodium hydride (304 mg, 7.6 mmol; 60% dispersion in oil) in DMF (10 cm^3). After evolution of hydrogen had ceased, the resulting solution was added to a stirring suspension of Merrifield resin (substitution level 0.76 mmol g^{-1}, 500 mg, 0.38 mmol) in DMF (15 cm^3). The suspension was then stirred at 60°C for 4 hours. Water (5 cm^3) was added carefully, then the resin was filtered and washed with water, dichloromethane and methanol (2 x 20 cm^3 each). The resin was then dried *in vacuo* at 50°C.

ν_{max}/cm^{-1} (KBr): 2724 (aldehyde C-H), 1702 (st, aldehyde carbonyl), 1601, 1493, 1453 (st, polystyrene), 1259 (C-O-C ether).

Formation of resin-bound imine with 4-fluorobenzylamine, 124

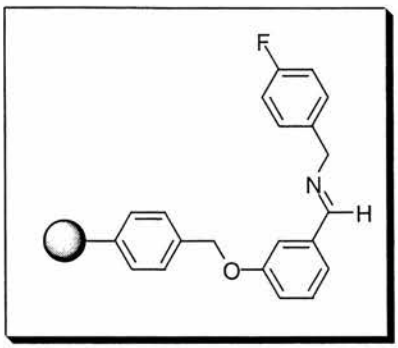

The resin-supported aldehyde **111** (substitution level 1.82 mmol g^{-1}, 200 mg, 0.36 mmol) was suspended in trimethylorthoformate, **115** (10 cm^3) and stirred. To this suspension was added 4-fluorobenzylamine **118** (250 mg, 226 mm^3, 2 mmol). The suspension was then left to stir overnight at room temperature. The resin was then filtered and washed with THF (2 x 30 cm^3) and methanol (30 cm^3) then dried *in vacuo* at 50°C.

ν_{max}/cm^{-1} (KBr): 1647 (m, C=N imine), 1601, 1492, 1452 (st, polystyrene), 1221 (m, C-O-C ether).

δ_F (298 MHz; $C_6{}^2H_6$): -115.6

Formation of resin-bound imine with 3-fluorobenzylamine, 123

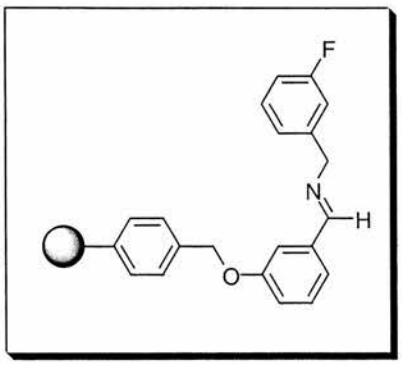

The resin-supported aldehyde **111** (substitution level 1.03 mmol g^{-1}, 566 mg, 0.58 mmol) was suspended in trimethylorthoformate, **115** (10 cm^3) and stirred. To the suspension was added 3-fluorobenzylamine (350 mg, 319 mm^3, 2.8 mmol). The suspension was then left to stir overnight at room temperature. The resin was filtered and washed with dichloromethane and methanol (2 x 20cm^3 of each) then dried *in vacuo* at 50°C.

ν_{max}/cm^{-1} (KBr): 1647 (m, C=N imine), 1601, 1492, 1452 (st, polystyrene), 1248 (m, C-O-C ether).

δ_F (298 MHz; $C_6{}^2H_6$): -113.2

Formation of resin-bound imine with 2-fluorobenzylamine, 122

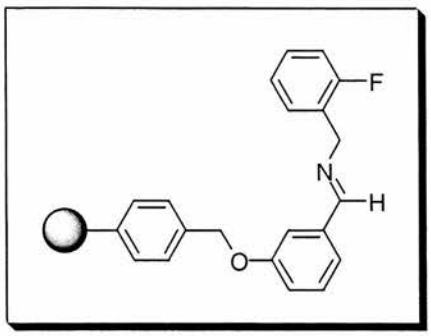

The resin-supported aldehyde, **111** (substitution level 1.03 mmol g^{-1}, 504 mg, 0.52 mmol) was suspended in trimethylorthoformate, **115** (10 cm^3) and stirred. To this suspension was added 2-fluorobenzylamine, **116** (626 mg, 572 mm^3, 5 mmol). The mixture was then left to stir overnight. The resin was filtered and washed with dichloromethane and methanol (2 x 20cm^3 of each) then dried *in vacuo* at 50°C.

ν_{max}/cm^{-1} (KBr): 1647 (m, C=N imine), 1601, 1492, 1452 (st, polystyrene), 1229 (m, C-O-C ether).

δ_F (298 MHz; $C_6{}^2H_6$): -118.5

Formation of resin-bound imine with 2,3-difluorobenzylamine, 125

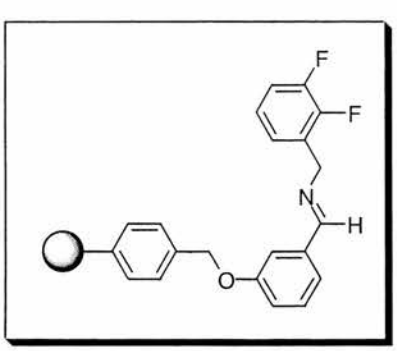

The resin-supported aldehyde, **111** (substitution level 1.03 mmol g^{-1}, 500 mg, 1 mmol) was suspended in trimethylorthoformate, **115** (10 cm^3) and stirred. To this suspension was added 2,3-difluorobenzylamine, **119** (716 mg, 592 mm^3, 5 mmol). The mixture was

then left to stir overnight at room temperature. The resin was then filtered and washed with dichloromethane and methanol (2 x 20cm^3 of each) then dried *in vacuo* at 50°C.

ν_{max}/cm^{-1} (KBr): 1645 (m, C=N imine), 1600, 1492, 1452 (st, polystyrene), 1280 (m, C-O-C ether).

δ_F (298 MHz; $C_6{}^2H_6$): -139.0, -143.6.

Formation of resin-bound imine with 2,6-difluorobenzylamine, 126

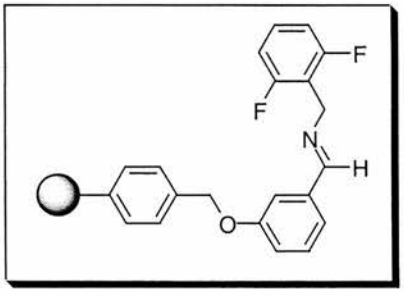

The resin-supported aldehyde, **111** (substitution level 1.03 mmol g^{-1}, 504 mg, 1 mmol) was suspended in trimethylorthoformate, **115** (10 cm^3) and stirred. To this suspension was added 2,6-difluorobenzylamine, **120** (716 mg, 598 mm^3, 5 mmol). The mixture was then left to stir overnight at room temperature. The resin was filtered and washed with dichloromethane and methanol (2 x 20cm^3 of each) then dried *in vacuo* at 50°C.

ν_{max}/cm^{-1} (KBr): 1647 (m, C=N imine), 1599, 1493, 1452 (st, polystyrene), 1264 (st, C-O-C ether).

δ_F (298 MHz; $C_6{}^2H_6$): -114.9

Formation of resin-bound imine with 3,5-difluorobenzylamine, 127

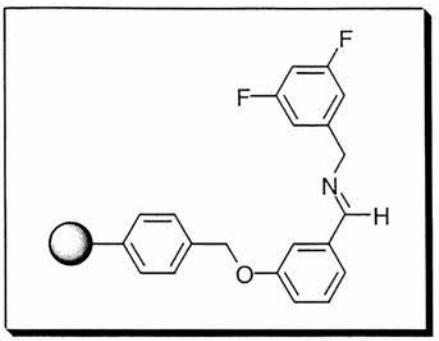

The resin-supported aldehyde, **111** (substitution level 1.82 mmol g^{-1}, 498 mg, 0.91 mmol) was suspended in trimethylorthoformate, **115** (10 cm^3) and stirred. To this suspension was added 3,5-difluorobenzylamine, **121** (716 mg, 594 mm^3, 5 mmol). The mixture was then left to stir overnight at room temperature. The resin was then filtered and washed with dichloromethane and methanol (2 x 20cm^3 of each) then dried *in vacuo* at 50°C.

ν_{max}/cm^{-1} (KBr): 1648 (m, C=N imine), 1598, 1492, 1452 (st, polystyrene), 1246 (st, C-O-C ether).

δ_F (298 MHz; $C_6{}^2H_6$): -109.6

Hydrolysis of resin-bound imine, 111 and 124.

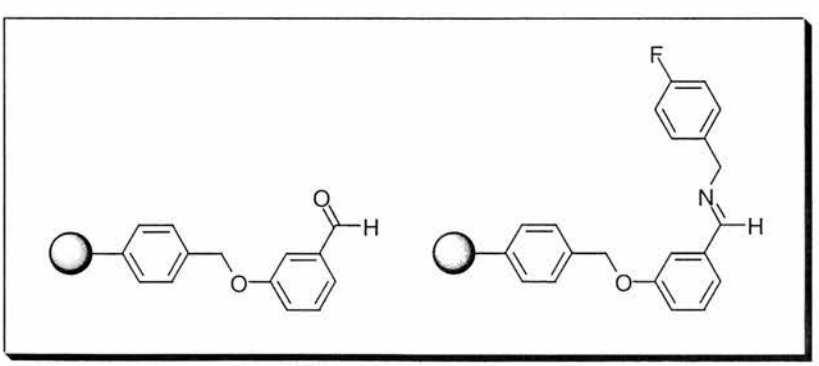

The resin-supported imine, **124** (substitution level 1.82 mmol g^{-1}, 100 mg, 0.18 mmol) was placed in a vial and to this was added water (5 cm^3). To aid solvation and to swell

the resin, THF (5 cm^3) was added, and the reaction mixture stirred at high speed for 30 minutes. The resin was then filtered and washed with THF (2 x 25 cm^3) and methanol (25 cm^3), then dried *in vacuo* at 50°C.

ν_{max}/cm^{-1} (KBr): 1699 (m, carbonyl), 1644 (m, C=N imine), 1600, 1492, 1452 (st, polystyrene), 1261 (m, C-O-C ether).

Grignard reaction with resin-bound imine 123 to form amine, 130.

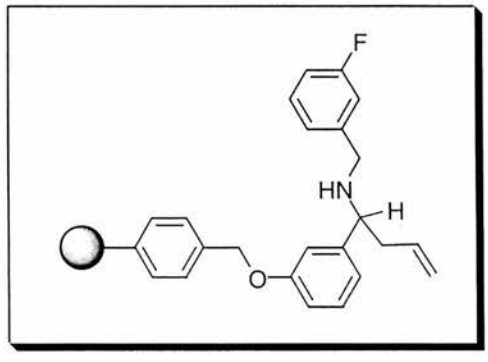

The resin-supported imine **123** (100 mg, approx. 0.1 mmol) was suspended in a 1:1 mixture of dry diethyl ether and dry toluene and stirred. To this suspension was added allylmagnesium bromide (1 mol dm^{-3} solution in diethyl ether, 500 mm^3, 0.5 mmol). The suspension was stirred at room temperature overnight, then filtered and washed with diethly ether (2 x 20 cm^3), toluene (2 x 20 cm^3), diethyl ether (20 cm^3) water (20 cm^3) and methanol (20 cm^3). After drying *in vacuo* at 50°C, the resin had changed appearance from light brown to yellow in colour.

ν_{max}/cm^{-1} (KBr): 3696 (m), 1637 (m, C=C), 1600, 1493, 1452 (st, polystyrene), 1257 (st, C-O-C ether).

Reaction of resin-bound imine 123 with TMS-cyanide, 129.

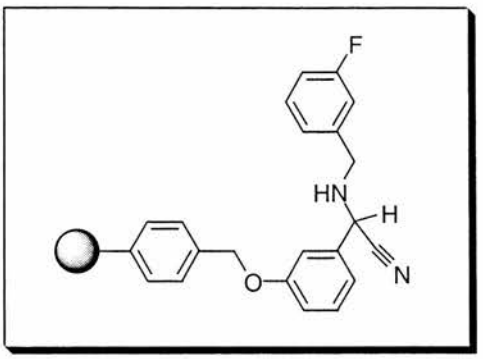

The resin-supported imine **123** (substitution level 1.03 mmol g^{-1}, 103 mg, 0.1 mmol) was suspended in dry THF (10 cm^3) and to this was added a catalytic amount of zinc (II) iodide (15 mg, 0.05 mmol) dissolved in dry THF (2 cm^3). The mixture was then stirred and to this was added trimethylsilyl cyanide (40 mg, 54 mm^3, 0.4 mmol). The reaction mixture was stirred overnight at room temperature, then filtered and washed with THF (3 x 25 cm^3), dichloromethane (2 x 25 cm^3), and methanol (25 cm^3). The resin was then dried *in vacuo* at 50°C.

ν_{max}/cm^{-1} (KBr): 2217 (m, nitrile), 1601, 1492, 1452 (st, polystyrene), 1254 (st, C-O-C ether).

Reduction of resin-bound imine 123 to form amine, 128.

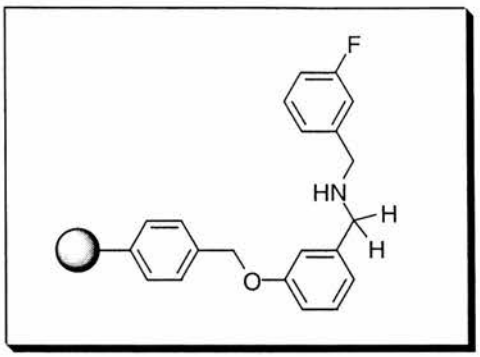

The resin-supported imine **123** (substitution level 0.86 mmol g^{-1}, 100 mg, 86 μmol) was suspended in dry dichloromethane (10 cm^3) an stirred. To the stirring suspension was added sodium triacetoxyborohydride (36 mg, 0.17 mmol), over 10 minutes. The reaction was stirred for a further 3 hours, then filtered and washed with water (25 cm^3), saturated sodium bicarbonate solution (25 cm^3), water (10 cm^3) then THF (25 cm^3). The resin was then dried *in vacuo* at 50°C.

ν_{max}/cm^{-1} (KBr): 1599, 1492, 1452 (st, polystyrene), 1233 (vst, C-O-C ether).

δ_F (298 MHz; $C_6{}^2H_6$):-112.5 (from secondary amine), -112.6 (from resin-bound imine, unreacted).

Attachment of 3-hydroxybenzaldehyde to Wang resin, 154.

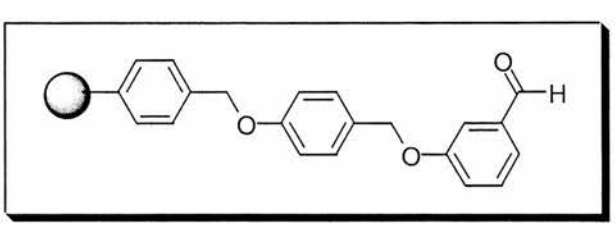

Wang (*p*-benzyloxybenzyl alcohol) resin (substitution level 1.16 mmol g^{-1}, 1.0 g, 1.16 mmol) was swollen in dry THF (10 cm^3) and to this was added triphenylphosphine (761 mg, 2.9 mmol) dissolved in dry THF (5 cm^3). The suspension was stirred at room temperature, and to it a solution of 3-hydroxybenzaldehyde, **110** (708 mg, 5.8 mmol) in

dry THF (5 cm^3) followed by diethyl azodicarboxylate (1.01 g, 913 mm^3, 5.8 mmol) was added. The reaction was stirred overnight, and then filtered and washed with DMF (5 x 10 cm^3), THF (3 x 10 cm^3) and methanol (3 x 10 cm^3).

ν_{max}/cm^{-1} (KBr): 2722 (w, C-H aldehyde), 1699 (st, carbonyl), 1600, 1493, 1453 (st, polystyrene), 1241 (C-O-C ether).

Immobilisation of perfluorododecanoic acid onto PTFE, 145.

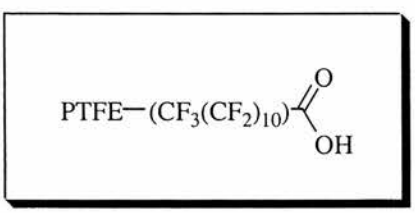

CD076 (co-polymer of TFE & approx. 0.1% HFP, 500 mg) was weighed out and placed in a Pasteur pipette, blocked with a small piece of glass wool. Perfluorododecanoic acid, **147**, (307 g, 0.5 mmol) was dissolved in diethyl ether (10 cm^3) and passed through the column of CD076 formed in the pipette. All the washings were collected, and this process was repeated 40-50 times, then the column was washed with diethyl ether (20 cm^3). All washings were collected and solvent removed under reduced pressure to give recovered unbound perfluorododecanoic acid **147** (280 mg, 0.46 mmol) and the resin-bound acid **149**.

ν_{max}/cm^{-1} (KBr): 1642 (w, carbonyl)

Immobilisation of perfluorododecanoic acid onto PTFE, 145a.

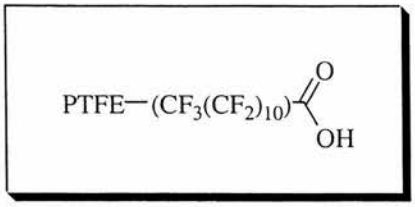

CD076 (500 mg) was suspended in diethyl ether (10 cm^3) and to this was added perfluorododecanoic acid **145** (300 mg, 0.51 mmol) dissolved in diethyl ether (10 cm^3). The mixture was stirred and heated at reflux for 4 hours. The CD076 was filtered and washed with diethyl ether (3 x 25 cm^3) and all washings collected. Removal of solvent under reduced pressure gave recovered unbound perfluorododecanoic acid (286 mg, 0.47 mmol), and the resin-bound acid **149**.

ν_{max}/cm^{-1} (KBr): 1641 (w, carbonyl).

Immobilisation of pentadecafluorooctanoic acid onto PTFE, 157.

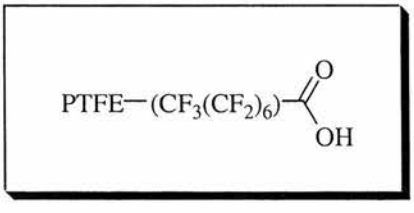

To a stirring suspension of CD076 (500 mg) in THF (10 cm^3) was added pentadecafluorooctanoic acid **156** (414 mg, 1 mmol) dissolved in THF (10 cm^3). The mixture was stirred at reflux for 24 hours. The CD076 was then filtered and washed with THF (2 x 50 cm^3) to give the resin-bound acid, **157**.

ν_{max}/cm^{-1} (KBr): 1682 (w, carbonyl).

The resin-bound acid, **157**, was further washed with THF (2 x 50 cm^3) and re-analysed.

ν_{max}/cm^{-1} (KBr): 1682 (weaker than previous, carbonyl).

Immobilisation of perfluorohexadecanoic acid onto PTFE, 150.

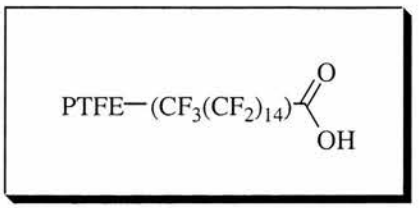

To a stirring suspension of CD076 (1 g) in THF (10 cm^3) was added perfluorohexadecanoic acid **148** (804 mg, 0.99 mmol). The mixture was then stirred at reflux overnight. After cooling, acid crystals were formed, which were decanted off with THF. Further additions of THF (2 x 50 cm^3) removed all traces of the perfluorohexadecanoic acid crystals. The polymer was then filtered and washed with THF (2 x 25 cm^3) to give the resin-bound acid, **150**.

ν_{max}/cm^{-1} (KBr): 1778 (w, carbonyl)

A portion of the PTFE immobilised acid was removed and washed further with THF (2 x 100 cm^3).

ν_{max}/cm^{-1} (KBr): 1778 (weaker than previous, carbonyl)

Formation of a PTFE immobilised rhodium catalyst, 151.

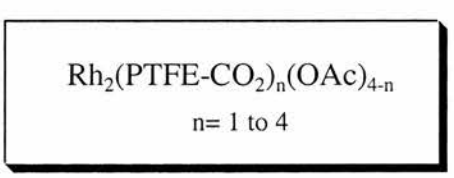

The CD076 bound perfluorohexadecanoic acid, **150** (493 mg) was suspensed in THF (10 cm^3) and to this was added a solution of dirhodium tetraacetate **131** (89 mg, 0.2 mmole) in THF (5 cm^3). The suspension was then stirred at reflux for 45.5 hours. When cool, a small portion of the polymer was removed, filtered and washed with THF (2 x 50 cm^3).

ν_{max}/cm^{-1} (KBr): 936 (w)

The mixture was then stirred and heated under reflux for a further 52 hours (97.5 hours total). When cool, the polymer was filtered and washed with THF (5 x 50 cm^3), to give the product polymer **151** as a slightly green coloured solid.

ν_{max}/cm^{-1} (KBr): 937 (w)

APPENDIX 1

1.

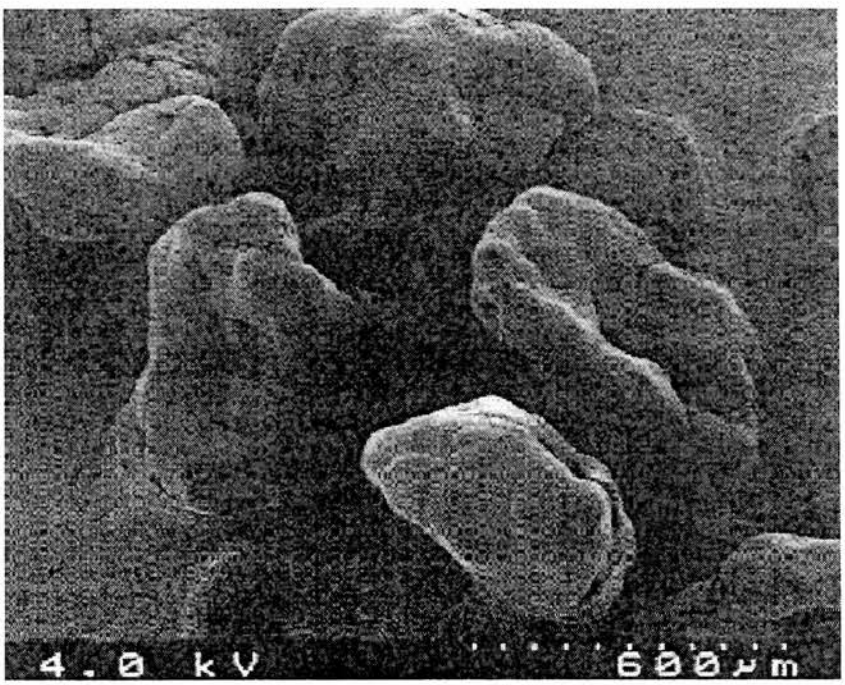

Picture 1 shows the external surface of the PTFE polymer. Points to note are the irregular and unique shape of each of the particles.

2.

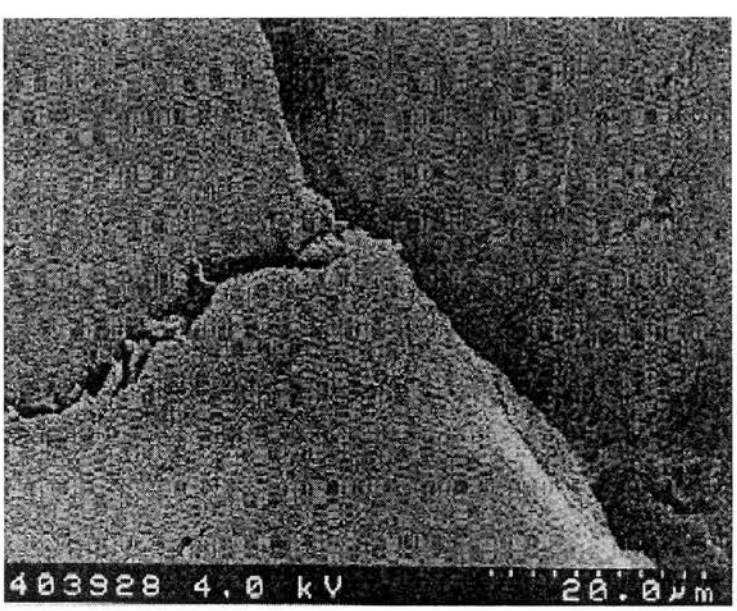

Magnification of the above picture gives a more detailed look at the surface of the PTFE particle. Notice the cracks and openings on the surface of the polymer.

3.

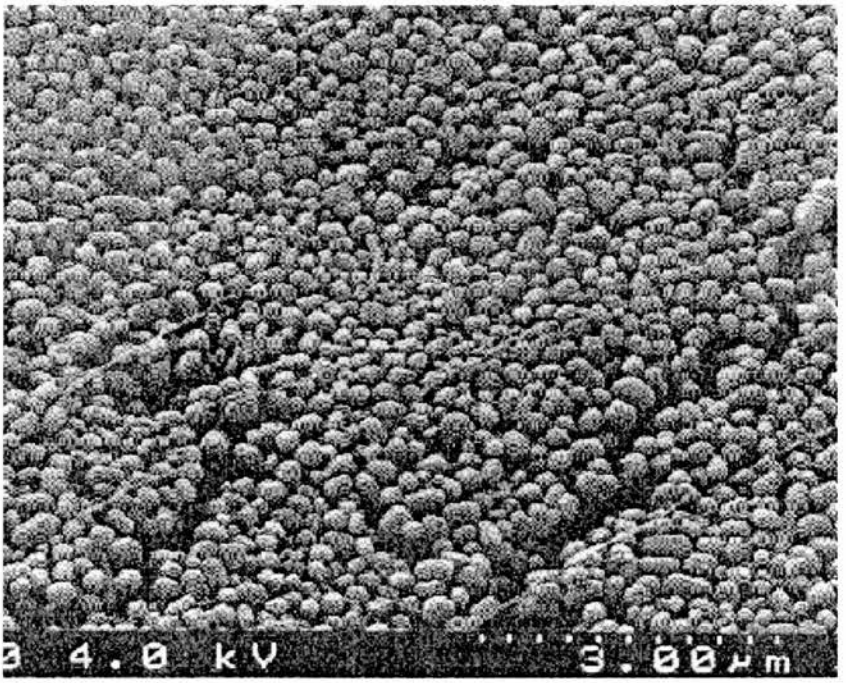

Picture 3 shows a greater magnification of the external surface of the polymer. Note the macroporous framework, and again, the cracks and openings in the surface.

4.

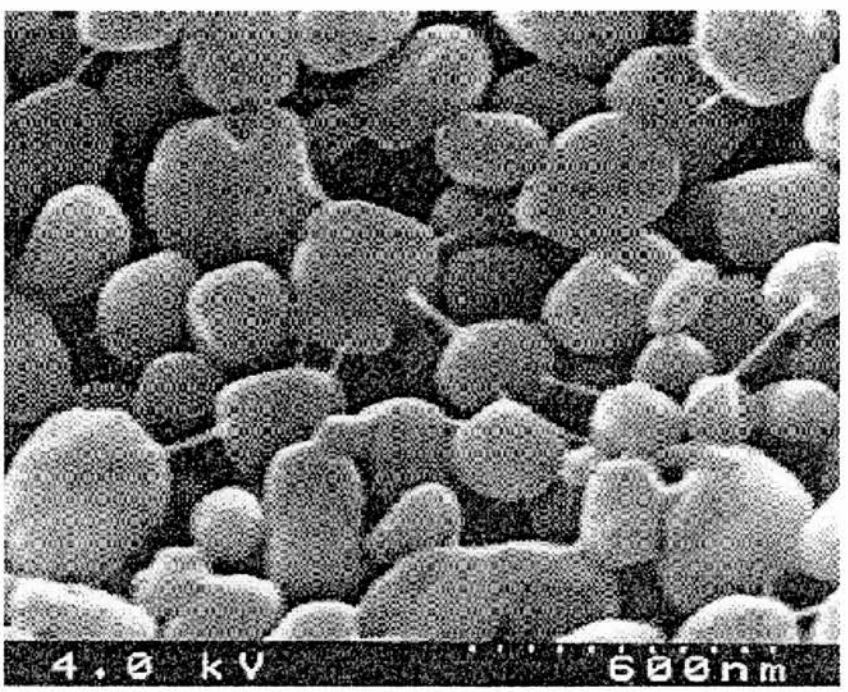

Further magnification shows in much greater detail the macroporous framework of the polymer discussed previously. It was thought that perfluorinated compounds could be passed into these openings in the surface shown, resulting in immobilised perfluorinated compounds.

5.

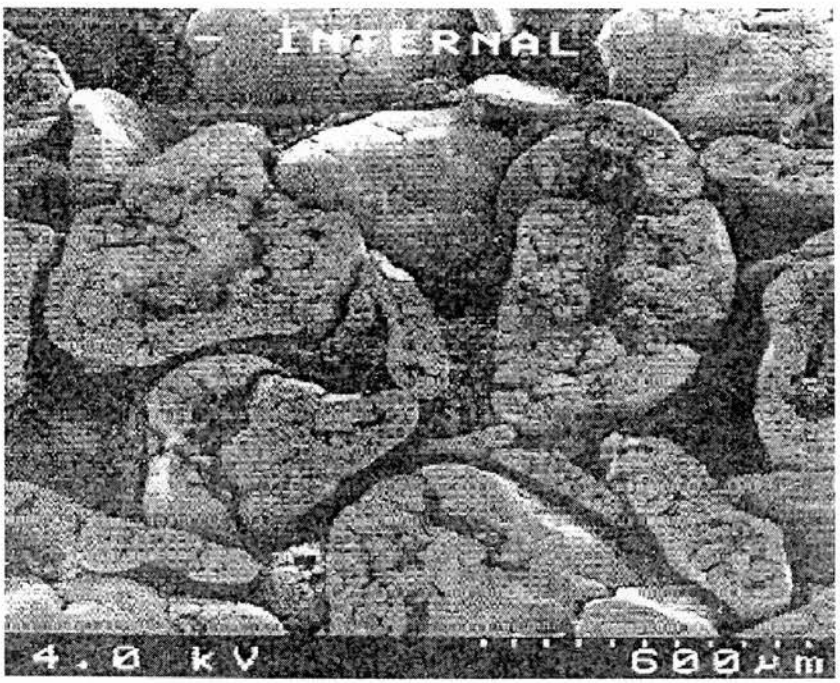

The above image shows the internal surface of the polymer. Again, note the irregular shapes and also the openings running through the polymer.

6.

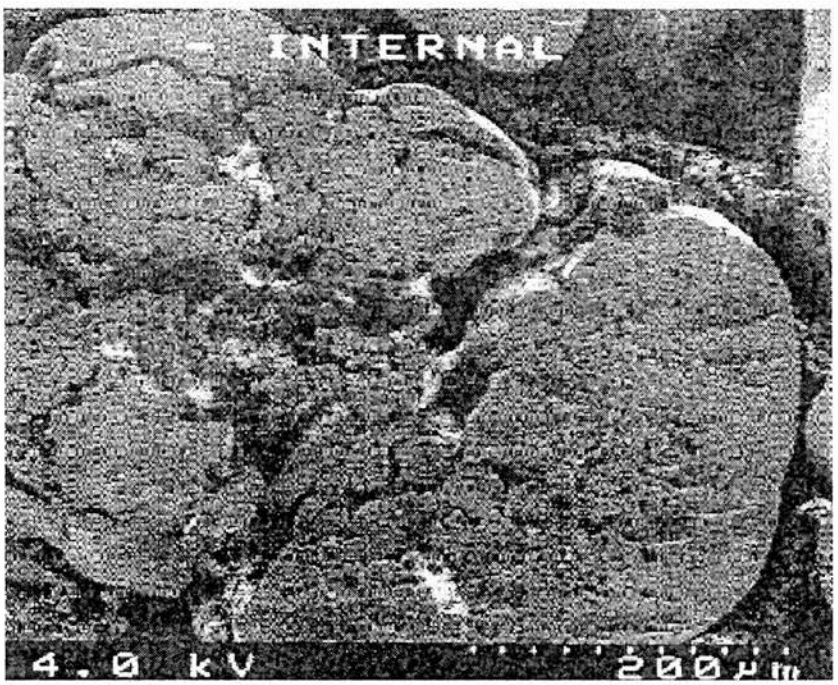

Magnification of picture 5 reveals the cracks in the framework inside the particle in greater detail.

7.

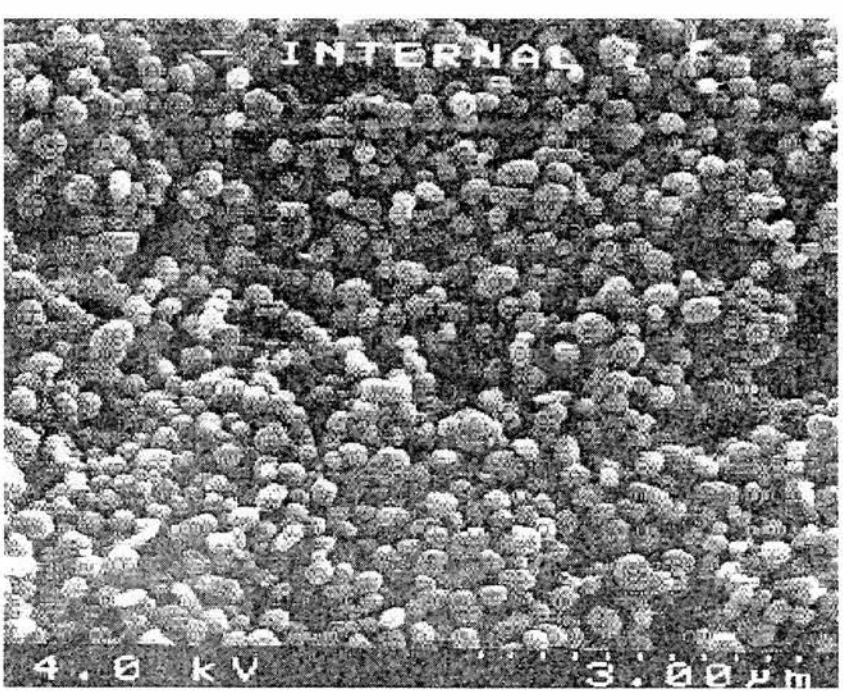

Again, the macroporous framework is revealed in this close up of the internal surface of the polymer. It is into these holes in the polymer that it was hoped that the perfluorinated acids would pass and hence be immobilised onto the PTFE, within the framework.

CHAPTER FOUR

REFERENCES

4 References.

1) Gallop, M. A.; Barrett, R. W.; Dower, W. J.; Fodor, S. P. A.; Gordon, E. M., *J. Med. Chem.,* 1994, **37**, 1233-1251.

2) Gordon, E. M.; Barrett, R. W.; Dower, W. J.; Fodor, S. P. A.; Gallop, M. A., *J. Med. Chem.,* 1994, **37**, 1385-1401.

3) Lebl, M., *Bioorg. Med. Chem. Lett.,* 1999, **9**, 1305-1310.

4) Krchñák, V., *Biotechnology and Bioengineering,* 1999, **61**, 135-141.

5) Cong, P.; Doolen, R. D.; Fan, Q.; Giaquinta, D. M.; Guan, S.; McFarland, E. W.; Poojary, D. M.; Self, K.; Turner, H. W.; Weinberg, W. H., *Angew. Chem. Int. Ed.,* 1999, **38**, 484-488.

6) Reetz, M. T.; Becker, M. H.; Klein, H.-W.; Stöckigt, D., *Angew. Chem. Int. Ed.,* 1999, **38**, 1758-1760.

7) Carell, T.; Wintner, E. A.; Bashir-Hashemi, A.; Rebek Jr., J., *Angew. Chem. Int. Ed. Engl.,* 1994, **33**, 2059-2061.

8) Carell, T.; Wintner, E. A.; Rebek Jr., J., *Angew. Chem. Int. Ed. Engl.,* 1994, **33**, 2061-2064.

9) Pirrung, M.C.; Chen, J., *J. Am. Chem. Soc.,* 1994, **117**, 1240.

10) Smith, P. W.; Lai, J. Y. Q.; Whittington, A. R.; Cox, B.; Houston, J. G.; Stylli, C. H.; Banks, M. N.; Tiller, P. R., *Bioorg. Med. Chem. Lett.,* 1994, **4**, 2821-2824.

11) Merrifield, R. B., *J. Am. Chem. Soc.,* 1963, **85**, 2149-2154.

12) Geysen, M. H.; Meloen, R. H.; Barteling, S. J., *Proc. Natl. Acad. Sci. USA,* 1984, **81**, 3998-4002.

13) Houghten, R. A., *Proc. Natl. Acad. Sci. USA,* 1985, **82**, 5131-5135.

14) Furka, A.; Sebestyen, F.; Asgedom, M.; Dibo, G., *Int. J. Pept. Prot. Res.,* 1991, **37**, 487-493.

15) Hermkens, P. H. H.; Ottenheijm, H. C. J.; Rees, D. C., *Tetrahedron,* 1996, **52**, 4527-4554.

16) Hermkens, P. H. H.; Ottenheijm, H. C. J.; Rees, D. C., *Tetrahedron,* 1997, **53**, 5643-5678.

17) Balkenhohl, F.; von dem Bussche-Hünnefeld, C.; Lansky, A.; Zechel, C., *Angew. Chem. Int. Ed. Engl.,* 1996, **35**, 2288-2337.

18) Santini, R.; Griffith, M. C.; Qi, M., *Tetrahedron Lett.,* 1998, **39**, 8951-8954.

19) MacDonald, A. A.; DeWitt, S. H.; Ghosh, S.; Hogan, E. M.; Kieras, L.; Czarnik, A. W.; Ramage, R., *Mol. Div.,* 1996, **1**, 183-186.

20) Atherton, E.; Clive, D. L. J.; Sheppard, R. C., *J. Am. Chem. Soc.,* 1975, **97**, 6584-6585.

21) Stahl, G., *Int. J. Pept. Prot. Res.,* , **15**, 331.

22) Gravert, D. J.; Janda, K. D., *Chem. Rev.,* 1997, **97**, 489-509.

23) Virgilio, A. A.; Ellman, J. A., *J. Am. Chem. Soc.,* 1994, **116**, 11580-11581.

24) Eby, R.; Schuerch, C., *Carbohyd. Res.,* 1975, **39**, 151-155.

25) Heckel, A.; Mross, E.; Jung, K.-H.; Rademann, J.; Schmidt, R. R., *Synlett,* 1998, 171-173.

26) Liu, S.; Akhtar, M.; Gani, D., *Tetrahedron Lett.,* 2000, **41**, 4493-4497.

27) Akhtar, M.; Kroll, F. E. K.; Gani, D., *Tetrahedron lett.,* 2000, **41**, 4487-4491.

28) Zhao, C.; Shi, S.; Mir, D.; Hurst, D.; Li, R.; Xiao, X.-Y.; Lillig, J.; Czarnik, A. W., *J. Comb. Chem.,* 1999, **1**, 91-95.

29) Xiao, X.-Y.; Zhao, C. F.; Potash, H.; Nova, M. P., *Angew. Chem. Int. Ed. Engl.,* 1997, **36**, 780.

30) Berg, R. H.; Pedersen, W. B.; Holm, A.; Tam, T. P.; Merrifield, R. B., *J. Am. Chem. Soc.,* 1989, **111**, 8024.

31) Matchi, S.; Kamel, I.; Silverman, J., *J. Polym. Sci. Part A-1,* 1970, **8**, 3329.

32) Mitchell, A. R.; Kent, S. B.; Engelhard, M.; Merrifield, R. B., *J. Org. Chem.,* 1978, **43**, 2845.

33) Gordon, K.; Balasubramanian, S., *Journal of Chemical Technology and Biotechnology,* 1999, **74**, 835-851.

34) Guillier, F.; Orain, D.; Bradley, M., *Chem. Rev.,* 2000, **100**, 2091-2157.

35) James, I. W., *Tetrahedron,* 1999, **55**, 4855-4946.

36) Kroll, F. E. K.; Morphy, R.; Rees, D.; Gani, D., *Tetrahedron Lett.,* 1997, **38**, 8573-8576.

37) Plunkett, M. J.; Ellman, J. A., *J. Org. Chem.,* 1995, **60**, 6006-6007.

38) Sauerbrei, B.; Jungmann, V.; Waldmann, H., *Angew. Chem. int. Ed.,* 1998, **37**, 1143-1146.

39) Stieber, F.; Grether, U.; Waldmann, H., *Angew. Chem. Int. Ed.,* 1999, **38**, 1073-1077.

40) Gutte, B.; Merrifield, R. B., *J. Biol. Chem.,* 1971, **246**, 1922-1941.

41) Yajima, H.; Fujii, N.; Ogawa, H.; Kawatani, H., *J. Chem. Soc. Chem. Commun.,* 1974, 107-108.

42) Karlsson, S.; Lindeberg, G.; Porath, J.; Ragnarsson, U., *Acta. Chem. Scand.,* 1970, **24**, 1010-1014.

43) Sparrow, J. T., *J. Org. Chem.,* 1976, **41**, 1350-1353.

44) Mitchell, A. R.; Kent, S. B. H.; Engelhard, M.; Merrifield, R. B., *J. Org. Chem.,* 1978, **43**, 2845-2852.

45) Mitchell, A. R.; Erickson, B. W.; Ryabtsev, M. N.; Hodges, R. S.; Merrifield, R. B., *J. Am. Chem. Soc.,* 1976, **98**, 7357-7362.

46) Wang, S.-S., *J. Am. Chem. Soc.,* 1973, **95**, 1328-1333.

47) Nugiel, D. A.; Wacker, D. A.; Nemeth, G. A., *Tetrahedron Lett.,* 1997, **38**, 5789-5790.

48) Raju, B.; Kogan, T. P., *Tetrahedron Lett.,* 1997, **38**, 4965-4968.

49) Ngu, K.; Patel, D. V., *Tetrahedron Lett.,* 1997, **38**, 973-976.

50) Orlowski, R. C.; Walter, R., *J. Org. Chem.,* 1976, **41**, 3701-3705.

51) Brown, D. S.; Revill, J. M.; Shute, R. E., *Tetrahedron Lett.,* 1998, **39**, 8533-8536.

52) Rink, H., *Tetrahedron Lett.,* 1987, **28**, 3787-3790.

53) Fréchet, J. M. J.; Haque, K. E., *Tetrahedron Lett.,* 1975, **16**, 3055-3056.

54) Fyles, T. M.; Leznoff, C. C., *Can. J. Chem.,* 1976, **54**, 935-942.

55) Fréchet, J. M. J.; Nuyens, L. J., *Can. J. Chem.,* 1976, **54**, 926-934.

56) Barlos, K.; Gatos, D.; Kallitsis, I.; Papaioannou, D.; Sotiriou, P., *Liebigs Ann. Chem.,* 1988, 1079-1081.

57) Morphy, J. R.; Rankovic, Z.; Rees, D. C., *Tetrahedron Lett.,* 1996, **37**, 3209-3212.

58) Heinonen, P.; Lönnberg, H., *Tetrahedron Lett.,* 1997, **38**, 8569-8572.

59) Barco, A.; Benetti, S.; De Risi, C.; Marchetti, P.; Pollini, G. P.; Zanirato, V., *Tetrahedron Lett.,* 1998, **39**, 7591-7594.

60) Chenera, B.; Finkelstein, J. A.; Veber, D. F., *J. Am. Chem. Soc.,* 1995, **117**, 11999-12000.

61) Rich, D. H.; Gurwara, S. K., *J. Chem. Soc. Chem. Commun.,* 1973, 610-611.

62) Pillai, V. N. R., *Synthesis,* 1980, 1-26.

63) Ajayaghosh, A.; Pillai, V. N. R., *J. Org. Chem.,* 1987, **52**, 5714-5717.

64) Ajayaghosh, A.; Pillai, V. N. R., *Tetrahedron Lett.,* 1995, **36**, 777-780.

65) Wang, S.-S., *J. Org. Chem.,* 1976, **41**, 3258-3261.

66) Sucholeiki, I., *Tetrahedron Lett.,* 1994, **35**, 7307-7310.

67) Forman, F. W.; Sucholeiki, I., *J. Org. Chem.,* 1995, **60**, 523-528.

68) Bray, A. M.; Chiefari, D. S.; Valerio, R. M.; Maeji, N. J., *Tetrahedron Lett.,* 1995, **36**, 5081-5084.

69) Kaiser, E.; Colescott, R. L.; Bossinger, C. D.; Cook, P. I., *Anal. Biochem.,* 1970, **34**, 595-598.

70) Reddy, M. P.; Voelker, P. J., *Int. J. Peptide Protein Res.,* 1988, **31**, 345-348.

71) Chu, S. S.; Reich, S. H., *Bioorg. Med. Chem. Lett.,* 1995, **5**, 1053-1058.

72) Ellman, G. L., *Arch. Biochem. Biophys.,* 1959, **82**, 70.

73) Epton, R.; Goddard, P., *Polymer,* 1980, **21**, 1367-1371.

74) Manatt, S. L.; Horowitz, D.; Horowitx, R.; Pinnell, R. P., *Anal. Chem.,* 1980, **52**, 1529-1532.

75) Jones, A. J.; Leznoff, C. C.; Svirskaya, P. I., *Organic Magnetic Resonance,* 1982, **18**, 236-240.

76) Blossey, E. C.; Cannon, R. G., *J. Org. Chem.,* 1990, **55**, 4464-4468.

77) Look, G. C.; Holmes, C. P.; Chinn, J. P.; Gallop, M. A., *J. Org. Chem.,* 1994, **59**, 7588-7590.

78) Look, G. C.; Murphy, M. M.; Campbell, D. A.; Gallop, M. A., *Tetrahedron Lett.,* 1995, **36**, 2937-2940.

79) Svennson, A.; Fex, T.; Kihlberg, J., *Tetrahedron Lett.,* 1996, **37**, 7649-7652.

80) Manatt, S. L., *Tetrahedron Lett.,* 1980, **21**, 1397-1400.

81) Shapiro, M. J.; Kumaravel, G.; Petter, R. C.; Beveridge, R., *Tetrahedron Lett.,* 1996, **37**, 4671-4674.

82) Svensson, A.; Berquist, K.-E.; Fex, T.; Kihlberg, J., *Tetrahedron Lett.,* 1998, **39**, 7193-7196.

83) Drew, M.; Orton, E.; Krolikowski, P.; Salvino, J. M.; Kumar, N. V., *J. Comb. Chem.,* 2000, **2**, 8-9.

84) Dorsey, J. G.; Cooper, W. T., *Anal. Chem.,* 1996, **68**, 515R-568R.

85) Bardella, F.; Eritja, R.; Pedroso, E.; Giralt, E., *Bioorg. Med. Chem. Lett.,* 1993, **3**, 2793-2796.

86) Johnson, C. R.; Zhang, B., *Tetrahedron Lett.,* 1995, **36**, 9253-9256.

87) Swayze, E. E., *Tetrahedron Lett.,* 1997, **38**, 8643-8646.

88) Maciel, G. E., *Science,* 1984, **226**, 282-288.

89) Keifer, P. A., *J. Org. Chem.,* 1996, **61**, 1558-1559.

90) Wehler, T.; Westman, J., *Tetrahedron Lett.,* 1996, **37**, 4771-4774.

91) Stöver, H. D. H.; Fréchet, J. M. J., *Macromolecules,* 1991, **24**, 883-888.

92) Anderson, R. C.; Jarema, M. A.; Shapiro, M. J.; Stokes, J. P.; Ziliox, M., *J. Org. Chem.,* 1995, **60**, 2650-2651.

93) Riedl, R.; Tappe, R.; Berkessel, A., *J. Am. Chem. Soc.,* 1998, **120**, 8994-9000.

94) Yan, B.; Fell, J. B.; Kumaravel, G., *J. Org. Chem.,* 1996, **61**, 7467-7472.

95) Russell, K.; Cole, D. C.; McLaren, F. M.; Pivonka, D. E., *J. Am. Chem. Soc.,* 1996, **118**, 7941-7945.

96) Chan, T. Y.; Chen, R.; Sofia, M. J.; Smith, B. C.; Glennon, D., *Tetrahedron Lett.,* 1997, **38**, 2821-2824.

97) Gosselin, F.; Di Renzo, M.; Ellis, T. H.; Lubell, W. D., *J. Org. Chem.,* 1996, **61**, 7980-7981.

98) Jung, G.; Beck-Sickinger, A. G., *Angew. Chem. Int. Ed. Engl.,* 1992, **31**, 367-383.

99) Meutermans, W. D. F.; Alewood, P. F., *Tetrahedron Lett.,* 1995, **36**, 7709-7712.

100) Egner, B. J.; Langley, G. J.; Bradley, M., *J. Org. Chem.,* 1995, **60**, 2652-2653.

101) Egner, B. J.; Cardno, M.; Bradley, M., *J. Chem. Soc., Chem. Commun.,* 1995, 2163-2164.

102) Fitzgerald, M. C.; Harris, K.; Shelvin, C. G.; Siuzdak, G., *Bioorg. Med. Chem. Lett.,* 1996, **6**, 979-982.

103) Czarnik, A. W., *Curr. Opin. Chem. Biol.,* 1997, **1**, 60-66.

104) Terrett, N. K. *Combinatorial Chemistry*; 1st Ed.; Oxford University Press Inc.:, 1998.

105) Edman, P., *Acta Chem. Scand.,* 1950, **4**, 283-293.

106) Ohlmeyer, M. H. J.; Swanson, R. N.; Dillard, L. W.; Reader, J. C.; Asouline, G.; Kobayashi, R.; Wigler, M.; Still, W. C., *Proc. Natl. Acad. Sci. USA,* 1993, **90**, 10922-10926.

107) Nestler, H. P.; Bartlett, P. A.; Still, W. C., *J. Org. Chem.,* 1994, **59**, 4723-4724.

108) Burbaum, J. J.; Ohlmeyer, M. H. J.; Reader, J. C.; Henderson, I.; Dillard, L. W.; Li, G.; Randle, T. L.; Sigal, N. H.; Chelsky, D.; Baldwin, J. J., *Proc. Natl. Acad. Sci. USA,* 1995, **92**, 6027-6031.

109) Borchardt, A.; Still, W. C., *J. Am. Chem. Soc.,* 1994, **116**, 373-374.

110) Borchardt, A.; Still, W. C., *J. Am. Chem. Soc.,* 1994, **116**, 7467-7468.

111) Boyce, R.; Li, G.; Nestler, H. P.; Suenaga, T.; Still, W. C., *J. Am. Chem. Soc.,* 1994, **116**, 7955-7956.

112) Wennemers, H.; Yoon, S. S.; Still, W. C., *J. Org. Chem.,* 1995, **60**, 1108-1109.

113) Baldwin, J. J.; Burbaum, J. J.; Hendreson, I.; Ohlmeyer, M. H. J., *J. Am. Chem. Soc.,* 1995, **117**, 5588-5589.

114) Nicolaou, K. C.; Xiao, X.-Y.; Parandoosh, Z.; Senyei, A.; Nova, M. P., *Angew. Chem. Int. Ed. Engl.,* 1995, **34**, 2289-2291.

115) Moran, E. J.; Sarshar, S.; Cargill, J. F.; Shahbaz, M. M.; Lio, A.; Mjalli, A. M. M.; Armstrong, R. W., *J. Am. Chem. Soc.,* 1995, **117**, 10787-10788.

116) Xiao, X.-Y.; Parandoosh, Z.; Nova, M. P., *J. Org. Chem.,* 1997, **62**, 6029-6033.

117) Crowley, J. I.; Rapoport, H., *Acc. Chem. Res.,* 1976, **9**, 135-144.

118) Camps, F.; Castells, J.; Font, J.; Vela, F., *Tetrahedron Lett.,* 1971, **12**, 1715-1716.

119) Heitz, W.; Michels, R., *Angew. Chem. Int. Ed. Engl.,* 1972, **11**, 298-299.

120) Heitz, W.; Michels, R., *Liebigs Ann. Chem.,* 1973, 227-230.

121) McKinkley, S. V.; Rakshys, J. W., *J. Chem. Soc., Chem. Commun.,* 1972, 134-135.

122) Ley, S. V.; Norman, J.; Griffith, W. P.; Marsden, S. P., *Synthesis,* 1994, 639-666.

123) Hinzen, B.; Ley, S. V., *J. Chem. Soc., Perkin Trans. 1,,* 1997, 1907-1908.

124) Ley, S. V.; Bolli, M. H.; Hinzen, B.; Gervois, A.-G.; Hall, B. J., *J. Chem. Soc., Perkin Trans. 1,,* 1998, 2239-2241.

125) Bernard, M.; Ford, W. T., *J. Org. Chem.,* 1983, **48**, 326-332.

126) Bolli, M. H.; Ley, S. V., *J. Chem. Soc., Perkin Trans. 1,,* 1998, 2243-2246.

127) Togo, H.; Nogami, G.; Yokoyama, M., *Synlett,* 1998, 534-536.

128) Ley, S. V.; Schucht, O.; Thomas, A. W.; Murray, P. J., *J. Chem. Soc., Perkin Trans. 1,,* 1999, 1251-1252.

129) Habermann, J.; Ley, S. V.; Scott, J. S., *J. Chem. Soc., Perkin Trans. 1,,* 1999, 1253-1255.

130) Kobayashi, S.; Nagayama, S., *J. Am. Chem. Soc.,* 1996, **118**, 8977-8978.

131) Kobayashi, S.; Nagayama, S.; Busujima, T., *Tetrahedron Lett.,* 1996, **37**, 9221-9224.

132) Kaldor, S. W.; Siegal, M. G.; Fritz, J. E.; Dressman, B. A.; Hahn, P. J., *Tetrahedron Lett.,* 1996, **37**, 7193-7196.

133) Ault-Justus, S. E.; Hodges, J. C.; Wilson, M. W., *Biotech. Bioeng.,* 1998, **61**, 17-22.

134) Coppola, G. M., *Tetrahedron Lett.,* 1998, **39**, 8233-8236.

135) Berridge, M. J.; Irvine, R. F., *Nature,* 1984, **312**, 315-321.

136) Berridge, M. J.; Irvine, R. F., *Nature,* 1989, **341**, 197-205.

137) Lückhoff, A.; Clapham, D. E., *Nature,* 1992, **355**, 356-358.

138) Potter, B. V. L.; Lampe, D., *Angew. Chem. Int. Ed. Engl.,* 1995, **34**, 1933-1972.

139) Kishimoto, A.; Takai, Y.; Mori, T.; Kikkawa, U.; Nishizuka, Y., *J. Biol. Chem.,* 1980, **255**, 2273-2276.

140) Leech, A. P.; Baker, G. R.; Shute, J. K.; Cohen, M. A.; Gani, D., *Eur. J. Biochem.,* 1993, **212**, 693-704.

141) Gani, D.; Downes, C. P.; Batty, I.; Bramham, J., *Biochem. Biophys. Acta,* 1993, **1177**, 253-269.

142) Ganzhorn, A. J.; Chanal, M.-C., *Biochemistry,* 1990, **29**, 6065-6071.

143) Spector, R.; Lorenzo, A. V., *Amer. J. Phys.,* 1975, **228**, 1510-1518.

144) Allison, J. H.; Blisner, M. E.; Holland, W. H.; Hipps, P. P.; Sherman, W. R., *Biochem. Biophys. Res. Commun.,* 1976, **71**, 664-670.

145) Hallcher, L. M.; Sherman, W. R., *J. Biol. Chem.,* 1980, **255**, 10896-10901.

146) Baker, R.; Leeson, P. D.; Liverton, N. J.; Kulagowski, J. J., *J. Chem. Soc., Chem. Commun.,* 1990, 462-464.

147) Baker, R.; Carrick, C.; Leeson, P. D.; Lennon, I. C.; Liverton, N. J., *J. Chem. Soc., Chem. Commun.,* 1991, 298-300.

148) Baker, R.; Kulagowski, J. J.; Billington, D. C.; Leeson, P. D.; Lennon, I. C.; Liverton, N. J., *J. Chem. Soc., Chem. Commun.,* 1989, 1383-1385.

149) Fauroux, C. M. J.; Lee, M.; Cullis, P. M.; Douglas, K. T.; Freeman, S.; Gore, M. G., *J. Am. Chem. Soc.,* 1999, **121**, 8385-8386.

150) Schulz, J.; Gani, D., *J. Chem. Soc., Perkin Trans. 1,* 1997, 657-670.

151) Piettre, S. R.; André, C.; Chanal, M.-C.; Ducep, J.-B.; Lesur, B.; Piriou, F.; Raboisson, P.; Rondeau, J.-M.; Scheler, C.; Zimmerman, P.; Ganzhorn, A. J., *J. Med. Chem.,* 1997, **40**, 4208-4221.

152) Piettre, S. R.; Ganzhorn, A. J.; Hoflack, J.; Islam, K.; Hornsperger, J.-M., *J. Am. Chem. Soc.,* 1997, **119**, 3201-3204.

153) Schnetz N.; Guedat, P.; Spiess, B.; Schlewer, G., *Bull. Soc. Chim. Fr.,* 1996, **133**, 205-208.

154) Gani, D.; Akhtar, M.; Kroll, F. E. K.; Smith, C. F. M.; Stones, D., *Tetrahedron Lett.,* 1997, **38**, 8577-8580.

155) Gani, D.; Akhtar, M.; Smith, C. F. M.; Stones, D., *Int. Pat.,* WO 97/40928, The University Court of The University of St Andrews, UK, 1997.

156) Perez, J. M.; Wilhelm, E. J.; Sucholeiki, I., *Bioorg. Med. Chem. Lett.,* 2000, **10**, 171-174.

157) Weerawarna, S. A.; Davis, R. D.; Nelson, W. L., *J. Med. Chem.,* 1994, **37**, 2856-2864.

158) Bray, A. M.; Lagniton, L. M.; Valerio, R. M.; Maeji, N. J., *Tetrahedron Lett.,* 1994, **35**, 9079-9082.

159) Young & Freedman *University Physics*; 9th ed.; Addison Wesley Educational Publishers, Inc.:.

160) Schulz, J.; Beaton, M. W.; Gani, D., *J. Chem. Soc., Perkin Trans. 1,* 2000, 943-954.

161) Sanders, J. K. M.; Hunter, B. K. *Modern NMR Spectroscopy: A guide for chemists.*; 2nd Ed.; Oxford University Press:, 1993.

162) Patrick, C. R.; Prosser, G. S., *Nature,* 1960, 1021.

163) Kariuki, B., *Personal Communication,* 2000.

164) Murphy, M. M.; Schullek, J. R.; Gordon, E. M.; Gallop, M. A., *J. Am. Chem. Soc.,* 1995, **117**, 7029.

165) Cornils, B.; Herrmann, W.A., *Applied Homogeneous Catalysis with Organometallic Compounds*; VCH: Weinheim, 1996.

166) Andersen, J. M.; Currie, A. W. S., *Chem. Commun.,* 1996, 1543.

167) Yoneda, N.; Nakagawa, Y.; Mimami, T., *Catal. Today,* 1997, **36**, 357.

168) Houghten, R. P.; Voyle, M.; Price, R., *J. Chem. Soc., Chem. Commun.,* 1980, 884.

169) Davies, H. M. C.; Kong, N., *Tetrahedron Lett.,* 1997, **38**, 4203.

170) Claver, C.; Ruiz, N.; Lahuerta, P.; Peris, E., *Inorg. Chim. Acta,* 1955, **233**, 161.

171) Andersen, J. M., *Plat. Metals Rev.,* 1997, **41**, 132-141.

172) Still, W. C.; Kahn, M.; Mitra, A., *J. Org. Chem.,* 1978, **43**, 2923-2937.